

# Final Report

## Sana'a Basin Water Management Project IDA Credit 3774-YEM

Contract No RFP No 2/04

- Republic of Yemen -

### Satellite Imagery/Data Analysis Study along with Ground Truth and Meteorological Monitoring

Prepared by:



Arnulfstr. 197, D-80634 Munich, Germany,

email: [info@gaf.de](mailto:info@gaf.de)

Tel: +49 89 1215 28-0

Fax: +49 89 1215 28-79

Web: [www.gaf.de](http://www.gaf.de)

In association with:

#### Vista GmbH

[www.vista-geo.de](http://www.vista-geo.de)  
Anton-Ferst-Str. 11  
D-82234 Wessling  
Germany

#### Ghayth Aquatech Ltd.

Harrat Assalam Building #8  
PO box 7219  
Sana'a  
Republic of Yemen

#### ISSUE:

Version 1.0  
26 June. 2007

### DOCUMENT IDENTIFICATION RECORD

Document No:	7192-Final Report
Issue No:	1.0
Date:	15-01-2007
Type:	Public
Distribution:	GAF-team GAF Internal File PN 7192
Authors:	T. Wever GAF
Contributions:	S. Saradeth, GAF P. Volk, GAF U. Steiner, GAF T. Kukuk, GAF H. Bach, VISTA A. Wagner, VISTA M. Al-Udaini, Ghayth
Review:	S. Saradeth
Quality Assurance:	S. Saradeth
Project Manager:	T. Wever

### REGISTER OR CHANGES OF THE DRAFT FINAL REPORT

Issue/Rev	Date	Page(s)	Reasons for change/Description	Author
1.0	14-09-05	All	First Document Issue - Draft	GAF / VISTA
1.2	23-09-06	All	Modifications according to recommendations of Final Workshop	GAF / VISTA
1.3	26-06-07	All	Modifications according to recommendations of Meeting on Feb. 2007	

## Abbreviations and Acronyms

AOI	Area of Interest
BCM	Billion Cubic Meter
COTS	Common-off-the-shelf
DB	Database
DCW	Digital Chart of the World
EO	Earth Observation
ESRI	Environmental Research Institute
ETa	actual Evapo-transpiration
ET	Evapo-transpiration
ETc	Crop evapo-transpiration under standard conditions
ETo	Reference evapo-transpiration
ETM	Enhanced Thematic Mapper
FAO	Food and Agriculture Organisation
GAF	Consulting Company
GC	General Conditions of Contract
GIS	Geographic Information System
GOY	Government of Yemen
GPS	Global Positioning System
GUI	Graphical User Interface
HW	Hardware
ICB	International Competitive Bidding
ICT	Information and Communication Technology
IDA	International Development Agency
IT	Information Technology
LAN	Local Area Network
LAI	Leave Area Index
MBR	Modified Bowen Ratio
MIS	Management Information System
MS	Milestone
MS	Microsoft
MS	Multi-spectral
MWE	Ministry of Water and Environment
NDVI	Normalized Differential Vegetation Index
NGO	Non-government Organisation
NIR	Near infra read
NSDI	National Spatial Data Infrastructure
NWRA	National Water Resources Authority
OS	Operating System
QA	Quality Assurance
QC	Quality Check
QCBS	Quality and Cost based Selection
pan	panchromatic
PCU	Project Coordination Unit
PMU	Project Management Unit
PROMET	process oriented multiscale evapo-transpiration
RDBMS	Relational Database Management System
RFP	Request for Proposal
RSGIS	Remote Sensing and Geographic Information System
SAR	Synthetic Aperture Radar
SBA	Sana'a Basin Agency
SB	Sana'a Branch
SC	Special Conditions of Contract
SEBAL	Surface Energy Balance Algorithm for Land
SBWM	Sana'a Basin Water Management
SBWMP	Sana'a Basin Water Management Project
SDI	Spatial Data Infrastructure
SRTM	Shuttle Radar Topography Mission
SW	Software
TA	Technical Assistance
tbd	to be discussed
TM	Thematic Mapper
ToR	Terms of Reference
USD	US Dollar
UTM	Universal Transverse Mercator
VHR	Very High Resolution
WAN	Wide Area Network
WGS	World Geodetic System
WP	Work-package
WUG	Water User Group
YER	Yemeni Rial

## **Table of Contents**

<b>1. Project Identification .....</b>	<b>4</b>
<b>2. Introduction .....</b>	<b>5</b>
2.1 Project Objectives .....	5
2.1.1 General Objectives .....	5
2.1.2 Specific Objectives .....	5
2.2 Purpose of the Document.....	5
2.3 Content of the Document .....	5
2.4 Referenced Documents.....	5
2.5 Project Background .....	6
<b>3. Tasks and Methodology.....</b>	<b>7</b>
3.1 Key Project Components.....	7
3.2 Data Acquisition and Pre-processing .....	7
3.2.1 Data Acquisition.....	7
3.2.2 Pre-processing.....	8
3.3 Field Survey and Ground Truth .....	13
3.3.1 Ground Truth .....	13
3.3.2 Field Survey.....	16
3.4 Irrigated Areas and Cropping Pattern.....	19
3.4.1 Irrigated Areas .....	19
3.4.2 Cropping Pattern.....	21
3.5 ET <sub>a</sub> Measurement.....	25
3.5.1 Specification of Ground Equipment for Measuring ET <sub>a</sub> .....	25
3.5.2 Procurement and Transport of Ground Equipment for Measuring ET <sub>a</sub> .....	25
3.5.3 Identification of Suitable Sites for Meteo-equipment.....	25
3.5.4 Installation of the MBR Station.....	27
3.6 Calculating Spatial Distributions of ET <sub>a</sub> from Satellite Data and Meteo-data	28
3.6.1 General Concept for Deriving the ET <sub>a</sub> .....	28
3.6.2 Calculation of ET <sub>o</sub> .....	29
3.6.3 Calculation of ET <sub>c</sub> .....	29
3.6.4 Calculation of ET <sub>a</sub> .....	30
3.6.5 Required Meteorological Measurements .....	30
3.7 Estimation of Net Groundwater Use by Agricultural .....	31
3.8 Other Information Analysis .....	32
3.8.1 Objectives .....	32
3.8.2 Compiled Geological Maps .....	32
3.8.3 Potential Infiltration Map .....	35
3.9 Training and Know-how Transfer .....	39
3.9.1 Background .....	39
3.9.2 Objectives.....	39
3.9.3 Training Needs .....	39



3.9.4	In-Country Training .....	39
3.9.5	External Training.....	41
<b>4.</b>	<b>Results and Accuracy Assessment .....</b>	<b>43</b>
4.1	Irrigation Acreage and Cropping Pattern .....	43
4.1.1	Irrigation Acreage .....	43
4.1.2	Cropping Pattern.....	45
4.1.3	Discussion of Results .....	51
4.2	ETa Measurements and ETa Model Results .....	55
4.2.1	Results from the MBR Station.....	55
4.2.2	Spectral Unmixing for Assessing the Fractional Vegetation Cover .....	58
4.2.3	Kc Values for the Sana'a Basin .....	80
4.2.4	Model Results for the Assessment of ETo .....	83
4.2.5	Calculation of ETo Based on Standard Meteorological Station Data .....	83
4.2.6	Calculation of ETo Based on MBR Station Data.....	86
4.2.7	Summary of ETo Calculations .....	88
4.2.8	Model Results for the Assessment of ETa .....	91
4.2.9	Calculation of ETa Using the Modified Bowen Ratio Method and MBR Data .....	91
4.2.10	Derivation of the Kc Value for Qat .....	91
4.2.11	Model Results for Spatial ETa Mapping.....	94
4.2.12	ETa Results per Crop Type .....	94
4.2.13	Results for Total ETa.....	100
4.2.14	Distribution of ETa in the Subwatersheds.....	103
4.2.15	Accuracy Assessment of ETa.....	104
4.3	Estimation of Ground Water Use by Agriculture .....	105
4.3.1	Spatial Interpolation of Annual Rainfall for the Investigation Period.....	105
4.3.2	Estimation of the Effective Rainfall .....	112
4.3.3	Summary of Net Ground Water Use by Agriculture .....	115
4.3.4	Problems Encountered and Solutions Found .....	119
4.4	Other Information Analysis .....	119
4.4.1	Compiled Geological Map.....	119
4.4.2	Potential Infiltration Map .....	125
4.5	Synthesis of Other Information Analysis.....	127
4.5.1	Artificial Recharge and Pollution in the Alluvium.....	127
4.5.2	Artificial Recharge in the Vulcanics.....	127
4.5.3	Artificial Recharge in the Tawilah.....	128
<b>5.</b>	<b>Conclusion.....</b>	<b>130</b>
<b>6.</b>	<b>Recommendations .....</b>	<b>133</b>
<b>7.</b>	<b>References .....</b>	<b>135</b>

## **List of Figures**

Figure 1: SPOT 5 false-colour image of the Sana'a Basin and its sub-catchments .....	3
Figure 2: SRTM 90m DEM of Sana'a Basin and perimeter .....	9
Figure 3: Radiance components affecting the measured signal at a satellite for non flat surfaces .....	10
Figure 4: Local solar direct irradiance (Ls) for the time of the SPOT 5 acquisition in the Sana'a basin .....	11
Figure 5: Atmospherically corrected SPOT image of the Sana'a basin from 5th Sep. 2004 (green, red, NIR) .....	12
Figure 6: Ground truth track and sample points in the Sana'a Basin and sub-basins, mission 1 .....	14
Figure 7: Ground truth track and sample points in the Sana'a Basin and sub-basins, mission 2 .....	15
Figure 8: GPS track (yellow) and observation points (red) surveyed during the GAF geological ground truthing campaign in 2004.....	17
Figure 9 - Left: Slope foot of the Tawilah sandstone with a fracture. In the front alluvium with arable land. Right Road cut outcrop showing stratified alluvium. ....	18
Figure 10: Spectra of healthy vegetation with the abrupt rise of the reflectance in the NIR; RED and NIR channels of SPOT 5	20
Figure 11: Schematic representation of the correlation between NDVI and healthy vegetation cover.....	21
Figure 12: Schematic process of creating thematic maps by logical pixel grouping .....	21
Figure 13: Processing workflow .....	24
Figure 14: SPOT 5 Image with location of the MBR Station .....	26
Figure 15: Micrometeorological Modified Bowen Ratio station (MBR station) after installation at Al-Qabil on 10th Feb. 2005 (Photo: W. Kaspari).....	27
Figure 16: Three step approach to calculate actual evapo-transpiration under non-standard conditions (ETa) based on the reference evapo-transpiration (ETo), and crop evapo-transpiration under standard conditions (ETc), (modified after FAO, 1998.) .....	28
Figure 17: Graphical user interface of the applied software with a geographically linked "four-window-screen" and a dynamic histogram stretch applied to the actual extension of the window. The example shows the comprehensive interpretation capabilities by the integration of all available input data. Top left: DEM; Top right: geological Map; Lower Left: Landsat ETM; Spot 5 .....	35
Figure 18: Sequential information derivation and iterative mapping and interpretation process.....	36
Figure 19: Input layers for the GIS analysis for the potential infiltration in the Sana'a plain. ....	39
Figure 20: Irrigation acreage in the Sana'a Basin (2004/2005) derived from multitemporal SPOT 5 imagery combined with actual evapo-transpiration map .....	45
Figure 21: Class examples on the ground.....	47
Figure 22: Scattergrams with NIR/SWIR band from Sept. 2004 (A) und Feb. 2005 (B).....	48
Figure 23: Cropping pattern in the Sana'a Basin (2004/2005).....	49
Figure 24: Irrigation acreage (A), irrigation acreage including the class "rain fed crops/natural vegetation" (B), irrigation acreage in Feb. 2005 (C) and evapo-transpiration map (D).....	53
Figure 25: Comparison between SPOT 5 PAN/MS Merge with 2,5m spatial resolution and SPOT MS with 10m resolution .....	55
Figure 26: Optimal coverage of a typical parcel (0,3ha; 40x75m) with Landsat TM (30x30m) and SPOT 5 data (10x10m) demonstrating the mixed pixel problem .....	55
Figure 27: Grapes cultivated in rows covered by 1 Landsat TM pixel of 30x30m (A); by 9 SPOT 5 pixel of 10x10m (B) and by 144 SPOT 5 pixel of 2,5x2,5m (C) .....	55

Figure 28: Temperature measurements during February 2005 at the MBR station at Al-Qabil, lower figure: 2m level, upper figure: 5 m level;.....	57
Figure 29: Measurements of energy fluxes and rainfall during February 2005 at the MBR station at Al-Qabil.....	58
Figure 30: ETa measured during February 2005 at the MBR station at Al-Qabil.....	59
Figure 31: Endmember spectra used for the calculation of the fractional vegetation cover from the SPOT images.....	60
Figure 32: Land use map and illustration of location of example subareas and the installed micro-meteorological station at Al-Qabil.....	62
Figure 33: Subarea of calculated fractional vegetation cover of qat on 5th Sep 2004 (top), 24th Feb 2005 (center) and 13th June 2005 (bottom), fc is calculated on 10m pixel.....	63
Figure 34: Subarea of calculated fractional vegetation cover of grapes on 5th Sep 2004 (top), 24th Feb 2005 (center) and 13th June 2005 (bottom), fc is calculated on 10m pixel.....	64
Figure 35: Subarea of calculated fractional vegetation cover of mixed crops on 5th Sep 2004 (top), 24th Feb 2005 (center) and 13th June 2005 (bottom); fc is calculated on 10m pixel.....	65
Figure 36: Subarea of calculated fractional vegetation cover of fruit orchards on 5th Sep 2004 (top), 24th Feb 2005 (center) and 13th June 2005 (bottom); fc is calculated on 10m pixel.....	66
Figure 37: Calculated Kc_adj of qat on 5th Sep 2004 for the Sana'a basin; Kc_adj is calculated on 10m pixel and rescaled to 100m cell resolution.....	67
Figure 38: Calculated Kc_adj of qat on 24th Feb 2005 for the Sana'a basin; Kc_adj is calculated on 10m pixel and rescaled to 100m cell resolution.....	68
Figure 39: Calculated Kc_adj of qat on 13th June 2005 for the Sana'a basin; Kc_adj is calculated on 10m pixel and rescaled to 100m cell resolution.....	69
Figure 40: Calculated Kc_adj of grape on 5th Sep 2004 for the Sana'a basin; Kc_adj is calculated on 10m pixel and rescaled to 100m cell resolution.....	70
Figure 41: Calculated Kc_adj of grape on 24th Feb 2005 for the Sana'a basin; Kc_adj is calculated on 10m pixel and rescaled to 100m cell resolution.....	71
Figure 42: Calculated Kc_adj of grape on 13th June 2005 for the Sana'a basin; Kc_adj is calculated on 10m pixel and rescaled to 100m cell resolution.....	72
Figure 43: Calculated Kc_adj of mixed crops on 5th Sep 2004 for the Sana'a basin; Kc_adj is calculated on 10m pixel and rescaled to 100m cell resolution.....	73
Figure 44: Calculated Kc_adj of mixed crops on 24th Feb 2005 for the Sana'a basin; Kc_adj is calculated on 10m pixel and rescaled to 100m cell resolution.....	74
Figure 45: Calculated Kc_adj of mixed crops on 13th June 2005 for the Sana'a basin; Kc_adj is calculated on 10m pixel and rescaled to 100m cell resolution.....	75
Figure 46: Calculated Kc_adj of fruit orchards on 5th Sep 2004 for the Sana'a basin; Kc_adj is calculated on 10m pixel and rescaled to 100m cell resolution.....	76
Figure 47: Calculated Kc_adj of fruit orchards on 24th Feb 2005 for the Sana'a basin; Kc_adj is calculated on 10m pixel and rescaled to 100m cell resolution.....	77
Figure 48: Calculated Kc_adj of fruit orchards on 13th June 2005 for the Sana'a basin; Kc_adj is calculated on 10m pixel and rescaled to 100m cell resolution.....	78
Figure 49: Standard temporal course of the crop coefficient Kc for the land use classes under investigation in the Sana'a basin (compilation of literature values, adapted to the Sana'a basin). The dates of the satellite images are illustrated as black vertical line.....	82
Figure 50: Temporal interpolation of Kc_adj for qat (dotted line) obtained from standard Kc course and 3 satellite acquisitions.....	83

Figure 51: Temporal interpolation of Kc_adj for mixed crops (green line) obtained from standard Kc course (blue line) and 3 satellite acquisitions (black vertical columns).....	83
Figure 52: Mean daily temperature used for ETo calculation measured at Sana'a Airport by CAMA .....	85
Figure 53: Daily values of relative humidity used for ETo calculation measured at Sana'a Airport by CAMA.....	85
Figure 54: Daily values of mean wind speed used for ETo calculation measured at Sana'a Airport by CAMA .....	86
Figure 55: Daily values of solar radiation used for ETo calculation measured in Sana'a by Sana'a Branch.....	86
Figure 56: Daily values of calculated ETo values for Sana'a .....	87
Figure 57: Daily courses of calculated ETo values [mm/20 min] using data of the MBR station .....	88
Figure 58: Calculated ETo [mm/day] using data of the MBR station after aggregation to daily values .....	88
Figure 59 Calculated ETo [mm/day] using data of the MBR station after aggregation to monthly values in comparison to the results obtained in the ITC report for the year 1989 (ITC, 2001) .....	89
Figure 60: Total monthly sum of simulated ETo in mm for the Sana'a basin. (Upper row: Jan to Apr 2005; centre row: May and Jun 05, Jul and Aug2004, bottom row: Sep to Dec 2004).....	90
Figure 61: Total annual sum of simulated ETo in mm for the Sana'a basin (size of model raster cell = 1 ha).....	91
Figure 62: Calculated ETo and ETa [mm/day] using data of the MBR station after aggregation to daily values; only days where valid ETa results were obtained are displayed. ....	92
Figure 63: Calculated Kc_adj using daily ETo and ETa results of the MBR station (illustrated in Fig. 38).....	93
Figure 64: Kc values for qat derived from 4 different dates using Kc_adj, satellite estimates of the fractional cover fc (24. Feb. or 13. June) or local assessments (13. Feb., 27. June).....	94
Figure 65: Map of annual sum of ETa for qat in the Sana'a basin for the period 1. July 2004 to 30. June 2005. The model used daily meteorological data, information on fractional vegetation cover from three satellite images and information on topography as input.....	96
Figure 66: Map of annual sum of ETa for grapes in the Sana'a basin for the period 1. July 2004 to 30. June 2005. The model used daily meteorological data, information on fractional vegetation cover from three satellite images and information on topography as input.....	97
Figure 67: Map of annual sum of ETa for mixed crops in the Sana'a basin for the period 1. July 2004 to 30. June 2005. The model used daily meteorological data, information on fractional vegetation cover from three satellite images and information on topography as input.....	98
Figure 68: Map of annual sum of ETa for fruit orchards in the Sana'a basin for the period 1. July 2004 to 30. June 2005. The model used daily meteorological data, information on fractional vegetation cover from three satellite images and information on topography as input.....	99
Figure 69: Monthly water use calculated for the crops in the Sana'a basin for the period 1. July 2004 to 30. June 2005	101
Figure 70: Map of annual sum of total ETa in the Sana'a basin for the period 1. July 2004 to 30. June 2005. The raster size for the simulation is 100m x 100m. Each value represents the average ETa per ha.....	102
Figure 71: Monthly maps of calculated total ETa distribution in the Sana'a basin . (Upper row: Jan to Apr 2005; centre row: May and Jun 05, Jul and Aug2004, bottom row: Sep to Dec 2004).....	103
Figure 72: Total monthly water use calculated in the Sana'a basin for the period 1. July 2004 to 30. June 2005. ....	104
Figure 73: Illustration of total annual ETa for the sub-watersheds of the Sana'a basin .....	105
Figure 74: Comparison of ETa modelled and ETa measured between 11.02.05 and 03.08.05.....	107
Figure 75: Long term average rainfall distribution for the Sana'a basin as prepared by WEC (University of Sana'a)..	108
Figure 76: Increase of annual precipitation with elevation in the Sana'a watershed during the investigation period 2004/2005 .....	110
Figure 77: Increase of annual precipitation with elevation in the Sana'a watershed based on annual rainfall sums measured in the period 1972 to 1998 .....	111

Figure 78: Annual sum of rainfall for the Sana'a basin during the investigation period 1. July 2004 to 30. June 2005. This year had approx. 20% more rainfall than the long term average.....	112
Figure 79: Isoline illustration of the annual rainfall for the Sana'a basin during the investigation period 1. July 2004 to 30. June 2005 .....	113
Figure 80: Estimation of Ground Water Use by Agriculture .....	117
Figure 81: Water Balance for groundwater use by agriculture for the subwatersheds in the Sana'a basin during the investigation period 2004/2005 (estimation).....	119
Figure 82: Compiled geological map of the Sana'a basin with relevance to hydrogeology.....	125
Figure 83: Potential infiltration map of the Sana'a basin.....	127
Figure 84: bottom of a dried reservoir with a concrete closed fracture (in between yellow lines, hand lens in the bottom middle as scale) .....	129
Figure 85: Sketch of the Sana'a basin with a coloured shaded relief, zones of high groundwater pollution risk (red) and areas of good infiltration properties (blue – see potential infiltration map). Suitable dam construction for recharge of the alluvium is within the lines of light blue colour. Indirect recharge for Tawilah Sandstone in the Sana'a city area is assumed south of the green line (subsurface cropping Tawilah).....	130

## **List of Tables**

Table 1: Satellite data .....	7
Table 2: Ancillary data.....	8
Table 3: Alluvium Infiltration classification (1) .....	38
Table 4: Alluvium Infiltration classification .....	38
Table 5: In country training 2005.....	42
Table 6: Training schedule for external training in Germany March- April 2005 .....	43
Table 7: Irrigation acreage broken down by sub-catchments (2004/2005) .....	44
Table 8: Cropping pattern broken down by sub-catchments .....	50
Table 9: Irrigation acreage and cropping pattern broken down by sub-catchments.....	51
Table 10: Confusion matrix of cropping pattern .....	52
Table 11: Accuracy matrix of cropping pattern .....	52
Table 12: Statistics of retrieved fraction cover values for the four land use classes .....	61
Table 13: Statistics of retrieved fractional cover values for the three land use classes and the subcatchments of the Sana'a basin (Definition of subcatchments from BGR, 2004) .....	79
Table 14: Comparison of fractional covers obtained from spectral unmixing using the 10m SPOT data and from classification of the 2.5m Panchromatic SPOT data .....	81
Table 15: Retrieved values of Kc_adj, fc / fc dense and the resulting Kc using the MBR data of 2005. For 24th Feb and 13th June satellite images could be used to get fc / fc dense .....	94
Table 16: Results for ETa calculations for each crop type and month. ....	100
Table 17: Results for total ETa calculations per month.....	104
Table 18: Total annual ETa for the sub-watersheds of the Sana'a basin.....	106
Table 19: Sum of ETa modelled in mm compared to ETa measured in mm.....	107
Table 20: Monthly rainfall values used for rainfall interpolation for the investigation period in 2004 and 2005.....	109
Table 21 Total annual rainfall for the subwatersheds in the Sana'a basin for the investigation period in 2004/2005 obtained from spatial interpolation of station data.....	113
Table 22 Total annual rainfall and effective rainfall from surface runoff for the subwatersheds in the Sana'a basin for the investigation period in 2004/2005 .....	114
Table 23 Infiltration after heavy rainfall for the Sana'a basin in 2004/2005 derived from soil water balance simulations	115
Table 24: Infiltration rates and effective rainfall from infiltration for the subwatersheds of Sana'a basin in 2004/2005	116
Table 25: Water balance components of the subwatersheds of the Sana'a basin and resulting ground water use by agriculture. Negative values in the water balance mean that the ground water is overused.....	118
Table 26: Litho-stratigraphical division into submembers with reference to the BGR map. *) taken from International Lexicon of Stratigraphy, Volume III, Republic of Yemen, IUGS Publications No.34 .....	121

## Executive Summary

The Sana'a Basin suffers from rapid and extreme depletion of groundwater, being the only water resource for domestic, industrial and agricultural use. The use of water by far exceeds the natural recharge including irrigation and wastewater return flow, and is inefficient and totally unregulated throughout the Basin. The Sana'a Basin is a highland area of some 3200 sqkm with a population of 1.8 million growing at 7% per annum. About 75% of the population depends wholly on agriculture activity, which mainly comprises qat and fruit growing and livestock rearing.

To tackle this serious water crisis, the Government's Natural Water Resources Authority (NWRA) has started working on a Sana'a Basin Water Master Plan, which helped defining the basis of the phase 1 program of the IDA Sana'a Basin Water Management Project. NWRA is also supposed to implement hydrological monitoring, well inventory and other information collection means needed for basin planning

The key issue is to increase the usable lifetime of the aquifers of the Sana'a Basin – thereby postponing long-distance high-lift import of water and allowing time for a shift to a less water-based economy.

The project therefore aimed generally at obtaining up-to-date information about the agricultural practice and water consumption in the Sana'a Basin in order to establish a sustainable water resource management. In addition, this study should act as a benchmarking indicator for the success of the Sana'a Basin Water Master Plan and for this purpose will be repeated three times.

Specifically within the project frame an actual map of the irrigation acreage broken-down by crop type (September 2004, February 2005, June 2005), an actual map of the evapo-transpiration (ET<sub>a</sub>) measurements by crop type and an actual map of the net groundwater use were produced.

All products were derived from multi-temporal SPOT 5 and ancillary data (ground truth, meteorological data etc.).

The derivation of crop types and irrigated areas based on the experience of the Land Use/Land Cover processing chains established at GAF. The technical environment was based on COTS image processing software ERDAS IMAGINE including standard automatic image classification routines, on-screen digitizing tools for the manual post-editing and verification tools. For ortho-correction the standard COTS image processing software PCI Geomatics was used.

Two ground truth campaigns were performed which were nearly synchronized with the first and second satellite image acquisition in order to gather in-situ data for calibration and verification of the land use classification.

For calculation of the potential evapo-transpiration ET<sub>o</sub> based on the FAO Penman-Monteith equation the hydrological model PROMET was applied at VISTA. Meteorological measurements and simulations provided daily values of reference evapo-transpiration ET<sub>o</sub> in a spatially distributed way. Depending on the land use, the respective crop coefficients (K<sub>c</sub>) and their evolution with time were ascertained. Using these K<sub>c</sub> coefficients the potential evapo-transpiration can be converted into the crop

evapotranspiration  $ET_c$ , which is valid only for optimum growing conditions without water or nutrient stress.

The actual evapo-transpiration  $ET_a$  was deduced through adapting the standard optimal phenological development, as described in the standard  $K_c$  curves, to the realistic, non-optimum case using the satellite observations. For each crop type separately the fractional vegetation cover was calculated in a spatially distributed way using the SPOT scenes from September, February and June as input. The fractional vegetation cover is used to calculate an adjusted  $K_c$  value, ( $K_{c\_adj}$ ), the factor for deriving the actual evapo-transpiration from  $ET_o$ . For three dates the information on the fractional vegetation cover was obtained from the satellite analyses. These three dates were temporally interpolated using the shape of the standard  $K_c$  curves for each crop type. Thus it was possible to derive spatially distributed maps of  $K_{c\_adj}$  for each day of the year. Multiplying  $ET_o$  with  $K_{c\_adj}$  provided for each day a map of the actual evapo-transpiration ( $ET_a$ ) for each crop type and after summation of all crop types also of the total  $ET_a$ .

One difficulty that had to be overcome was the lack of standard  $K_c$  coefficients for qat in literature. Therefore it was necessary to measure actual evapo-transpiration at a newly implemented micro-meteorological ground station in a qat field in order to derive the crop coefficient  $K_c$  for qat.

A rough estimation of agricultural net ground water use was finally calculated from the difference of effective rainfall and Water Use for Crops. The calculation of the effective rainfall is based on spatially distributed rainfall interpolation, basic assumptions on the infiltration in wadis from surface runoff and infiltration assessments from a simple soil water balance module. The Water Use for Crops results from the  $ET_a$  simulations and takes an irrigation efficiency of 60% for irrigated crops into account.

The total ground water use by agriculture during the investigation period in 2004/2005 was 133 Mio  $m^3$ . This value was obtained from the  $ET_a$  simulation results with an assumed irrigation efficiency of 60% for irrigated crops. The total annual rainfall was 867 Mio  $m^3$ . The total effective rainfall can only be estimated and amounts 8.6 to 27.1 Million  $m^3$  from which 6.2 to 12.8 Million  $m^3$  infiltrated after heavy rainfall events and 2.4 to 14.3 Million  $m^3$  infiltrated in the wadis from surface runoff. This results in a net ground water use by agriculture between 105.6 and 124.2 Mio  $m^3$ . The net ground water use is however not equally distributed in the Sana'a basin. Some wadis show higher net ground water use than others. E.g. Wadi bani Huwat showed the highest negative water balance, i.e. had the highest net ground water use, with  $-30.5$  Mio  $m^3$ .



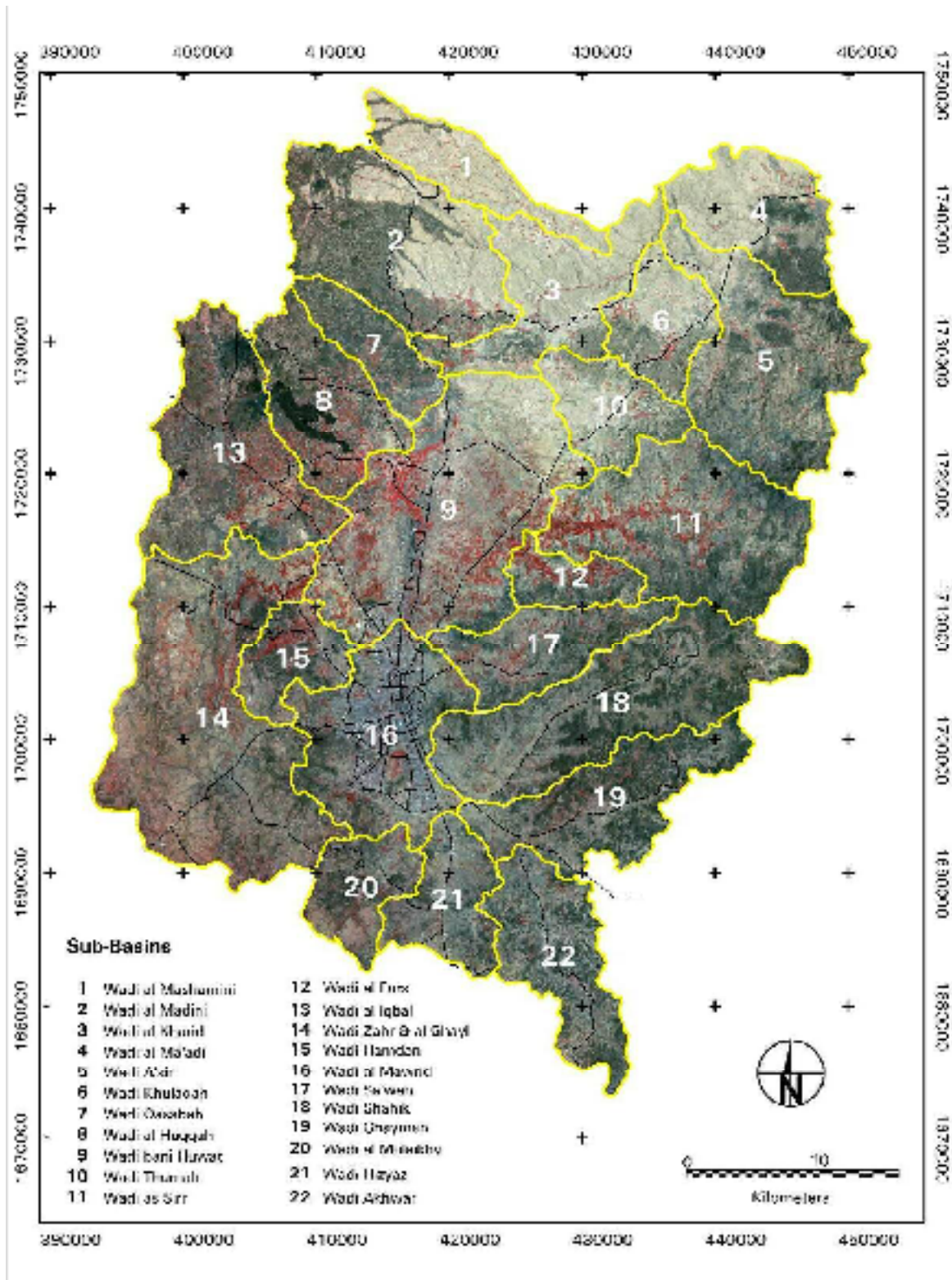


Figure 1: SPOT 5 false-colour image of the Sana'a Basin and its sub-catchments

# 1. Project Identification

Country	Republic of Yemen
Project Name	Sana'a Basin Water Management Project
Loan/Credit	IDA Credit 3774-YEM
Title of Consulting Services	Satellite imagery/data analysis study along with required ground truth work and meteorological monitoring
Client	REPUBLIC OF YEMEN Ministry of Water and Environment Sana'a Basin Water Management Project PROJECT Coordination Unit ( PCU)
Project	SANA'A BASIN WATER MANAGEMENT PROJECT (SBWMP)
RFP	RFP No 2/04 Request for Proposal For Satellite imagery/data analyses study along with required ground truth work and meteorological monitoring
Contract Partner Address	Mr. Mohamed Saad Harmal Director of PCU Sana'a – ROY P. O. Box 11014 Phone : 00967 1 469159/6/7 Mobile: 00967 73218300 Facsimile: 00967 1 469158 E-mail : sbwmp@y.net.ye
MWE	Ministry of Water and Environment
<b>Subcontractors:</b>	
VISTA GmbH	Dr. Heike Bach, General Manager Anton-Ferstl-Str.11 D-82234 Wessling Germany Phone: +49 89 523 89 802 www.vista-geo.de email: Bach@vista-geo.de
Ghayth Aquatech Ltd.	Mr. Mahmoud Al-Udaini, General Manager Harrat Assalam Building # 8 PO box 7219 Sana'a Republic of Yemen Phone: 00967 1 413863 Mobile: 00967 73217777 Fax: 00967 1 412325 email: water-ye@ye.net.ye

## **2. Introduction**

### **2.1 Project Objectives**

#### **2.1.1 General Objectives**

The general objective of the study is to estimate cropped and irrigated areas as well as cropping patterns and evapo-transpiration levels, all of which are important for water balance analysis in the Sana'a Basin.

#### **2.1.2 Specific Objectives**

The specific objectives of the project are:

- Perform advanced remote sensing / satellite imagery studies with comprehensive ground truthing at two points in time
- Estimate cropped and irrigated areas in three seasons
- Identify the cropped areas by crop type (qat, grapes and cereals etc.)
- Determine the classification accuracy by use of ground truth
- Determine actual evapo-transpiration levels for crop types in the basin
- Spatially determine net groundwater use in the basin
- Provide information on all geographic levels: field, catchment area, sub-basin and basin.
- Identify potential recharge enhancement areas by analysis of hydro-geological information
- Prepare maps and reports demonstrating the results of the analyses

### **2.2 Purpose of the Document**

The purpose of this document is to describe the activities and achievements reached in meeting the objectives as set out in the study scope of work. As such, the Draft Final Report gives an overview of all performed activities and highlights any major deviations from the original project plan updated in the Inception Report. It refers to the time period from 10/09/04 up to 14/09/05.

### **2.3 Content of the Document**

This report includes a detailed description of studies performed. It takes into account the project objective, up-to-date results, project deviations and problems encountered.

### **2.4 Referenced Documents**

The following documents are referenced:

- Contract RFP No 2/04, dated 10/09/2004
- GAF Technical and Financial proposal, dated on 21/06/2004
- ToR, IFB "Satellite imagery/data analyses study along with required ground truth work and meteorological monitoring" as part of the "Sana'a Basin Water Management Project", World Bank Credit No. 3774-YEM, RFP No 2/04 Request for Proposal
- Inception Report dated 20/10/2004

- Technical Note 1 (Ground Truth Mission 1) dated on 15/11/2004
- Technical Note 2 (Training Plan) dated on 26/11/2004
- Draft Interim Report dated on 14/01/2005
- Final Interim Report dated on 11/04/2005
- Progress Report 1 dated on 01/06/2005
- Progress Report 2 dated on 01/08/2005
- Draft Final Report Vers. 1.0 dated on 14/09/2005
- Draft Final Report Vers. 1.1 dated on 23/09/2006

## 2.5 Project Background

The Sana'a Basin suffers from rapid and extreme depletion of groundwater, being the only water resource for domestic, industrial and agricultural use. The use of water by far exceeds the natural recharge including irrigation and wastewater return flow, and is inefficient and totally unregulated throughout the Basin. The Sana'a Basin is a highland area of some 3200 km<sup>2</sup> with a population of 1.8 million growing at 7% per annum. About 75% of the population depends wholly on agriculture activity, which mainly comprises qat and fruit growing and livestock rearing.

To tackle this serious water crises, government's Natural Water Resources Authority (NWRA) has started working on a Sana'a Basin Water Master Plan, which helped defining the basis of the phase 1 program of the IDA Sana'a Basin Water Management Project. NWRA is also supposed to implement hydrological monitoring, well inventory and other information collection means needed for basin planning

The key issue is to increase the usable lifetime of the aquifers of the Sana'a Basin – thereby postponing long-distance high-lift import of water and allowing time for a shift to a less water-based economy.

Irrigation is the main water consumption factor in the Sana'a Basin. Therefore, the project aimed to obtain an up-to-date map of the acreage of irrigated crops cultivated in the Sana'a Basin. Also the actual crop evapo-transpiration (ET<sub>a</sub>) in the Sana'a Basin and the net ground water use was determined reflecting the local irrigation practices and local groundwater consumption. Another prioritized activity was to identify possible recharge enhancement areas in the Sana'a Basin because the hydro-geological information as well as hydrological monitoring data are quite limited. Altogether, the project delivered all input data for water balance modelling necessary for a sustainable water resource management.

### 3. Tasks and Methodology

#### 3.1 Key Project Components

As defined in the ToRs and outlined in the Technical Proposal the project consisted of the following key components, discussed in detail in the sections below.

- Data acquisition and pre-processing
- Field survey and ground truth
- Mapping of cropping pattern and irrigated areas
- Actual evapo-transpiration measurement
- Determination of net groundwater use
- Other information analysis
- Training and Know-how transfer

#### 3.2 Data Acquisition and Pre-processing

##### 3.2.1 Data Acquisition

Satellite data to be used in the project were pre-defined in the ToRs. Therefore, the crop by crop irrigation acreage and the digital cropping pattern were derived from multi-temporal/multi-spectral SPOT 5 data (10m) while the hydrological and geological information was mapped on the basis of Landsat ETM data. In addition, one SPOT PAN (2,5m) scene was acquired to derive background information. Beside satellite data a number of ancillary data were acquired necessary for production of the required products. The following tables give an overview of all data acquired in the framework of the project.

Table 1: Satellite data

Satellite Data	Specification	Path/Row	Acquisition Date
Landsat ETM	1 PAN Band (15 m ) 3 VIS Bands (30 m ) 1 NIR Band (30 m ) 2 SWIR Bands (30 m )	166/49	06/01/2000
SPOT 5	1 PAN Band (2,5m) 2 VIS Bands (10m) 1 NIR Band (10m) 1 SWIR Band (10m)	146/318 +60% 146/319 +60%	05/09/2004
SPOT 5	2 VIS Bands (10m) 1 NIR Band (10m) 1 SWIR Band (10m)	146/318 +60% 146/319 +60%	24/02/2005
SPOT 5	2 VIS Bands (10m) 1 NIR Band (10m) 1 SWIR Band (10m)	146/318 +60% 146/319 +60%	13/06/2005
JERS	1 L-Band (12,5 m)	230/274 230/275	07/01/1996
SRTM DEM	C-Band (90 m)		Feb./2000

Table 2: Ancillary data

Other Data	Scale	Date
Geological Map	Robertson 15G 1:250,000	1990
Hydro-geological Map	Robertson 15G 1:250,000	1990
Meteorological Data	rainfall; radiation; humidity, wind speed; NWRA Stations alphanumeric	1974-2004 different quality and information level; some gaps
Watershed boundaries	ArcGIS file	2001
Topographic maps	1:50.000	1979 -1998
SBWMP maps	MS-word print files	2001-2004

### 3.2.2 Pre-processing

#### 3.2.2.1 Ortho-correction

The geometric correction of satellite images is a basic step in acquiring a reliable geometric basis for mapping and overlay procedures, especially for multi-temporal applications using different images over time and GIS analysis.

In order to ensure a proper geometric accuracy necessary for this project, ground control points (GCPs) were collected with a GPS device during the ground truth mission 1 in October 2004. The GPS measurements were made using a Garmin GPS12xl. The accuracy of the measurements is given as an EPE (estimated position error) by the device. The EPE is a measurement of the horizontal positioning error in meters, based upon several factors including dilution of precision (DOP) and satellite signal quality. A minimum of 50% of the measurements from the Garmin device are within this given range. All measurements in the field were equal to or better than 5m EPE.

The GPS measurements described above were made on objects which could be clearly identified in the images. These Ground Control Points (GCPs) were fed into the geometric processing for the geo-referencing and ortho-correction of the highest resolution imagery SPOT PAN, with 2.5m synthetic GSD. Subsequently, all multi-spectral XI-scenes with 10m GSD were geo-referenced using the same GPS points and GCPs identifying the same object as in the Pan imagery. This led to a co-registration of the SPOT PAN and XI-bands of three different acquisition dates to match the same geometry.

After geo-referencing the images were ortho-corrected using PCI Geomatica 9.1 Ortho Engine. For the ortho-correction the SRTM 3" (90m resolution) digital elevation model (DEM) was used. This is a degraded product from the original 1" DEM data (30m resolution) which has a horizontal accuracy of 20m and a height accuracy of 16m. After ortho-correction the PAN and XI data (1<sup>st</sup> SPOT data set) were merged for the mapping basis. The XI-images were used for the classification.

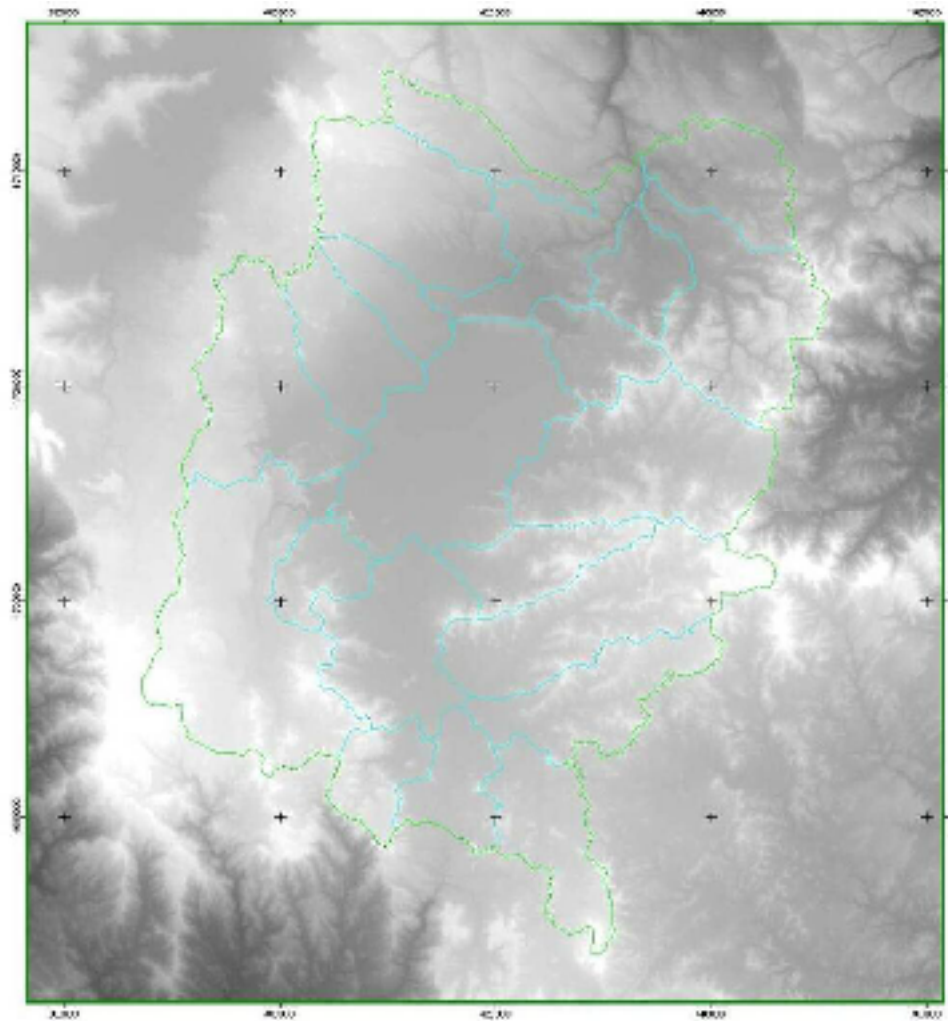


Figure 2: SRTM 90m DEM of Sana'a Basin and perimeter

### 3.2.2.2 Radiometric Correction

The correction of atmospheric and illumination effects in the satellite images is a required processing step for change detection and analysis of multi-temporal imagery because, especially in mountainous regions, the irradiance conditions vary strongly depending on the slope and aspect of each pixel.

For this radiometric correction of the SPOT 5 imageries the atmospheric correction procedure MODREF, developed at VISTA, was used.

MODREF models the irradiance of each pixel depending on topographic information (elevation, slope, local solar incidence angle), atmospheric information (visibility or radiosonde profile) and sensor information (time of acquisition, observation geometry, spectral band). Changing atmospheric conditions are taken into consideration, depending on elevation and the different illumination of each pixel, which is determined by the local solar incidence angle and terrain irradiance. The total signal measured by a sensor is modelled as 4 components, as illustrated in fig. 4, and described in the following equation. This allows for consideration of the variation of direct and diffuse irradiance, as well as the terrain irradiance and the path radiance for each pixel. The results of this atmospheric correction are surface reflectance values for each spectral band.

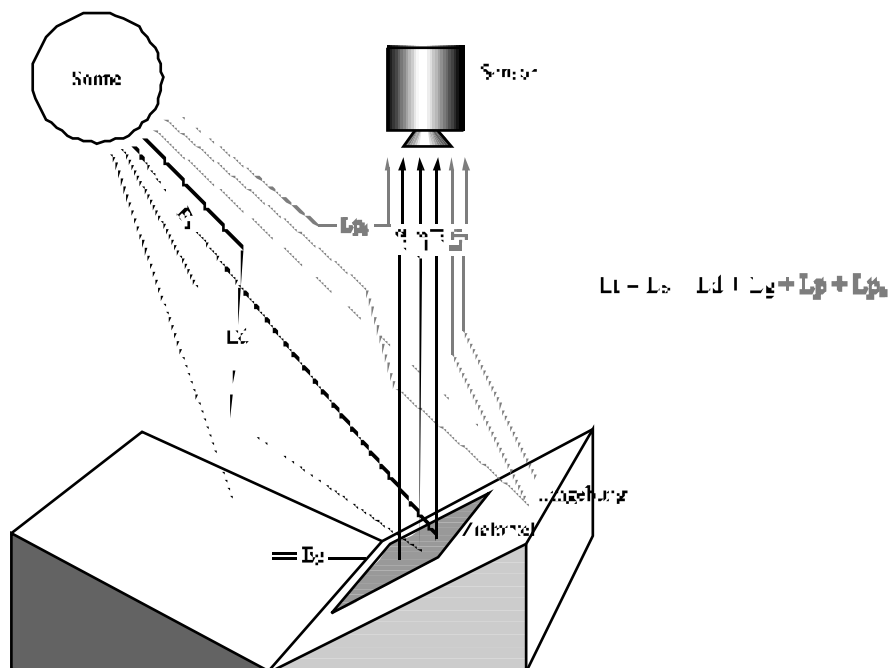


Figure 3: Radiance components affecting the measured signal at a satellite for non flat surfaces

$$L_{total} = L_s \frac{\sin(sz) \sin(s) \cos(az_{rel}) + \cos(sz) \cos(s)}{\cos(sz)} \quad \text{(direct irradiance component) (1)}$$

$$+ L_d \frac{1 + \cos(s)}{2} \quad \text{(diffuse irradiance component)}$$

$$+ (L_d + L_s) \left[ 1 - \frac{1 + \cos(s)}{2} \right] \quad \text{(terrain irradiance component)}$$

$$+ L_p + L_{p0} \quad \text{(path radiance component)}$$

where:

- $L_{total}$  = total irradiance over an inclined surface
- $L_s$  = direct irradiance over a horizontal surface
- $L_d$  = diffuse irradiance over a horizontal surface
- $L_p + L_{p0}$  = path radiance reaching a sensor
- $sz$  = solar zenith angle
- $s$  = slope of pixel
- $az_{rel}$  = relative azimuth between sun and sensor

The horizontal visibility parametrizes the optical depth of the atmosphere. It is a function also of aerosol content and varies with elevation. For a proper atmospheric correction in mountainous areas the consideration of the influence of the vertical change of the optical depth is crucial. In order to allow for this, an increase in the horizontal visibility with increasing elevation was incorporated into the radiative transfer modelling of the atmosphere. This incorporation results in a spectrally dependent decrease of path radiance and diffuse irradiance ( $L_p + L_{p0}$ ,  $L_d$ ) with decreasing elevation, while the direct irradiance ( $L_s$ ) increases over high mountainous areas.

Using the radiative transfer calculations, based on the MODTRAN code, the image data are atmospherically corrected and “normalised” to simulate flat terrain



conditions. Figure 6 shows the resulting SPOT scene from 5th Sep 2004, where illumination effects (illustrated in Fig. 5) have been reduced as much as possible. Band 1, 2 and 3 (green, red and near infrared) were selected for illustration.

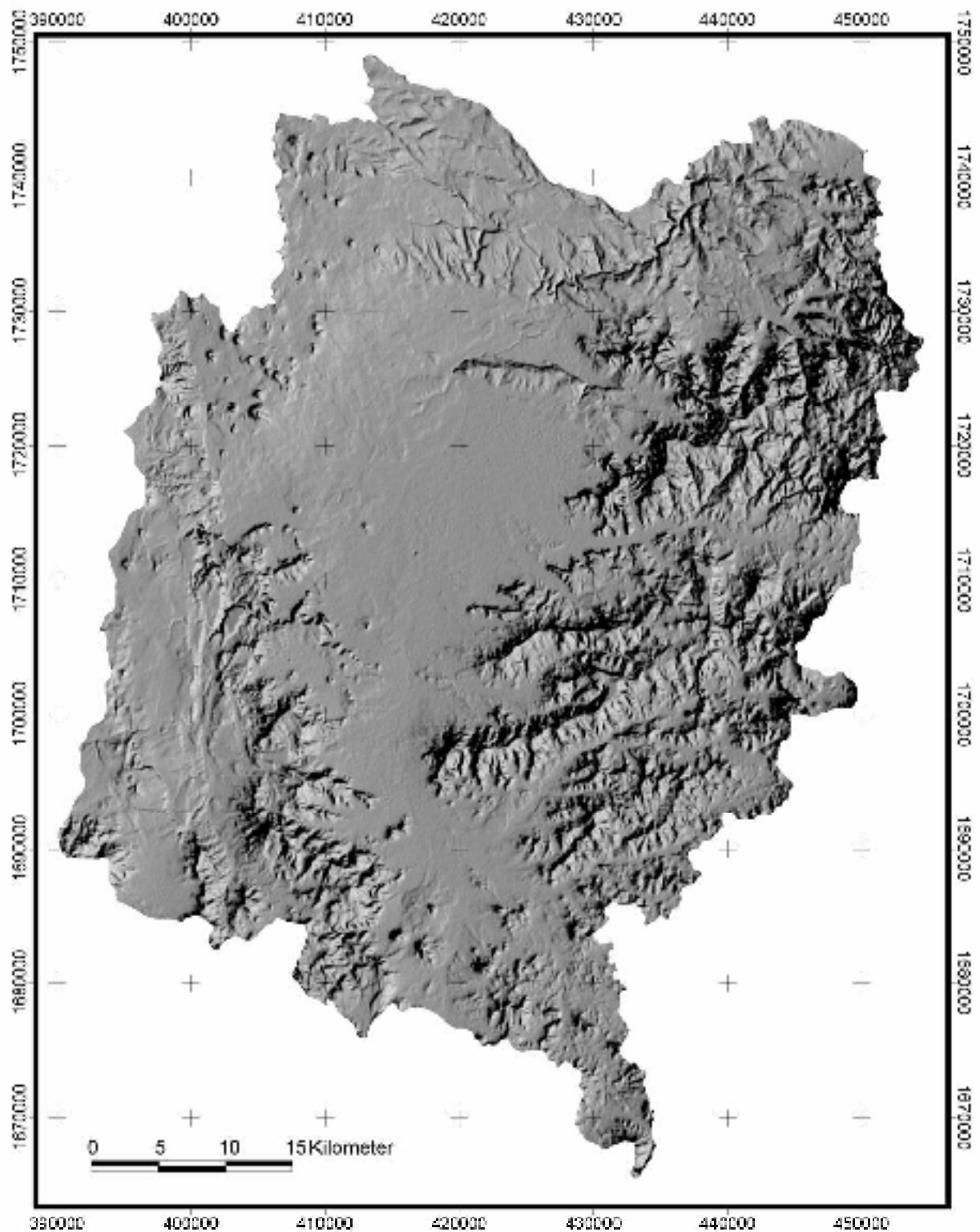


Figure 4: Local solar direct irradiance (Ls) for the time of the SPOT 5 acquisition in the Sana'a basin

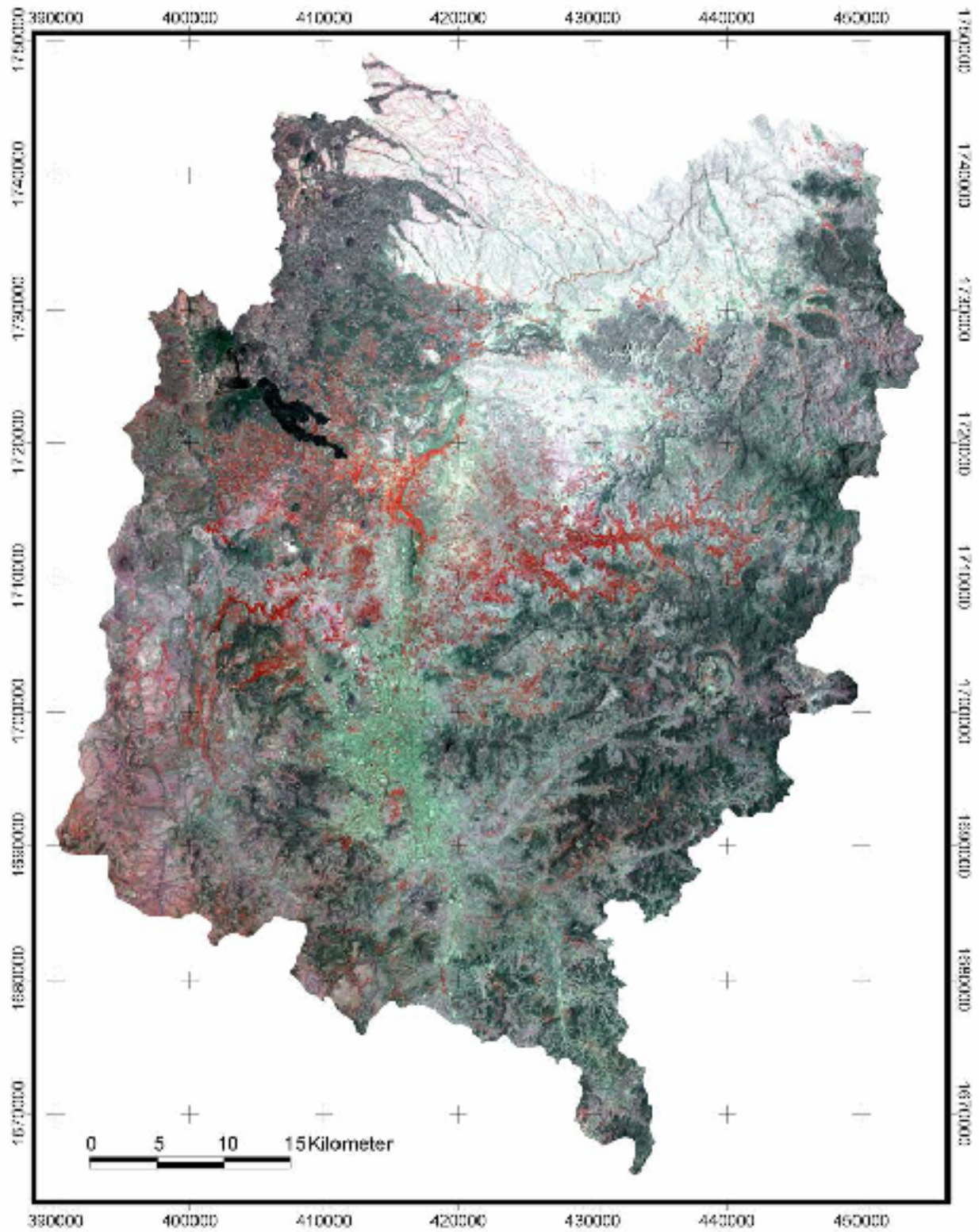


Figure 5: Atmospherically corrected SPOT image of the Sana'a basin from 5<sup>th</sup> Sep. 2004 (green, red, NIR)

### 3.3 Field Survey and Ground Truth

#### 3.3.1 Ground Truth

For calibration and verification of the satellite imagery derived cropping pattern, two ground truth campaigns were performed during the project. Both campaigns were nearly synchronized with satellite overpasses and acquisitions and executed in October 9 – 21, 2004 and February 7 - 22, 2005.

During the first mission to Yemen in addition GCPs were collected for the geometric correction of the image data. The GCPs were measured with a Garmin GPS 12 in the field. About 58 objects were identified in the images which could easily be seen in the SPOT XI and the PAN bands. These objects appear easy to access in the field and ensure avoidance of military installations.

For planning and realization of the ground truth campaigns the first SPOT image data were used. To get a rough figure of the cropped area in the Sana'a basin a NDVI mask was calculated and a qualitative threshold visually fixed. About 30,000ha of active vegetation was found. Following the specifications (JRC IPSC/G03/P/HKE/hke D(2004)(3486)) of the JRC (EU Directorate General Joint Research Center) for sampling in agricultural areas for crop interpretation, about 300 agricultural parcels were sampled during the first mission and 400 during the second mission to Yemen, distributed over all sub-basins. Transects were driven through the whole Sana'a basin, in order to cover all crops of interest that occur. The predominant crop was qat followed by grapes, cereals, fruit trees vegetables and alfalfa. For the "qat" crop type the density height pattern and irrigation features were also collected.

During the fields surveys two counterparts from NWRA/SBWMP joined partly the field team for on-the-job training.

In detail the following crops were sampled in the field:

- Qat
- Grapes
- Fruit trees
- Cereals (predominantly maize, barley)
- Vegetables (predominantly tomatoes, onions)
- Alfalfa
- Shrub land

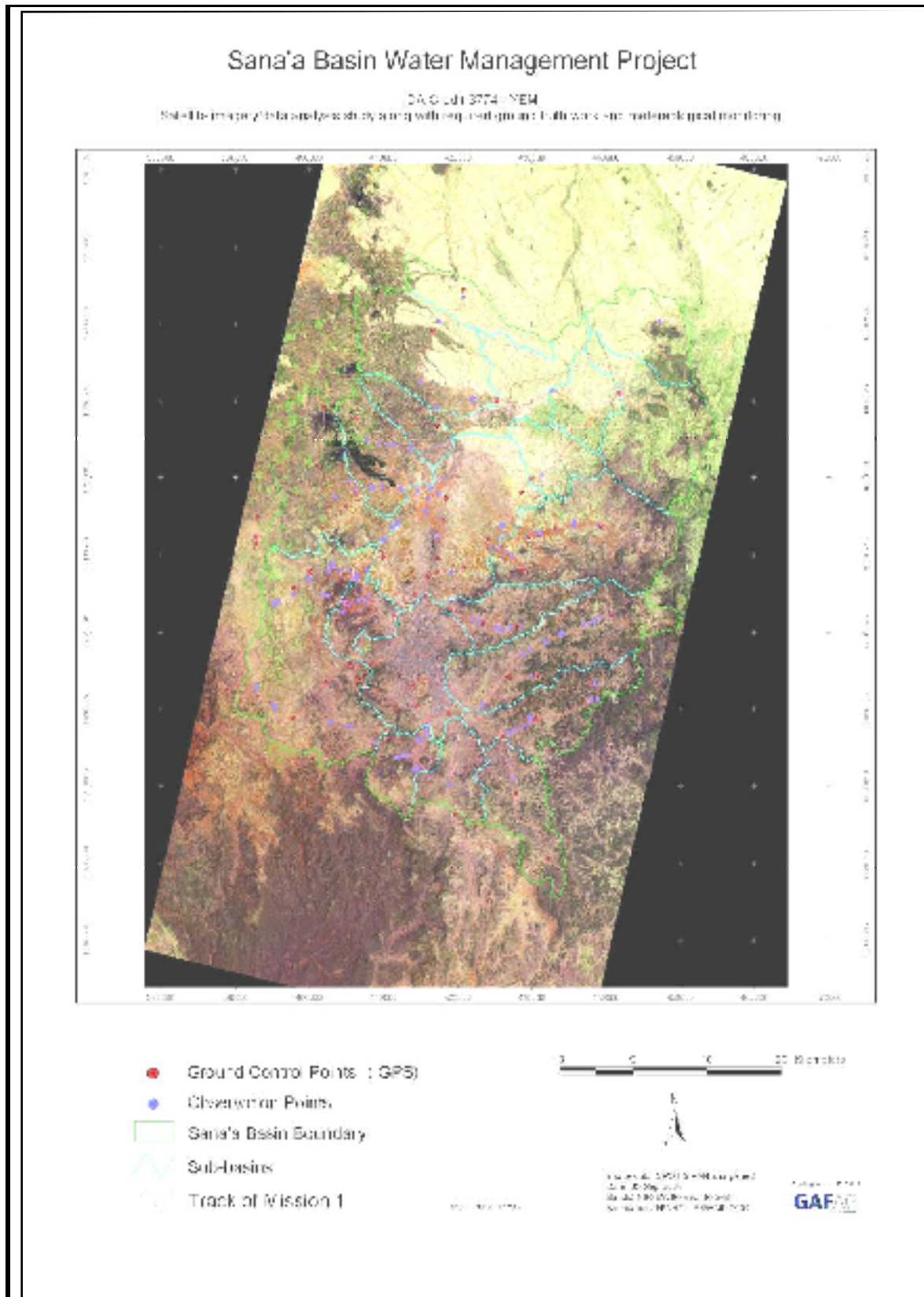


Figure 6: Ground truth track and sample points in the Sana'a Basin and sub-basins, mission 1



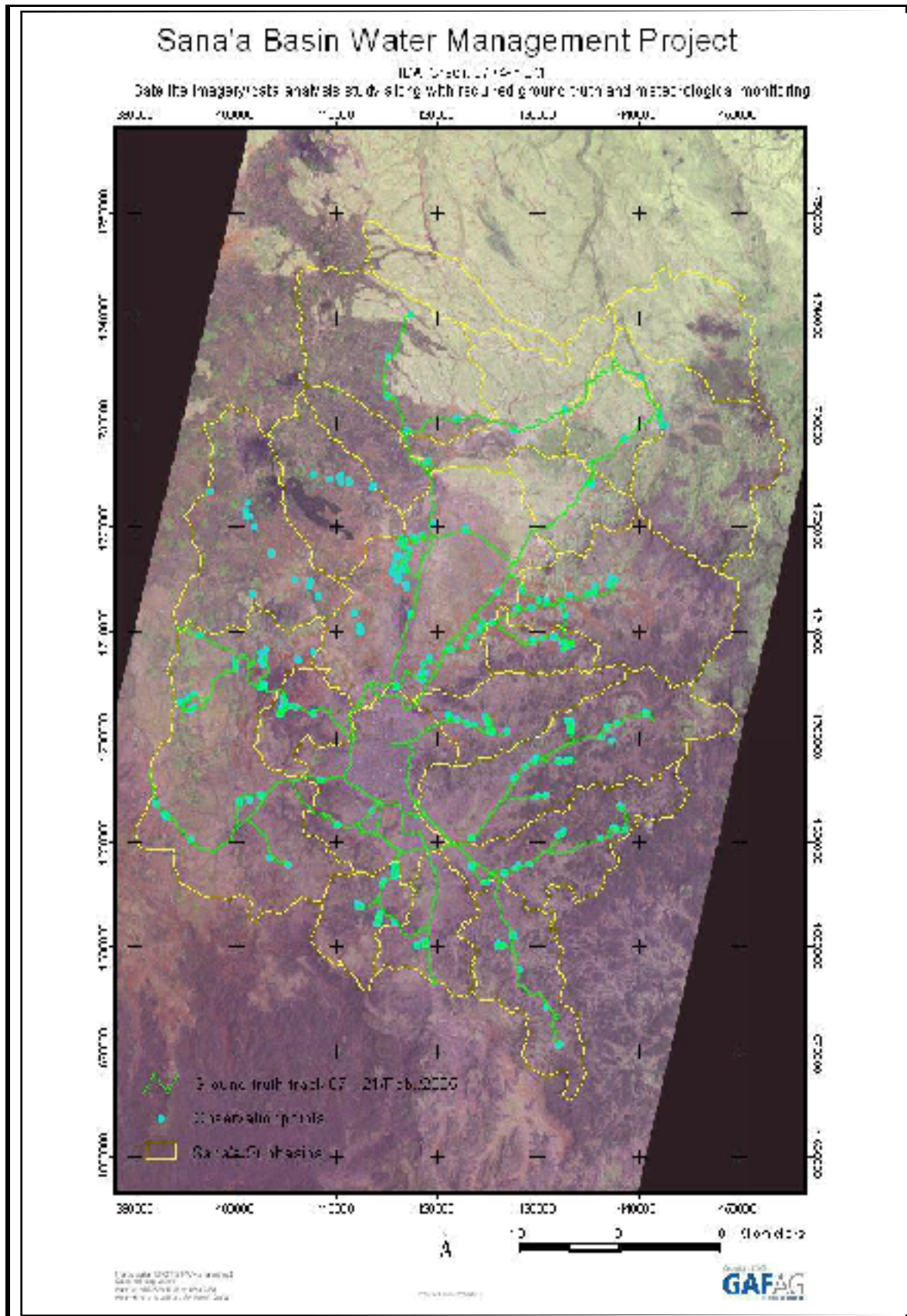


Figure 7: Ground truth track and sample points in the Sana'a Basin and sub-basins, mission 2

### 3.3.2 Field Survey

As stipulated in the Technical Proposal a two-week geological field survey was performed to verify geological data analysis and calibrate the lithospectral and geomorphological interpretation.

The field team consisted of (participation see chapter 3.9)

Mr. **Ulrich Steiner** (GAF) – Remote Sensing Geologist  
Mr. **Abdul Aziz** Al Arika(Gyath) - Hydrogeologist  
Mr. **Abdullah Abdulwahid Saif Al-Adimi** - Geologist  
Mr. **Nabil A. Qader** – GIS Expert

The specific objective of this short term field survey was to visit previously selected locations and to collect general hydrogeological, geological and geomorphological ground information which was regarded as significant for a area wide mapping. It turned out during the on-site mission that the geological field knowledge available through the local experts was inadequate concerning a detailed lithostratigraphical legend as it is required for a 1:50 000 map. Additionally some areas were due to security reasons in the NE of the Sanaa basin no accessible.

For the survey the geological field mapping software “GeoRover” was used, running on a field laptop with an online GPS connection to navigate and to localize the onsite position on-screen.

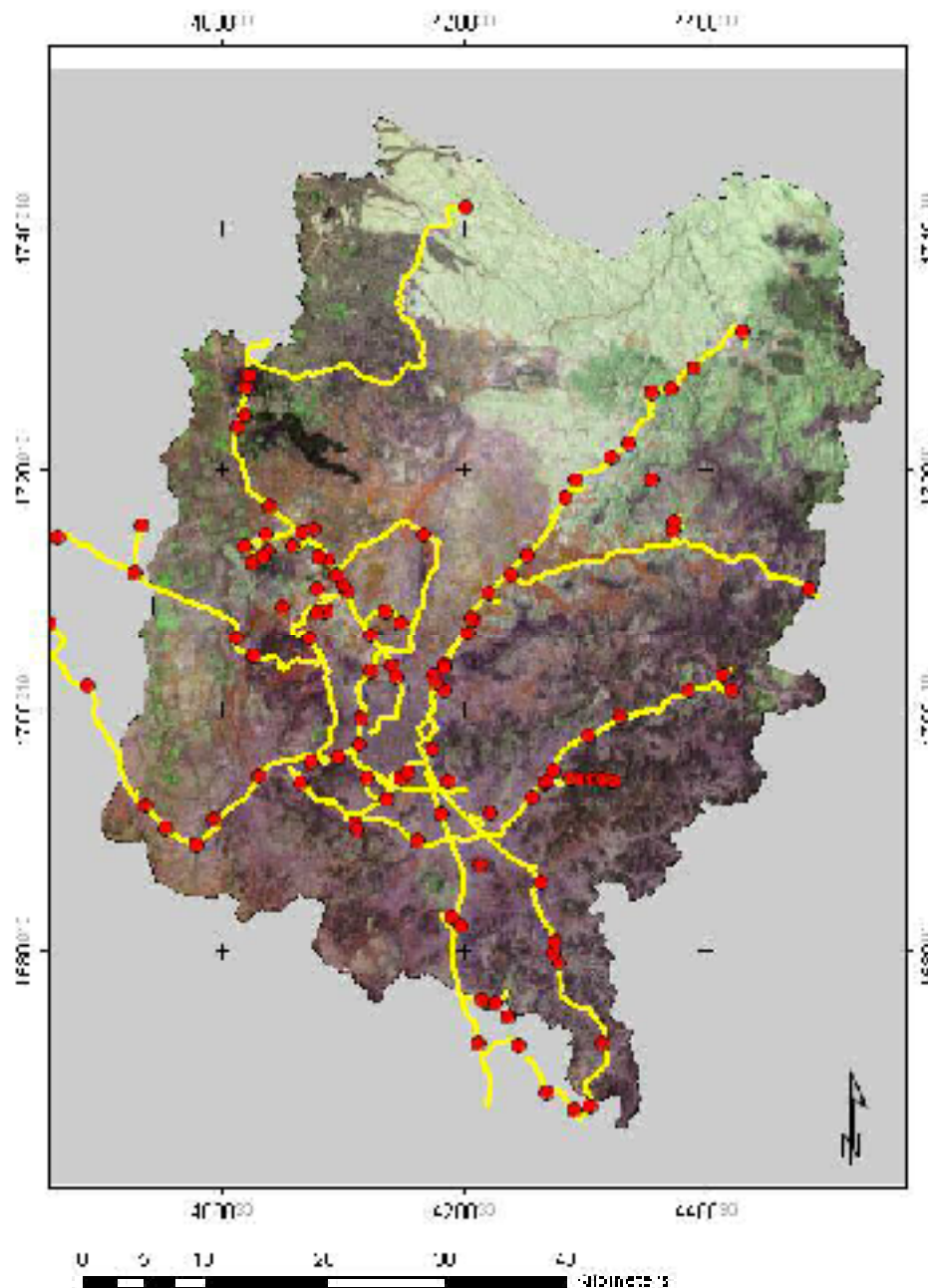


Figure 8: GPS track (yellow) and observation points (red) surveyed during the GAF geological ground truthing campaign in 2004

The following items are compiled as the most relevant field observations for the study objective:

- Tawilah sandstone shows a pink to purple colour in Landsat 741 band composite and its spatial extension is less than indicated in reference geological maps. The sandstone often forms steep escarpments with slope foets with low infiltration potential due to rapid surface runoff
- The overlying basal basalt caps bigger parts of Tawilah Sandstone, so they stretch more over the Tawilah than indicated in the reference geological maps. In close contact to the Tawilah it is of bright blue to blue color in the 741 composite.
- The Yemen Volcanic Group are very heterogeneous and it was not possible to separate stratigraphical subdivisions/members in the outcrop based on the



available knowledge in the field. The whole Tertiary Yemen Volcanic Group was assigned in the field as Trapp Basalts based on the fact that further, detailed local geological field knowledge was not available for this specific study. The subdivision in different submembers was done later in the office, based on the available literature, map and remotely sensed data (lithospectral and textural image properties as well as morphology).

- Quaternary basalts: the youngest basalts are relatively easy to identify due to the fact that they are often in vicinity to a volcanic cone. The older quaternary volcanics get the more difficult it is to differentiate them lithologically from Tertiary volcanics.
- Alluvium is assumed to be widespread in the central Sana'a basin plain and the surrounding wadis. Arable soils and loess covers the Alluvium in patches. It is generally hard to distinguish loess from beds with strata of finer material in the Alluvium. The loess cover and strata of fine material reduce the infiltration properties of the Alluvium.

Fractures in the Amran and Tawilah units can easily be verified in the field, but in the Tertiary and Neogene volcanics structural features are badly expressed and their verification in the field is very limited.



*Figure 9 - Left: Slope foot of the Tawilah sandstone with a fracture. In the front alluvium with arable land. Right: Road cut outcrop showing stratified alluvium.*



### 3.4 Irrigated Areas and Cropping Pattern

The derivation of irrigation acreage and cropping pattern is based on SPOT 5 imageries with a spatial resolution of 10m from September 2004, February 2005 and June 2005. The use of multi-temporal satellite data was strongly required to delineate the inventory of the land use of the Sana'a Basin in general and the irrigation area in particular. Especially the differentiation of the perennial crop types like qat, grape and fruit trees which are semi-dormant in the winter season, have demanded the use of multi-temporal data to cover the different phenological cycles.

For calibration and verification of the classification a SPOT 5 MS/PAN merge with a spatial resolution of 2,5m together with the ground truth data were used.

#### 3.4.1 Irrigated Areas

##### 3.4.1.1 Introduction

Generally, it can be assumed that under the prevailing climatic conditions in the Sana'a Basin nearly all vegetation cover is irrigated. Therefore, vegetated areas, detected in the satellite images are nearly identical with the irrigation acreage. However, rainfall prior to a satellite image acquisition can falsify this general picture because the presence of natural vegetation and green rain fed crops will also be classified as "irrigated areas" which results in an overestimation of the irrigation acreage. This is the case e.g. for the September 2004 SPOT 5 scene.

In addition, it should be mentioned that irrigation acreage derived from satellite images and evapo-transpiration measures record the current status of the vegetation and do not consider that some parcels are only partly cultivated or just harvested. Therefore, census data based on field surveys or cadastral data representing the irrigation acreage by parcel or ownership boundaries give always higher values than data derived from satellite.

Therefore, the classification of the irrigation acreage was based on a two step approach:

- In a first step a vegetation / non-vegetation mask was generated using the NDVI of all SPOT 5 acquisition dates. This derived vegetation acreage, outlining all pixels in the images having a fraction of vegetation cover, still includes natural vegetation and rain fed crops resulting in an overestimation of the irrigation acreage.
- To derive the real **acreage irrigated by groundwater** natural vegetation and rainfed crops had to be excluded from the general vegetation acreage. Because a spectral discrimination of the class "natural vegetation/rain fed crops" from "irrigated crops" is per se not possible, the vegetation acreage was merged with the actual evapo-transpiration map under consideration that evapo-transpiration levels higher than 240 mm/sqm corresponding to longtime average rainfall over the last years are irrigated by groundwater.

### 3.4.1.2 Technique

#### Normalised Difference Vegetation Index NDVI

The spectral signature of healthy vegetation generally shows a strong increase in the reflectance at 0.7  $\mu\text{m}$  (Fig. 10), while bare soils or outcrops feature a more continuous, linear characteristic. The more active the chlorophyll of the plants is, the more largely is the rise of the reflection degree in the near infrared (NIR).

Apart from the distinction of the vegetation from other objects thus the strength and vitality of vegetation can be derived. This circumstance is used with the computation of the NDVI:

$$\text{NDVI} = (\text{NIR} - \text{RED}) / (\text{NIR} + \text{RED})$$

The NDVI forms a measure for the photo-synthetic activity and is strongly correlated with density and vitality of the vegetation covering. The standardisation (by quotient formation) reduces topographic and atmospheric effects and increases the differences in the reflectance of different surfaces in the RED and NIR range of the electromagnetic spectra.

Figure 11 demonstrates schematically the nearly linear correlation between NDVI values and density of vegetation cover. Only in the upper and lower parts this linearity is not warranted. To define the lower NDVI threshold for the discrimination of vegetation and non vegetated areas, the NDVI response of pixels known to have no green crop fraction at the time of image acquisition (outcrops, urban areas etc.) were determined.

For determination of the ETa, in addition, the fraction of vegetation within each pixel of the irrigated areas was investigated using spectral unmixing techniques.

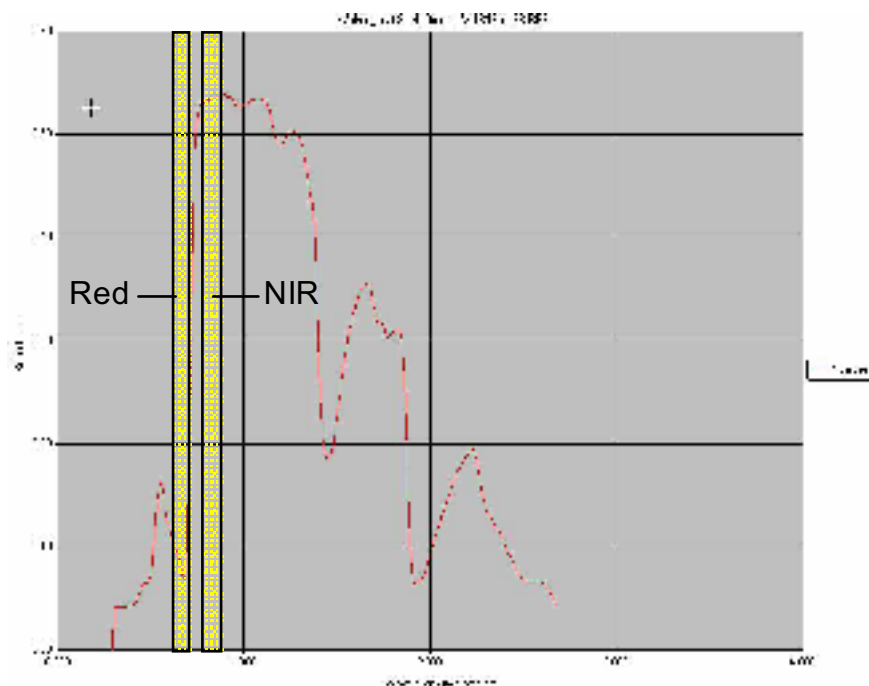


Figure 10: Spectra of healthy vegetation with the abrupt rise of the reflectance in the NIR; RED and NIR channels of SPOT 5

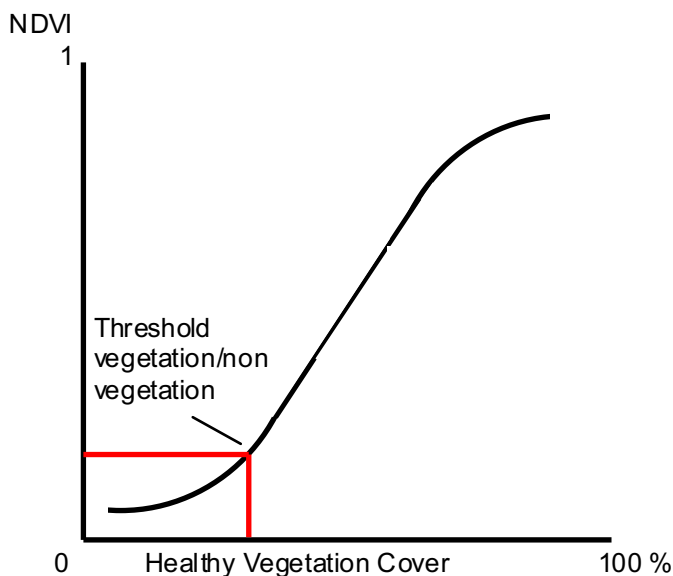


Figure 11: Schematic representation of the correlation between NDVI and healthy vegetation cover

### 3.4.2 Cropping Pattern

#### 3.4.2.1 Introduction

Image classification is the process of creating thematic maps from satellite imagery. A thematic map is an informational representation of an image which shows the spatial distribution of a particular theme. Themes can be as diversified as their areas of interest.

Digital image classification uses the spectral information represented by the digital numbers in one or more spectral bands, and attempts to classify each individual pixel based on this spectral information. This type of classification is termed spectral pattern recognition. In either case, the objective is to assign all pixels in the image to particular classes or themes (e.g. water, coniferous forest, deciduous forest, corn, wheat, etc.). The resulting classified image is comprised of a mosaic of pixels, each of which belong to a particular theme, and is essentially a thematic "map" of the original image.

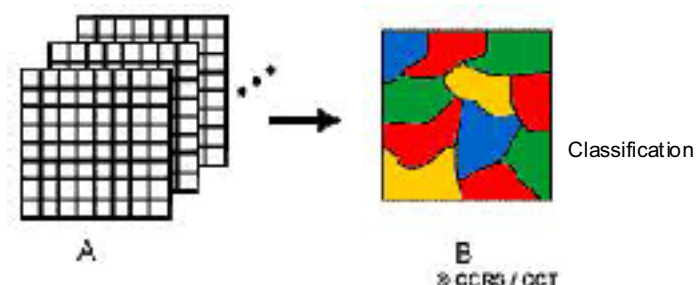


Figure 12: Schematic process of creating thematic maps by logical pixel grouping

When talking about classes, it is necessary to distinguish between information classes and spectral classes. Information classes are those categories of interest that the analyst is actually trying to identify in the imagery, such as different kinds of crops, different forest types or tree species, different geologic units or rock types, etc.

Spectral classes are groups of pixels that are uniform (or near-similar) with respect to their brightness values in the different spectral channels of the data. The objective is to match the spectral classes in the data to the information classes of interest. Rarely is there a simple one-to-one match between these two types of classes. Rather, unique spectral classes may appear which do not necessarily correspond to any information class of particular use or interest to the analyst. Alternatively, a broad information class (e.g. qat) may contain a number of spectral sub-classes with unique spectral variations. Using the qat example, spectral sub-classes may be due to variations in age, species, and density, or perhaps as a result of shadowing or variations in scene illumination.

Common classification procedures can be broken down into two broad subdivisions based on the method used:

- Supervised classification
- Unsupervised classification

In a supervised classification, the analyst identifies in the imagery homogeneous representative samples of the different surface cover types (information classes) of interest. These samples are referred to as training areas. The selection of appropriate training areas is based on the analyst's familiarity with the geographical area and their knowledge of the actual surface cover types present in the image. Thus, the analyst is "supervising" the categorization of a set of specific classes. The numerical information in all spectral bands for the pixels comprising these areas are used to "train" the computer to recognize spectrally similar areas for each class. The computer uses a special program or algorithm (of which there are several variations), to determine the numerical "signatures" for each training class. Once the computer has determined the signatures for each class, each pixel in the image is compared to these signatures and labeled as the class it most closely "resembles" digitally. Thus, in a supervised classification we are first identifying the information classes which are then used to determine the spectral classes which represent them.

Unsupervised classification in essence reverses the supervised classification process. Spectral classes are grouped first, based solely on the numerical information in the data, and are then matched by the analyst to information classes (if possible). Programs, called clustering algorithms, are used to determine the natural (statistical) groupings or structures in the data. Usually, the analyst specifies how many groups or clusters are to be looked for in the data. In addition to specifying the desired number of classes, the analyst may also specify parameters related to the separation distance among the clusters and the variation within each cluster. The final result of this iterative clustering process may result in some clusters that the analyst will want to subsequently combine, or clusters that should be broken down further - each of these requiring a further application of the clustering algorithm. Thus, unsupervised classification is not completely without human intervention. However, it does not start with a pre-determined set of classes as in a supervised classification.

Both techniques, supervised and unsupervised classification were used for the analysis of agricultural land use in the Sana'a Basin.

After several tests classifications the following approach was chosen due to our experience in other similar geographic regions and the best combination of supervised and unsupervised classification. In a first step the unsupervised

classification was used to obtain a basic set of classes from the signatures of SPOT 5 image data. The automatically derived classes are then assigned to the classes found in the field and utilized for the task using a supervised reclassification. If necessary, classes were clustered together.

The SPOT-PAN data were not included in the classification approach because the texture would become too dominant, due to the very high resolution which leads to a degradation of the classification result.

### 3.4.2.2 Approach

Principally the derivation of crop types and irrigated areas based upon the experience of the Land Use/Land Cover processing chains established at GAF. The applied method involved the compilation of land coverage mapping from satellite imagery using an optimised and multi-step processing strategy and is based on the utilisation of multi-temporal data. Figure 13 gives an overview about the general workflow for the derivation of the land use classes respectively the cropping pattern.

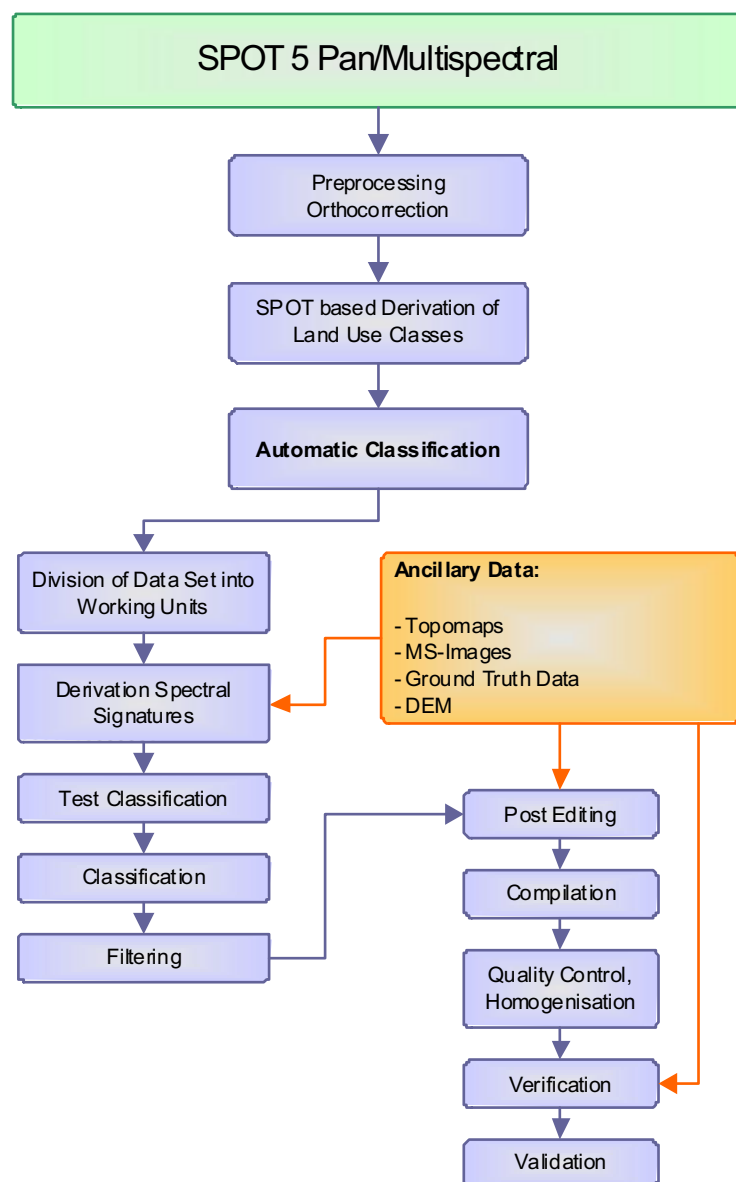


Figure 13: Processing workflow

## **Input**

The final classification is based on the radiometric corrected, multi-temporal SPOT XI images of the three acquisition dates (Sept. 2004, Feb. 2005 and June 2007). These XI images were mosaiced during the radiometric processing and the Sana'a basin was extracted as an AOI for classification.

## **Masking**

In a first step a vegetation/non vegetation mask was generated from the NDVI images of each SPOT 5 acquisition data (chapter 2.4.1) and finally added up. The result is a vegetation layer representing only those parts of the image having fractional vegetation cover.

## **Splitting into Image Strata**

Due to differences in the appearance of the different landscape units causing a high variance in the spectral signatures the vegetation layer was split into different image strata which were then classified separately. Later on, the classified image strata were merged again to one vegetation layer broken down by crop type.

## **Classification**

Several multi-spectral classifiers exist in the literature and have been tested. Finally, in this approach the spectral distance classifier was used. This classifying approach uses the spectral distance and classifies the classes iteratively, then redefines the criteria for each class and classifies again so that the spectral distance patterns in the data gradually emerge. This process was repeated until either a maximum number of iterations have been performed, or a maximum percentage of unchanged pixel assignments have been reached between two iterations. The result of this unsupervised classification consisted of a thematic raster layer and a specific signature file consisting of 55 to 65 classes in the three strata.

The supervised part of the classification was finally the assignment of these individual spectral classes to the final defined crop / land use class interpreted in various parts of the images. This calibration was done on the base of the SPOT Multi-spectral/PAN merges together with the ground truth information.

## **Technical Environment for the Development, Integration, Testing, Validation and Operation**

The technical environment for the development of the Cropping Pattern Maps was the standard COTS image processing Software ERDAS IMAGINE. It includes all standard automatic image classification routines and on-screen digitizing tools for the manual post-editing. In addition, ERDAS IMAGINE includes verification tools.

## 3.5 ETa Measurement

### 3.5.1 Specification of Ground Equipment for Measuring ETa

In close cooperation with VISTA GmbH, responsible for meteorological measurements, the ground equipment for measuring actual evapo-transpiration  $ET_a$  has been specified. This has been done in accordance with the Technical Proposal, project demands and the proposed methodology.

As proposed in the Technical Proposal, the Modified Bowen Ratio Station is specified as follows and includes:

- two special Frankenberger psychrometers for measuring the temperature and air humidity at two height levels,
- a 3D-sonic anemometer.
- a precipitation pulse transmitter,
- two heat flux plates,
- a pyranometer to allow the calculation of the complete energy and water fluxes,
- a soil moisture measurement using a equitensiometer,
- a 6m adjustable aluminium mast with stainless steel guys for support,
- a data logger stores the measurements on a standard PC card,
- solar panels are used as power supply.

An overview of the specified MBR station is given in ANNEX A of this report.

### 3.5.2 Procurement and Transport of Ground Equipment for Measuring ETa

On October 18, 2004 the specified "Modified Bowen Ratio Station" was ordered at Theodor Friedrichs & Co .GmbH, Germany. The meteo-equipment was shipped on December 18, 2004 to Ghayth Aquatech Ltd. The meteo-station was implemented and installed during the second mission to Sana'a, Yemen, scheduled on February, 2005.

### 3.5.3 Identification of Suitable Sites for Meteo-equipment

During the first mission to Sana'a, Yemen, from October 9 – 21 2004, the first ground truth work was performed. In addition, one goal of this mission was the identification of a suitable site for the meteo-equipment. The main criteria for the placement of the meteo-equipment were as follows:

- The installation had to be implemented in a suitable place in a well kept qat stand. A limiting factor is the height of the qat trees because the installation is 6m high and should reach beyond the branches.
- The situation for the land owner and SBWMP should be stable and reliable. It was therefore beneficial that the farmer who owns the land was personally known to the local partner of GAF, Mr. Mahmoud Al-Udaini of Ghayth Aquatech. The farmer had to be assured that no damage will happen to his plants and supported the installation of the meteo-equipment wholeheartedly.
- The security of the station was ensured through the facts mentioned above and the existence of two bigger roads and a fence around the parcel. The station was obscured by surrounding qat and other trees.



- Easy access was given due to the proximity of the parcel to Sana'a (about 30mins drive) which was important for the maintenance and the regular data download from the installation.

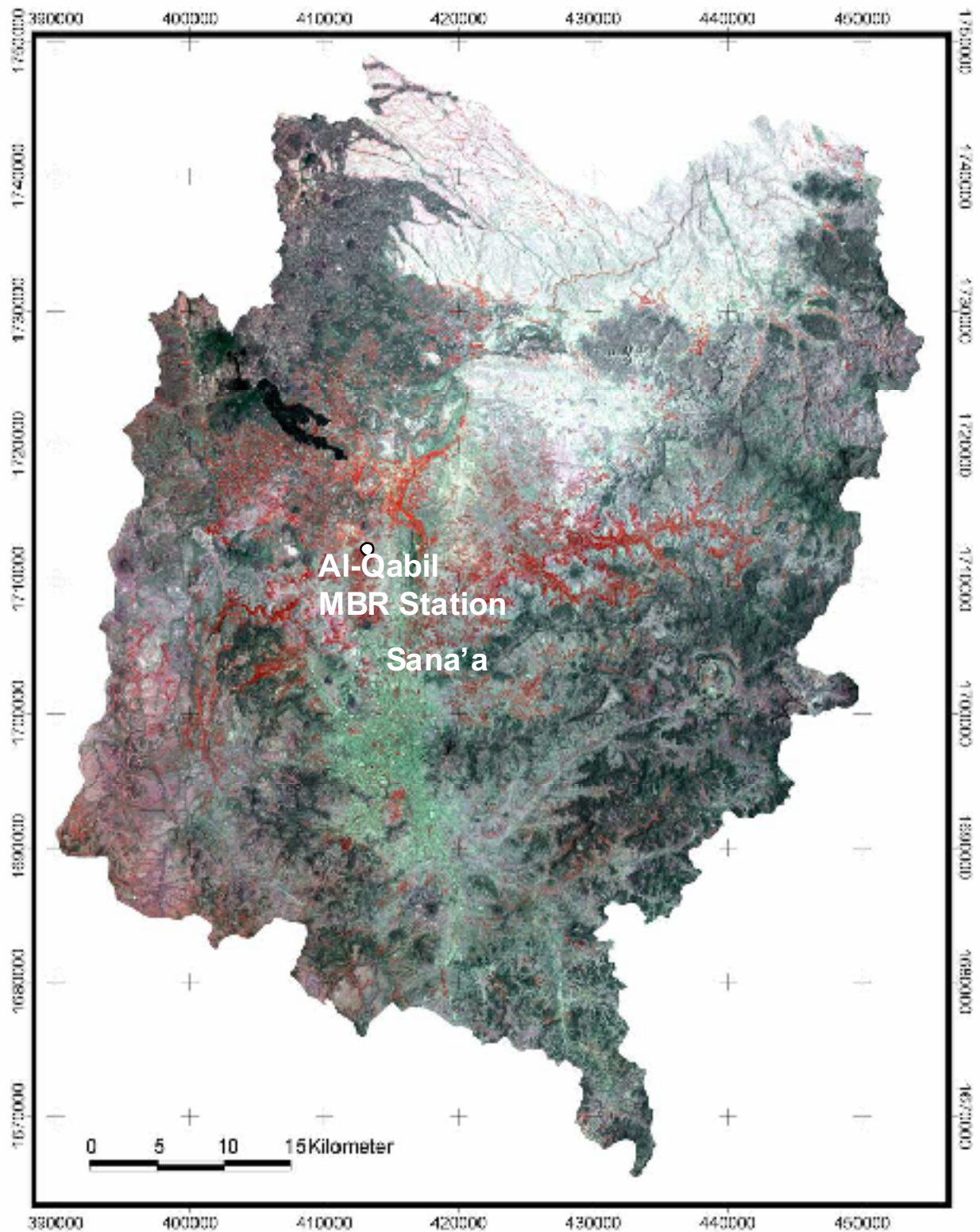


Figure 14: SPOT 5 Image with location of the MBR Station



### 3.5.4 Installation of the MBR Station

The Modified Bowen Ratio (MBR) station was installed during 9th and 10th of February 2005 with technical and personnel support provided by NWRA and the Sana'a branch. Since then it provides valuable data with some data failures however. Fig. 15 shows the station after installation at Al-Qabil. It is situated in the centre of a qat field. The qat leaves were just harvested a few weeks before the installation. Thus installing the station without destroying the plants was easier.



Figure 15: Micrometeorological Modified Bowen Ratio station (MBR station) after installation at Al-Qabil on 10th Feb. 2005 (Photo: W. Kaspari)

The MBR station is equipped with an ultrasonic anemometer, sensors for temperature, humidity and net radiation, two soil heat flux plates, a tensiometer and an automatic rain gauge. The data logger, a 6m tower and a solar power supplier complement the system. The two levels for temperature and humidity measurements are installed at 2 and 5m respectively. The temporal resolution of the stored measurements is 20 minutes.

The Modified Bowen Ratio method allows measuring the sensible heat flux and the latent heat flux using the eddy covariance method and the Bowen ratio similarity. For the MBR, a measurement system uses a sonic anemometer together with two level dry- and wet- temperatures to obtain sensible and latent heat fluxes. Because the classical Bowen ratio/energy balance method (BREB) is mainly influenced by the 'non-closed' surface energy balance, the MBR method uses the benefits of eddy covariance and BREB. In this method sensible and latent heat fluxes are determined without using the surface energy balance equation and therefore net radiation measurements. Results found in literature (Liu and Foken, 2001) and error analysis showed that the MBR can achieve more accurate results than BREB. It is however also possible to use the classical Bowen Ratio method with the data provided.

### 3.6 Calculating Spatial Distributions of ET<sub>a</sub> from Satellite Data and Meteo-data

This chapter describes the methodology for actual evapo-transpiration mapping, the required meteorological measurements and its application to the Sana'a basin. Another key aspect will be the utilisation of the satellite data in the ET<sub>a</sub> calculations.

#### 3.6.1 General Concept for Deriving the ET<sub>a</sub>

The methodology is based on standard hydrological techniques, which are supplemented with information from optical satellite data in the visible to short infrared wavelength region from the SPOT sensor.

The concept follows the guideline of FAO for computing crop water requirements - FAO Irrigation and drainage paper 56, 1998. Actual evapo-transpiration is determined based on the calculation of a reference evapo-transpiration ET<sub>o</sub> (of a hypothetical grass reference crop) through consideration of two correction factors: K<sub>c</sub> for the adaptation to crop evapo-transpiration and K<sub>a</sub> for the reduction to water stress as illustrated in Figure 16.

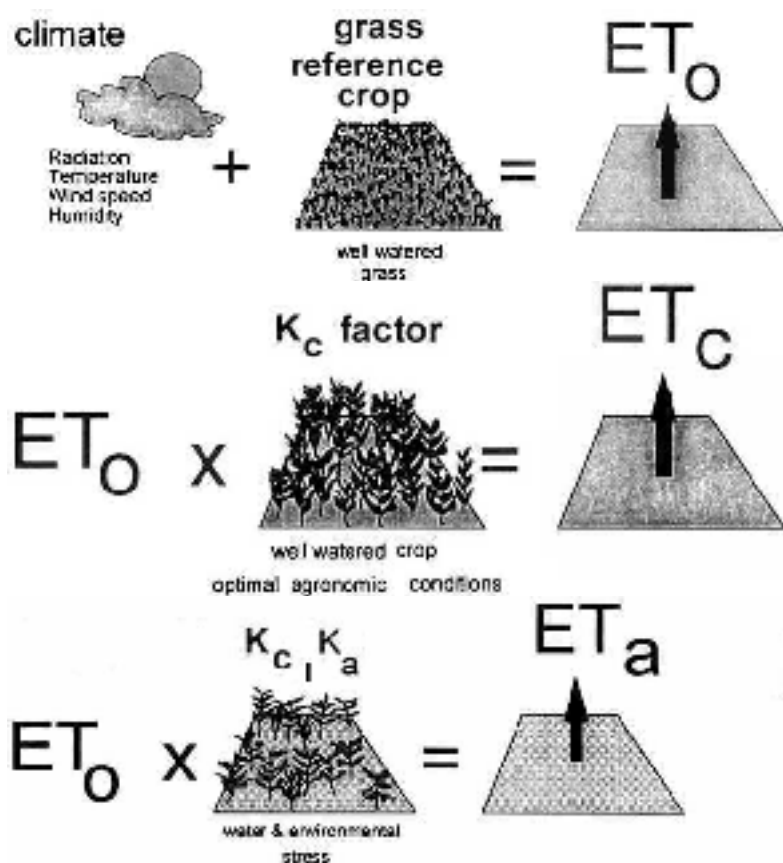


Figure 16: Three step approach to calculate actual evapo-transpiration under non-standard conditions (ET<sub>a</sub>) based on the reference evapo-transpiration (ET<sub>o</sub>), and crop evapo-transpiration under standard conditions (ET<sub>c</sub>), (modified after FAO, 1998.)

### 3.6.2 Calculation of ET<sub>o</sub>

ET<sub>o</sub> is calculated based on the FAO Penman-Monteith equation on a daily basis. The effects of various weather conditions on evapo-transpiration are incorporated into ET<sub>o</sub>.

The FAO Penman-Monteith method to estimate ET<sub>o</sub> is defined as

$$ET_o = \frac{0.409 \Delta (R_n - G) + \gamma \frac{900}{T + 273} u_2 (e_s - e_a)}{\Delta + \gamma (1 + 0.34 u_2)}$$

where

- ET<sub>o</sub> reference evapo-transpiration [mm day<sup>-1</sup>],
- R<sub>n</sub> net radiation at the crop surface [MJ m<sup>-2</sup> day<sup>-1</sup>],
- G soil heat flux density [MJ m<sup>-2</sup> day<sup>-1</sup>],
- T mean daily air temperature at 2 m height [°C],
- u<sub>2</sub> wind speed at 2 m height [m s<sup>-1</sup>],
- e<sub>s</sub> saturation vapour pressure [kPa],
- e<sub>a</sub> actual vapour pressure [kPa],
- e<sub>s</sub> - e<sub>a</sub> saturation vapour pressure deficit [kPa],
- Δ slope vapour pressure curve [kPa °C<sup>-1</sup>],
- γ psychrometric constant [kPa °C<sup>-1</sup>].

The reference evapo-transpiration, ET<sub>o</sub>, provides a standard to which: evapo-transpiration at different periods of the year or in other regions can be compared;

actual evapo-transpiration ET<sub>a</sub> of other crops can be calculated.

The equation uses standard climatological records of solar radiation (sunshine), air temperature, humidity and wind speed. No special meteorological equipment is needed for calculating ET<sub>o</sub>.

### 3.6.3 Calculation of ET<sub>c</sub>

The crop evapo-transpiration under standard conditions, denoted as ET<sub>c</sub>, is the evapo-transpiration from disease-free, well-fertilized crops, grown in large fields, under optimum soil water conditions, and achieving full production under the given climatic conditions.

The effects of characteristics that distinguish the cropped surface from the reference surface are integrated into the crop coefficient. ET<sub>c</sub> is determined by multiplying ET<sub>o</sub> by the crop coefficient K<sub>c</sub>

$$ET_c = K_c * ET_o$$

For many crops this coefficient is available in literature. However it does not exist for qat yet. Therefore measurements of ET<sub>c</sub> needed to be performed in order to derive K<sub>c</sub>.

### 3.6.4 Calculation of ET<sub>a</sub>

Where field conditions differ from the standard conditions, correction factors are required to adjust ET<sub>c</sub>. The adjustment reflects the effect of the environmental and management conditions on crop evapo-transpiration in the field. Where cover is reduced due to disease, stress, pests, or planting density, the values for K<sub>c</sub> can be reduced by a factor K<sub>a</sub> depending on the actual ground cover fraction (f<sub>c</sub>):

$$K_a = 1 - (f_c / f_{c \text{ dense}})^{0.5}$$

K<sub>a</sub> is subtracted from K<sub>c</sub> in order to obtain an adjusted K<sub>c</sub> value:

$$K_{c\_adj} = K_c - K_a$$

ET<sub>a</sub> can thus be calculated by multiplying ET<sub>o</sub> by the adjusted K<sub>c</sub> value.

$$ET_a = ET_o * K_{c\_adj}$$

### 3.6.5 Required Meteorological Measurements

In order to calculate ET<sub>o</sub> and ET<sub>a</sub> the following two inputs from meteorological measurements are required.

#### 3.6.5.1 Standard Meteorological Measurements

The spatial simulation of ET<sub>o</sub> uses standard climatological records of solar radiation (alternatively: sunshine duration or cloud cover), air temperature, humidity and wind speed. These meteorological data are measured at regular weather stations in Yemen. Daily values are needed at least, but higher temporal resolutions are advantageous. It is desirable to use data from several stations distributed in the basin for a better reflection of the spatial heterogeneity of ET<sub>o</sub>. Due to the crucial data quality one has however to carefully balance whether to use few stations with high quality meteo-data or a higher number of stations with lower quality.

#### 3.6.5.2 Measurements of ET<sub>a</sub>

The crop coefficient, K<sub>c</sub>, is used for the adaptation of the evapo-transpiration of the reference surface ET<sub>o</sub> to the cropped surface ET<sub>c</sub>. For many crops this coefficient is available in literature and can be applied after an adjustment to the conditions in the Sana'a basin. Because there exist no K<sub>c</sub> coefficients for qat based on experimental data in literature yet, the K<sub>c</sub> coefficient for qat had to be derived. Therefore measurements of ET<sub>o</sub> and ET<sub>c</sub> shall be performed for a qat field in order to derive K<sub>c</sub> for this crop.

Besides the use of lysimeters, the actual evapo-transpiration ET<sub>a</sub> can be measured indirectly with either a Bowen Ratio Station or An Eddy Covariance Station. In the first case the fluxes of energy and water are measured at 2 heights and the Bowen Ratio is calculated, in the second case the eddy covariance of fluxes is measured. A Modified Bowen Ratio (MBR) station is an instrument which is a mixture of both approaches, since it measures energy fluxes and also the covariance of the wind. This kind of station was selected for purchase and installation, since it is more robust

than the eddy covariance stations and more accurate than the classical Bowen ratio method.

The setup of the Modified Bowen Ratio station enables the determination of  $ET_o$  and  $ET_a$ . If the  $ET_a$  measurements are done under optimal growing conditions, the sensor also provides values for  $ET_c$ .

The new meteorological equipment is used in two ways in the project. Firstly, to derive the crop coefficient  $K_c$  for qat. Secondly, the measurements are used to determine the accuracy of the methodology by comparing measured actual evapo-transpiration rates with the ones calculated using satellite derived information as input. Application of the Concept to the Sana'a Basin

The hydrological model PROMET (Mauser & Schädlich, 1998) is applied to the Sana'a basin for the spatially distributed calculation of the potential evapo-transpiration  $ET_o$  based on the FAO Penman-Monteith equation. Calculations provide daily values of reference evapo-transpiration  $ET_o$  in a spatially distributed way. As meteorological inputs data of existing meteo-stations in Yemen are used and complemented with measurements of the newly equipped micrometeorological station situated in the Sana'a basin.

Depending on the land use, the respective crop coefficients  $K_{c\_adj}$  are applied in order to determine the evapo-transpiration  $ET_a$ . Information derived from satellite data are used in different ways. Firstly, the satellite images with a pixel size of 10 by 10m provide maps of land use, in order to assign  $K_c$  for each pixel. Secondly, the fractional vegetation cover is calculated in order to derive  $K_{c\_adj}$  for each pixel. The fractional vegetation cover can be obtained from the available satellite data using a spectral unmixing approach. This will be described in Chapter 3.3.2.

For temporal interpolation between the 3 observed satellite images the shapes of standard  $K_c$  curves are used. For most of the crops in Yemen coefficients for  $K_c$  are available in literature (FAO, 1998). These values were collected in a literature review. In order to derive  $K_c$  for qat, which was not available in literature, a micrometeorological station was purchased and installed. The station was supposed to measure the crop evapo-transpiration under optimal conditions ( $ET_c$ ) in order to derive  $K_c$ . Therefore the station needed to be installed in an irrigated region. The location of the station was selected based on the local logistic situation and supported by satellite data analyses. The choice fell on Al-Qabil.

### **3.7 Estimation of Net Groundwater Use by Agricultural**

Estimation of spatially distributed groundwater extraction and recharge for the 2004/2005 season shall be calculated using the mass balance between rainfall and  $ET_a$ . Therefore, the net groundwater use in agricultural fields in the basin will be estimated through calculation of the difference between rainfall and  $ET_a$ .

The rainfall distribution will be achieved by interpolation of the rainfall measurements considering the elevation dependency of the rainfall. In order to establish a correlation between rainfall and elevation, a longer time series (e.g. 10 years) of rainfall data was analysed.

The mass balance approach for calculating the net groundwater use is only an indirect method. Additional assumptions on the irrigation efficiency are therefore mandatory.

### 3.8 Other Information Analysis

The “Other Information Analysis” chapter contains compiled information about the aquifer properties and groundwater conditions in the Sana’a basin.

The general groundwater configuration has two major strata:

- the **shallow aquifers** (alluvium and volcanic), with water level depths from 10 m to about 50 m (AYELE & ALSHADILY, 2000)
- a **deep aquifer** (Tawilah aquifer), slanting from north to south, with a recorded water level depth in 1970 of up to 40 m in the main abstraction area. According to SBWRM (2001) it is declining by 2 to 4 m/year.

#### 3.8.1 Objectives

The overall aim of this chapter is to provide background information for decision makers on the potential infiltration and recharge in the Sana’a basin for further action planning.

The specific objective is to derive

- litho-stratigraphical and structural information from satellite imagery and existing geological data focussing on hydrogeology, (e.g. the Amran Limestones are from a groundwater aspect of low relevance for Sanaa and therefore mapped respectively in low resolution)
- geomorphological and hydrological information focussing on surface water runoff and potential infiltration

#### 3.8.2 Compiled Geological Maps

The Geological Maps, parts of the additional information compilation of this study are compiled with reference to the specifications described in the technical proposal (p. 45 ff., part of the contract). The technical proposal was submitted to the ITT and bases on the Terms of Reference (TOR’s). However, the specification in the TOR’s were not always clear with respect to what meaningful and reliable information can actually be derived from available remotely sensed data. GAF therefore adequately reviewed the TOR’s and the technical proposal. It is referenced in here that both, the TOR’s and the proposal are part of the contract and the present study bases on both documents.

##### 3.8.2.1 Discussion of problems faced during the compilation

It was identified during the map compilation that the map in a print scale of 1: 50 000 was adequate to the low degree of details of the available litho-stratigraphic information (legend). Referring to the technical proposal p. 47 “units/elements will be assessed as far as a discrimination is possible with the reference data” the consultant therefore concluded to compile the maps on the base of multispectral image visual on-screen interpretation using the maximum differentiation from lithospectral and textural image information and resulting in a number of members and submembers,

referring to the legend in the BGR map (BGR 1991). The BGR legend and map was for the purpose of this study reviewed in detail.

### 3.8.2.2 Input Data and Relevant Information Derived

#### Remote Sensing Data

Landsat ETM data (path 166 / row 49) with 30 m ground resolution was processed to a colour composite of 741 in RGB which is known to be most appropriate for geological related studies in arid areas. It provides a basic mapping scale of equal to or less than 1: 100 000. ETM data are ortho-corrected with a spatial accuracy of at least 50 Meters

A Spot 5 colour merge mosaic with a ground resolution of 2.5 m prepared with false colour combination of IR, red and green was used to derive structural features which were not identifiable in the Landsat ETM data.

The SRTM digital elevation model was acquired by NASA in 2000 with a ground resolution of 90 m. The vertical accuracy is given with 90% better than 5 m.

The DEM was used to support the Landsat ETM data interpretation of the single geological units in their morphological context.

#### Ancillary Data

Three geological maps (in the following referred to as geological reference maps) were scanned and geo-referenced:

1. Geological Map Sana'a', sheet 15 G, 1:250 000. The Natural Resources Project. Ministry of Oil and Mineral Resources, Oil and Mineral Cooperation, Mineral Exploration Board; Republic of Yemen. By Robertson Group
2. Geological Map of the Yemen Arab Republic, sheet Sana'a', 1:250 000, Ministry of Oil and Mineral Resources, Sana'a, Republic of Yemen/Federal Institute of Geoscience and Natural Resources Hanover, 1991, Federal Republic of Germany . By W. Kruck and U. Schäfer
3. Geological Map 1:100 000 by Jungfer (1987) published in „Zur Frage der Grundwasserneubildung in Trockenräumen – Fallstudie aus der Arabischen Republik Jemen und dem Königreich Marokko“ Erlanger Geologische Arbeiten, Sonderband 18.

The cited geological maps differ in their information content and thematic focus. From each of the maps specific information was derived considering its background:

Ref 1. The Robertson Group Map has an emphasis on the lithology. The map was created mainly on the base of satellite imagery with very limited field work

Ref 2. BGR Map pronounces more the stratigraphy, it was also derived from satellite imagery with limited field observations.

Ref 3. Jungfer Map; the ratio of field work and remote sensing interpretation is unknown. The Jungfer Map as the only one of the three maps, that refers to the initial subdivision of Italconsult (1973) as most of the authors in the literature and was prepared in bigger scale of 1:100000.

#### In-situ Data

For the in-situ data refer to chapter 3.3.2.



### 3.8.2.3 Integrated Data Analysis / Interpretation

#### Visual interpretation

The processed image products have been loaded into a digital image interpretation software allowing simultaneous analysis of the data sets on the screen. The advantage of digital interpretation is the online generation of digital polygons, lines and point data and their storage and manipulation in a standard Geographic Information System (GIS) format (Figure 17).

Visual analysis is the only way to assess the geological/structural/other categories of information needed in sufficient precision and detail. Automatic processes are yet not satisfying the requirements in practise. In order to calibrate and verify the analysed information, additional information is needed.

A geodatabase containing about 100 observation points was created during the field survey and integrated in the GIS mapping software. So field data (stratigraphical /lithological information; field photos) could be spatially linked, visualized and finally integrated in the on-screen interpretation.

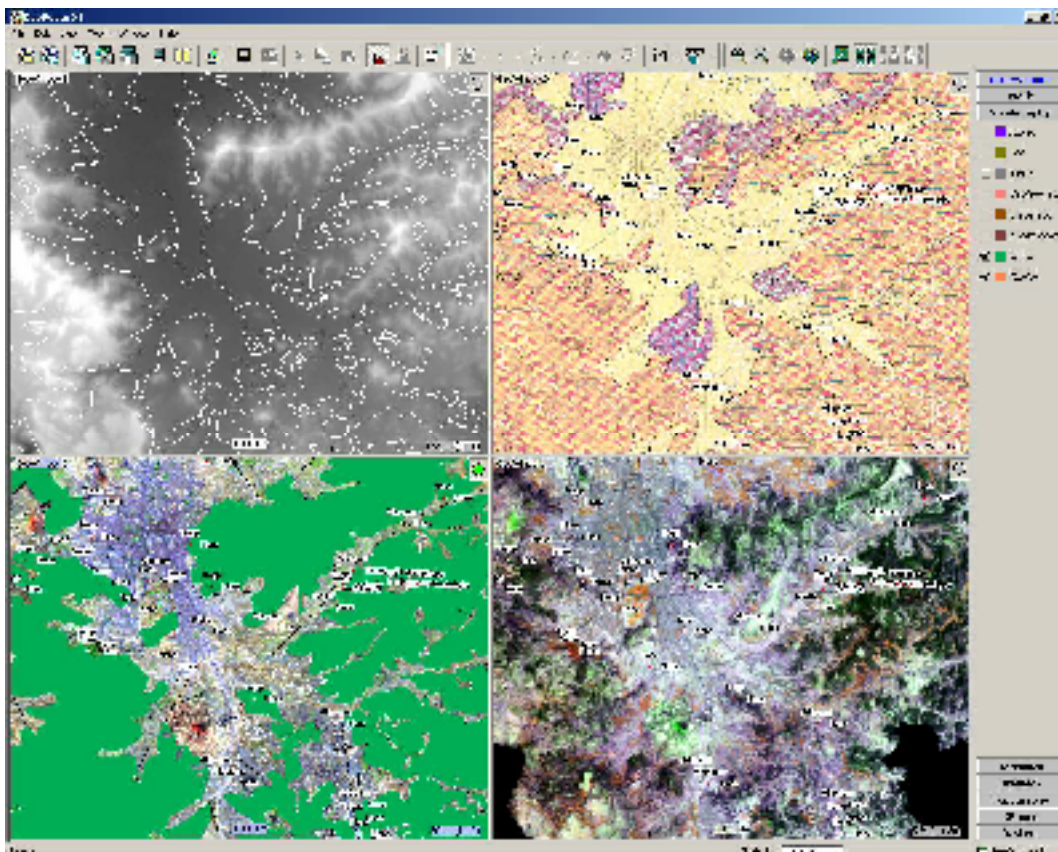


Figure 17: Graphical user interface of the applied software with a geographically linked "four-window-screen" and a dynamic histogram stretch applied to the actual extension of the window. The example shows the comprehensive interpretation capabilities by the integration of all available input data. Top left: DEM; Top right: geological Map; Lower Left: Landsat ETM; Spot 5



The mapping can be described as an iterative process of information extraction, calibration and refinement.

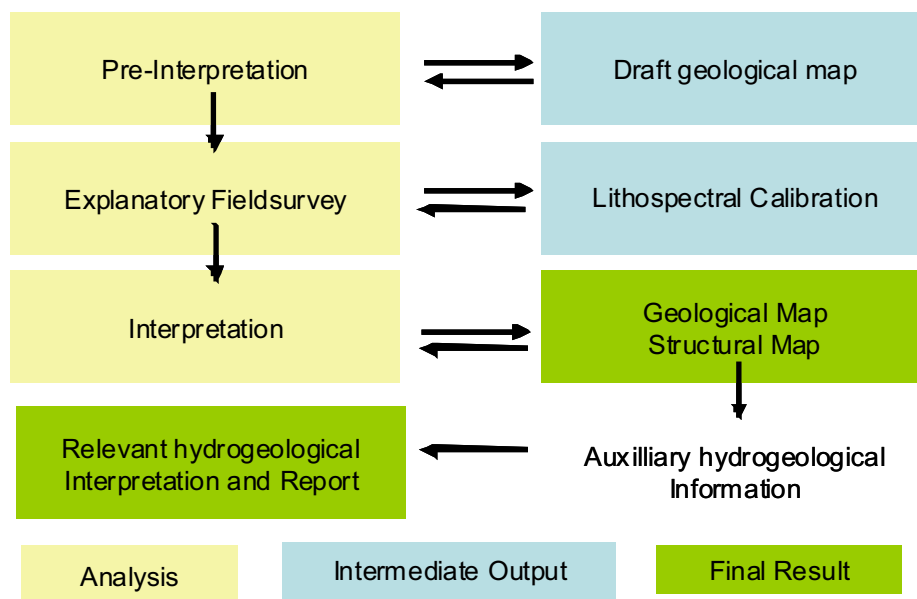


Figure 18: Sequential information derivation and iterative mapping and interpretation process

### 3.8.3 Potential Infiltration Map

The “Potential Infiltration Map” is prepared at a scale of 1 : 100 000. It includes geomorphological and hydrological information derived from remote sensing data and geological maps.

#### 3.8.3.1 Input Data

##### Remote Sensing Data

Spot 5 and Landsat ETM were used as a basic source for the mapping of wadis and reservoirs.

JERS SAR data with a wavelength of 23,5 cm and a ground resolution of 12,5 m is known to be appropriate for structural and geological mapping at scales up to 1:100 000. Scenes 230/247 and 230/275 were referenced image to image on the base of Landsat, speckle filtered and mosaiced. The result was generalized (reduced resolution of to 90 meters) to apply for the GIS analysis a common spatial resolution with the other layers.

Radar data records surface physical properties reflecting differences in surface roughness.

SRTM data was used to derive a slope angle map. For the potential infiltration in the alluvium slopes with an angle higher than 1° were masked out. It has to be mentioned at this point that the Digital Terrain Model slopes are very much related to

its ground resolution, slope angles in the data do in most cases not reveal the actual slope angle in the field.

### **Ancillary data**

The Robertson Group Map was used in combination with Spot 5 data as a basic input for the delineation of wadi courses. The majority of authors assume that the main natural groundwater recharge takes place through the wadi bed during flood events. (e.g. Sawas 1996).

The extension of the Alluvium in the Sana'a plain was used to mask out the other geological units, because the surface roughness is there assumed to be of less relevance for infiltration properties.

Vegetation cover from land use mapping (refer to chapter 2.4.1).

Vegetation classification was used from the land use classification to mask out these areas. It is assumed that vegetated areas, like farmed land will not significantly contribute to natural recharge, due to enhanced evapo-transpiration and the limited infiltration through sealing properties of arable soils.

### **3.8.3.2 Integrated Data Analysis / Interpretation**

#### **Visual interpretation**

- dams
- reservoirs
- wadi course

The major natural surface water infiltration is assumed during floods in wadi beds. Artificial infiltration can be achieved by dams and reservoirs. Wadi course and reservoirs were identified from Spot 5 image based on the hydrogeological map from the Robertson Group and digitized onscreen.

#### **Automatic classification**

##### *Slope Angle*

The slope angle is known for its significance for the infiltration of surface water; the steeper the slope the higher is the surface runoff and the less is the time for infiltration. Contrary, in flat areas the water accumulates and has the chance to penetrate little by little into the ground.

The one-degree slope angle in the DEM is an empirical defined boundary to classify areas with values

- below 1° as flat and
- above 1° as slightly oblique to steep slopes.

##### *Surface Roughness*

Generally radar signals are sensitive for surface roughness. The baseline for the roughness classification of bare surfaces is that the rough material (gravels) in the alluvial plain allows generally for a better infiltration than smooth surface material (sand and silt).

A simple slicing method was applied to the JERS data. The threshold was set empirical to classify two classes with

- a “smooth” class for dark areas (poor backscattering of the signal) and
- a “rough” one for brighter areas (significant backscattering)

## GIS Analysis

A simple GIS analysis was applied to intersect all relevant information. First the area was masked out where other natural factors (vegetation cover, slope angle, geology) cause a generally low infiltration.

*Table 3: Alluvium Infiltration classification (1)*

	“No data”	“Potential infiltration”	Remarks
Vegetation cover	Vegetated	Not vegetated	Surface roughness parameters can be derived by radar data only for non-vegetated areas. Vegetation can influence the radarsignal and can thus mislead in the interpretation.
Slope angle	Steep Slopes (>1°)	Flat Slopes 0-1°	Surface water runoff is too fast to efficiently infiltrate into the rock
Geology	Non alluvium	Alluvium	The basic assumption is that in the alluvium the surface roughness gives indication on the potential infiltration; infiltration in other outcropping geological units is more determined by other factors

*Table 4: Alluvium Infiltration classification*

	“Poor infiltration”	“Fair infiltration”	Remarks
Surface roughness	smooth	rough	A rough surface means a material with a significant space between the components (e.g. gravel) with better infiltration properties than smooth material (e.g. sand, silt)

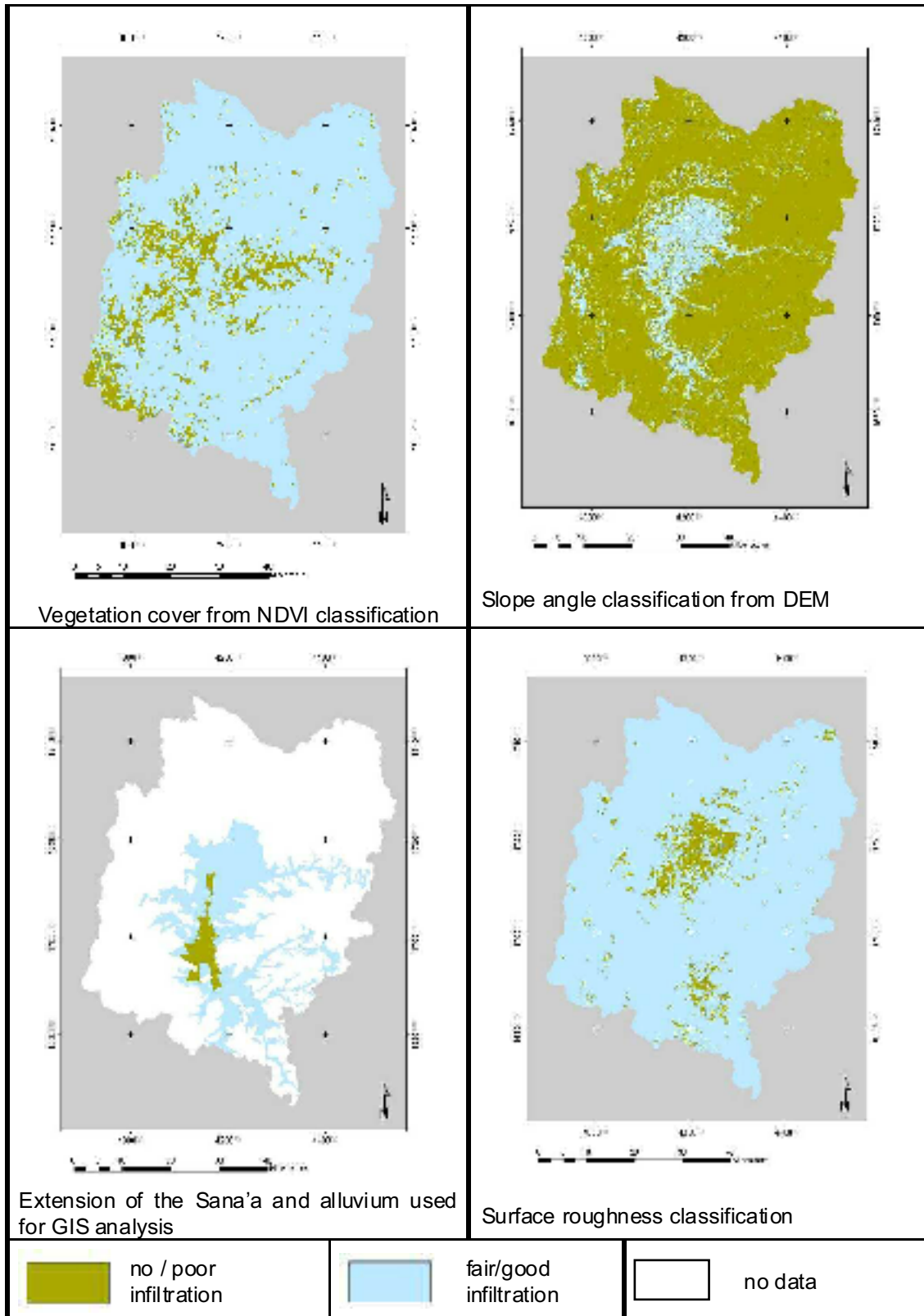


Figure 19: Input layers for the GIS analysis for the potential infiltration in the Sana'a plain.

## 3.9 Training and Know-how Transfer

### 3.9.1 Background

The effective transfer of knowledge and skills was one important component of the project and considered a priority deliverable.

The training was an on-going activity and commitment throughout the whole project, consisting of two dedicated training periods and will include one final workshop.

In October 2004 the client assigned **Mr. Abdullah Abdulwahid Saif Al-Adimi** and **Mr. Mohammed Hamid Ahmed Emad** for the in-country training and the training abroad. The counterpart staff was selected by the client according to their professional capacity and availability to the SBWMP after end of this contract. After the 20 day in-country training by Ghayth, in December 2004 **Mr. Mohammed Hamid Ahmed Emad** was replaced by **Nabil A. Qader**.

### 3.9.2 Objectives

The objectives of the in-country and external training were as follows:

- to build-up the knowledge of general GIS and Remote Sensing techniques for the two assigned engineers of NWRA Sana'a Branch
- to build-up the understanding of the project's methodology in general
- to cross-train specialists so that they are able to perform multiple tasks in the relevant fields efficiently and safely
- to prepare specialists for establishment of continuing professional development to ensure the sustainability of the project results
- to organise monitoring activities to ensure a trouble-free progress of the project

The objectives of the final workshop are as follows:

- to use the final workshop as a forum for an in-depth discussion with all participants on improvements and enlargements
- to discuss results of the services/products and their implementation
- to familiarise a bigger group of workshop attendees with procedures and project activities
- to consult the beneficiaries regarding of HW/ SW and data procurement

### 3.9.3 Training Needs

Needs in training was assessed in-depth by Ghayth Aquatech Expert Mr. Khalil Gubran after counterpart staff assignment in October 2004. Beside the ToRs and project objectives this assessment analysis was the main input for the training plan as outlined in chapter 2 and 3 of the Technical Note 2 "Training Plan".

### 3.9.4 In-Country Training

Comprehensive in-country training was held during the first phase of the project on-site. The training was structured into several parts, covering the training needs and was conducted jointly by experts of GAF/Ghayth Aquatech/Vista. The total duration of the in-country training was 32 days for 2 trainees. The detailed training content is outlined in the delivered training material.

## The following topics were addressed within the in-country training

1. Evapo-transpiration field monitoring instruments (VISTA)
  - Theory of the measurements
  - Set-up, operation and maintenance
  - Data logging
  - Interpretation of measurements – limitations
2. Conducting ground truth work for cropping pattern classification (GAF)
  - Planning
  - Performance
  - Use of satellite data and GPS together with Geover software as a field mapping tool
3. Conducting ground truth for geological and hydrogeological mapping (GAF)
  - Planning
  - Field verification
  - Use of satellite data and GPS together with Geover software as a field mapping tool
  - Satellite image interpretation with focus on:
    - Geology
    - Structural inventory
    - Hydro-geology
    - Infrastructure
4. Training on satellite remote sensing and image processing (GHAYTH)
  - Training of software (ERDAS Imagine) fundamentals
    - Import/Export of digital data (raster, vector)
    - Image enhancement
    - Georeferencing
    - Image mosaicking
    - Image libraries and catalogues
    - Compositions of maps
    - Unsupervised classification
    - Supervised classification
5. GIS Training (GHAYTH)
  - Training of GIS fundamentals
    - Access to the data from within the GIS
    - Data visualisation
    - Query maps and databases for information
    - Thematic map generation of data
    - Colour code maps using symbols for geological, land use, hydrological etc. data
    - Produce high quality maps
    - Overlay analysis
    - Layout design and printing
    - Recovery procedures/Backup / archiving
    - GIS database design and management

- Editing spatial and attribute data
- Spatial analysis functions

#### 6. GeoRover Training (GAF)

- General overview about the SW
- Training of SW fundamentals
  - Project set-up
  - Data formats to be used
  - GIS functionality
  - GPS functionality

*Table 5: In country training 2005*

Topics	Duration (days)	Time frame	Responsibility
Training on satellite remote sensing and image processing	10	Oct./Nov. 2004 -	Ghayth
GIS Training	10	Nov. 2004 -	Ghayth
Evapo-transpiration field monitoring instruments	4	Feb. 2005	VISTA
Conducting ground truth work for cropping pattern classification	3	Feb. 2005	GAF
Conducting ground truth work for geological and hydro-geological mapping	3	Jan. 2005	GAF
GeoRover Training	2	Jan. 2005	GAF

### 3.9.5 External Training

The external training took place in Munich, Germany at GAF and VISTA premises. The training was performed during a period of 5 weeks duration after the second mission dealing with the second set of imagery.

As outlined in the technical proposal the external training was initially planned to be fully on-the-job. However, expertise of counterpart staff necessitated a more operational and basic training. Nevertheless, together with the experts of the GAF/VISTA team the trainees were trained and made fully acquainted with the applied methodology for image processing, processing of ground truth and ancillary data, image classification, GIS and data analysis and interpretation, ETa measurement and modelling as well as development of report structure and annexes. Finally, the trainees were provided with theoretical explanations and literature and then stepped through the whole sequence of image processing, modelling and information extraction and presentation.

The topics of the training were in line with the thematic focal points of the project and were performed with those data acquired in the frame of the project.

**The following topics were covered by the GAF team:**

1. Image processing
  - Image enhancement
  - Image statistics
  - land use and land cover classification
  - accuracy assessment/verification
2. Generation and layout of output maps
3. Other information analysis, with a focus on geological, structural and hydrological analysis of the remote sensing imagery.
  - Interpretation of infrastructure, geomorphology, ecology and geology from satellite images
  - Fracture Analysis
  - Hydrogeological interpretation
4. Reporting

**The following topics were covered by the VISTA team:**

1. Modelling and determination of ETa
  - Introduction into mathematical modelling
  - Theoretical background of evapo-transpiration model
  - Adjusting a model to “real” data
  - Analysing the results of a model
  - Detection of change of results over time
  - Interpretation
  - Produce high quality maps for the plotter, tabular outputs and statistics

**Modelling of spatially distributed groundwater extraction**

*Table 6: Training schedule for external training in Germany March- April 2005*

Date	Days	Topics	Responsibility
14.3.05 – 17.3.05	4	<ul style="list-style-type: none"> <li>• Introduction ERDAS</li> <li>• Ortho-correction</li> </ul>	GAF
18.3.05	1	<ul style="list-style-type: none"> <li>• Radiometric Correction</li> </ul>	VISTA
21.3.05 – 24.3.05	4	<ul style="list-style-type: none"> <li>• Classification</li> <li>• Accuracy Assessment</li> </ul>	GAF
29.3.05 – 30.3.05	2	<ul style="list-style-type: none"> <li>• Combination autumn/winter classification</li> </ul>	GAF
31.3.05 – 6.4.05	5	<ul style="list-style-type: none"> <li>• Eta modelling               <ul style="list-style-type: none"> <li>• Sana’a Basin</li> <li>• Sub-catchments</li> </ul> </li> <li>• Calculation of net ground water use</li> </ul>	VISTA
07.04.05 – 08.04.05	5	<ul style="list-style-type: none"> <li>• Other information analysis               <ul style="list-style-type: none"> <li>• Geology</li> <li>• Structures</li> <li>• Hydro-geology</li> </ul> </li> </ul>	GAF
11.04.05 – 14.04.05	4	<ul style="list-style-type: none"> <li>• GIS/Map layout</li> </ul>	GAF
15.04.05	1	<ul style="list-style-type: none"> <li>• Reporting</li> </ul>	GAF



## 4. Results and Accuracy Assessment

### 4.1 Irrigation Acreage and Cropping Pattern

#### 4.1.1 Irrigation Acreage

The method for the calculation of the irrigation acreage is described in detail in chapter 2.4.1. It is based on the calculation of the NDVI of all 3 satellite acquisition dates, covering nearly the entire phenological cycle of the crops and the assumption that vegetation with an evapo-transpiration level lower than 240 mm/m<sup>2</sup>, corresponding to long-time average rainfall over the last years, are not irrigated.

Table 7: Irrigation acreage broken down by sub-catchments (2004/2005)

Sub-Catchments	No.	Area			Irrigated Area	
		(qm)	(ha)	(%)	(ha)	(%)
Wadi al Mashamini	1	77778536	7777,9	2,4	69,0	0,9
Wadi al Madini	2	213300000	21330,0	6,6	351,6	1,6
Wadi al Ma'adi	4	111330000	11133,0	3,4	100,2	0,9
Wadi al Kharid	3	138210000	13821,0	4,3	237,5	1,7
Wadi A'sir	5	208750000	20875,0	6,4	593,2	2,8
Wadi Khulaqah	6	75677104	7567,7	2,3	180,5	2,4
Wadi Qasabah	7	64517144	6451,7	2,0	186,1	2,9
Wadi al Huqqah	8	120270000	12027,0	3,7	1176,1	9,8
Wadi al Iqbal	13	202940000	20294,0	6,3	1538,1	7,6
Wadi Thumah	10	77045984	7704,6	2,4	125,5	1,6
Wadi bani Huwat	9	327030000	32703,0	10,1	4825,5	14,8
Wadi as Sirr	11	218550000	21855,0	6,7	2603,2	11,9
Wadi Zahr & al Ghayl	14	360830000	36083,0	11,1	1297,2	3,6
Wadi al Furs	12	45815372	4581,5	1,4	855,9	18,7
Wadi Sa'wan	17	95936120	9593,6	3,0	1054,9	11,0
Wadi Shahik	18	238660000	23866,0	7,4	1032,4	4,3
Wadi Hamdan	15	63496708	6349,7	2,0	788,8	12,4
Wadi al Mawrid	16	179160000	17916,0	5,5	739,0	4,1
Wadi Ghayman	19	143340000	14334,0	4,4	533,2	3,7
Wadi Hizyaz	21	81874360	8187,4	2,5	205,6	2,5
Wadi al Mulaikhy	20	69657048	6965,7	2,2	269,0	3,9
Wadi Akhwar	22	125600000	12560,0	3,9	190,8	1,5
<b>Total</b>	<b>22</b>	<b>3239768376</b>	<b>323976,8</b>	<b>100,0</b>	<b>18953,2</b>	<b>5,9</b>

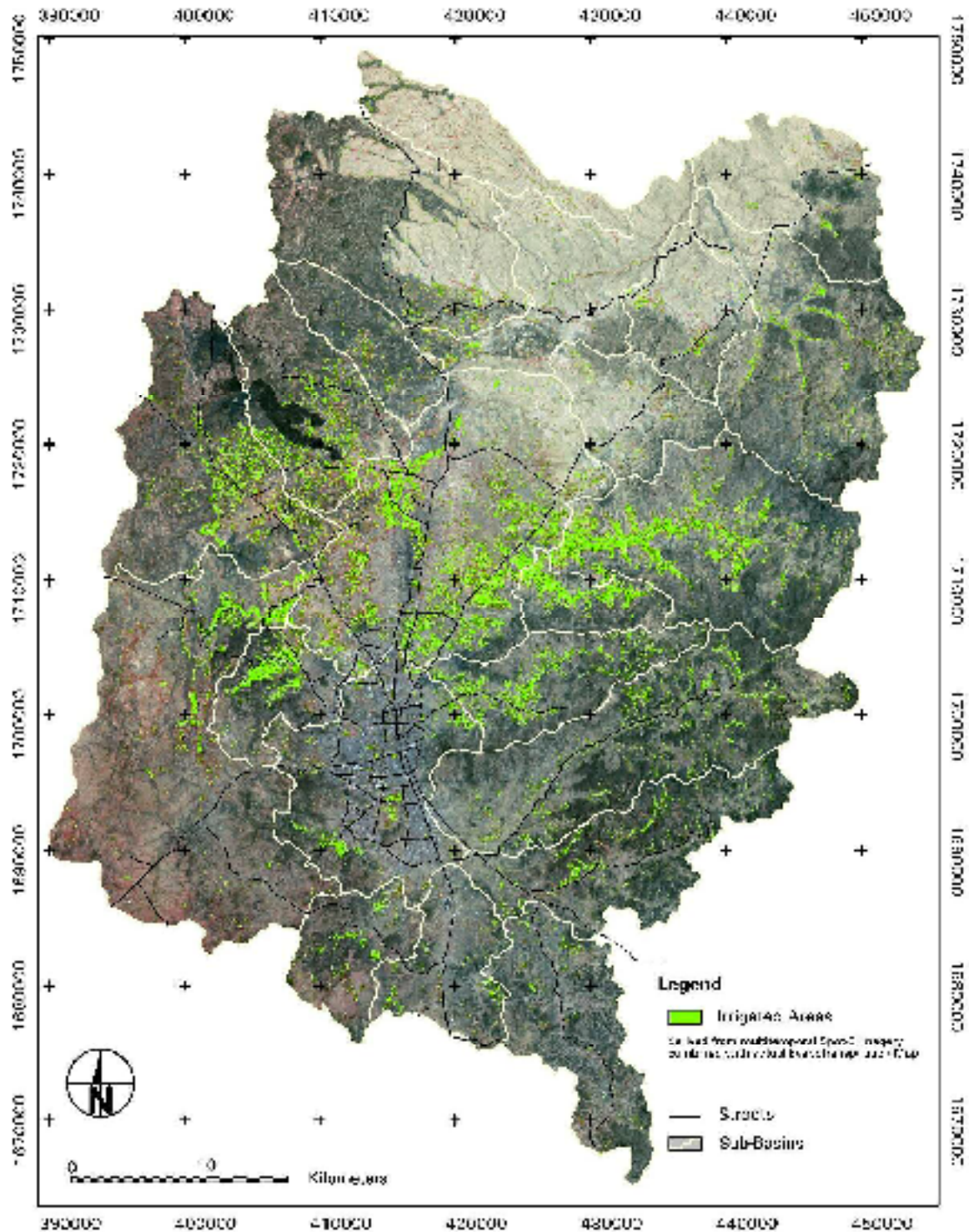


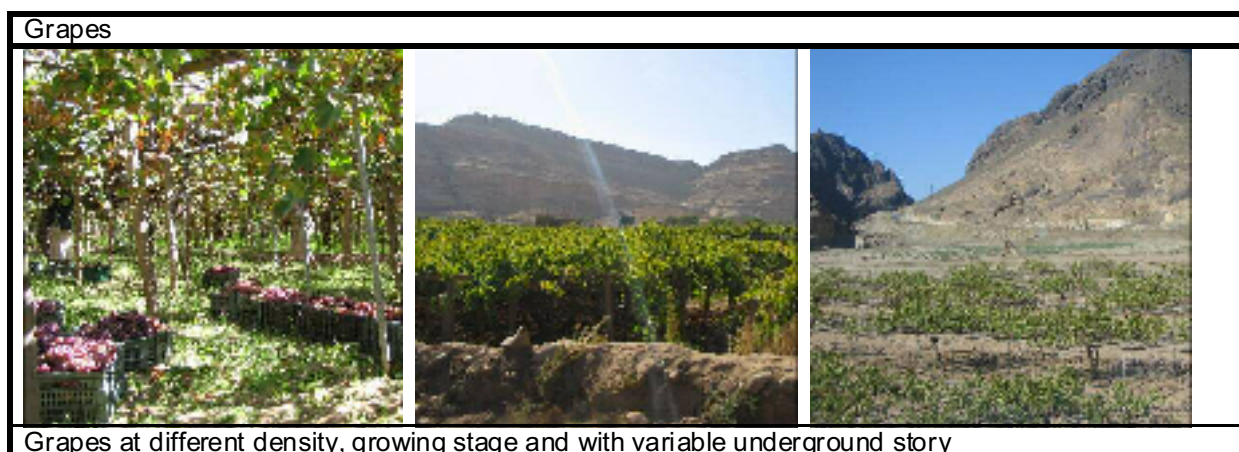
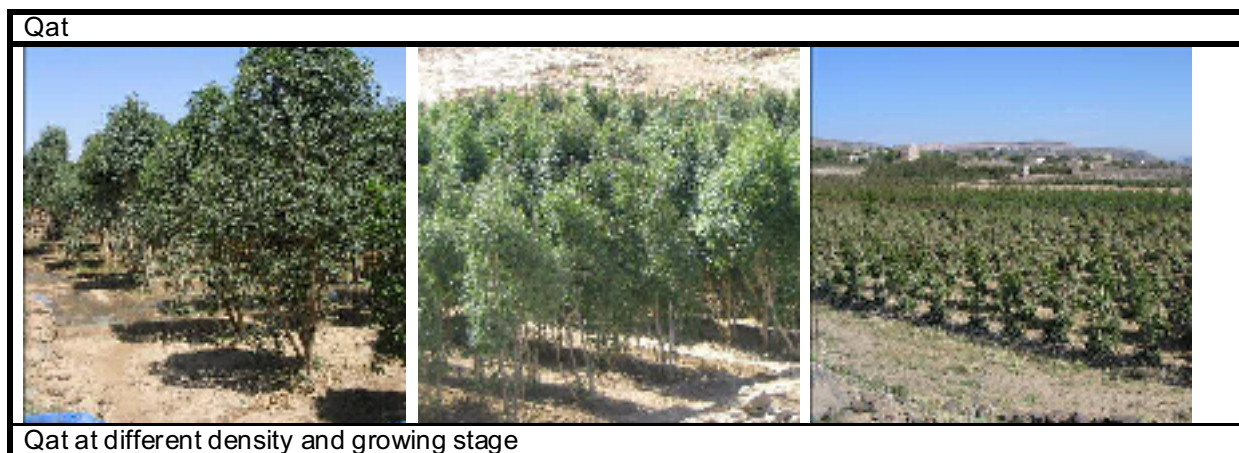
Figure 20: Irrigation acreage in the Sana'a Basin (2004/2005) derived from multi-temporal SPOT 5 imagery combined with actual evapo-transpiration map

### 4.1.2 Cropping Pattern

Based on the experience of the consultant and the first image classification (Sept. 2004) it was agreed during the second Progress Meeting in February 2005 in Sana'a, Yemen to classify the following classes:

- Qat
- Grapes
- Orchades
- Irrigated mixed crops
- Rain fed crops/natural vegetation

The small parcels, a variable underground story and different density/growing stages of the classes caused a high variance within each class. Therefore, for the final classification at last all 3 SPOT 5 acquisition dates were used for the final classification to reach an adequate accuracy (Tab. 10, 11). Figure 21 gives an impression of the variability of the different classes on the ground. The class "irrigated mixed crops" comprises cereals and vegetable. All classes especially the classes Qat and orchards may contain up to 30% trees and bushes due to the practice to surround fields with trees and bushes to protect the field from wind.





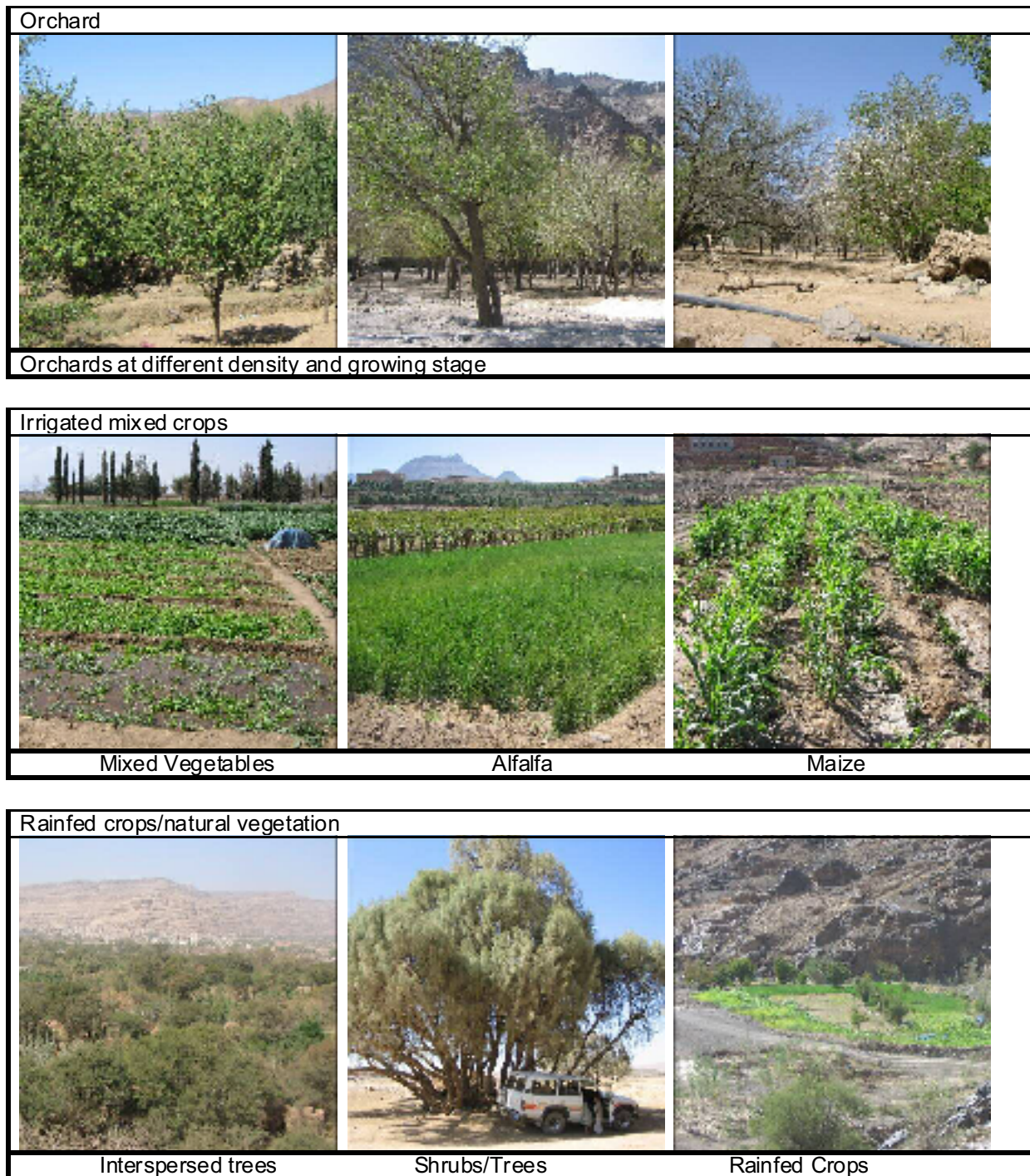


Figure 21: Class examples on the ground

As outlined also in all previous studies qat and grape are the most dominant, irrigated cultivations in the Sana'a basin. In the present study 91% of the irrigation acreage is covered by these two classes. Beside these cultivations the cropping pattern is dominated by vegetables, cereals and orchards. The dominant cash crops qat and grapes are both perennial crops and occur in various phenological stages causing a high spectral variance and hence a great class overlap. Because of winter season only in the February 2005 SPOT imagery qat could be clearly separated from grapes due to the fact that qat is an evergreen crop (Fig. 22).

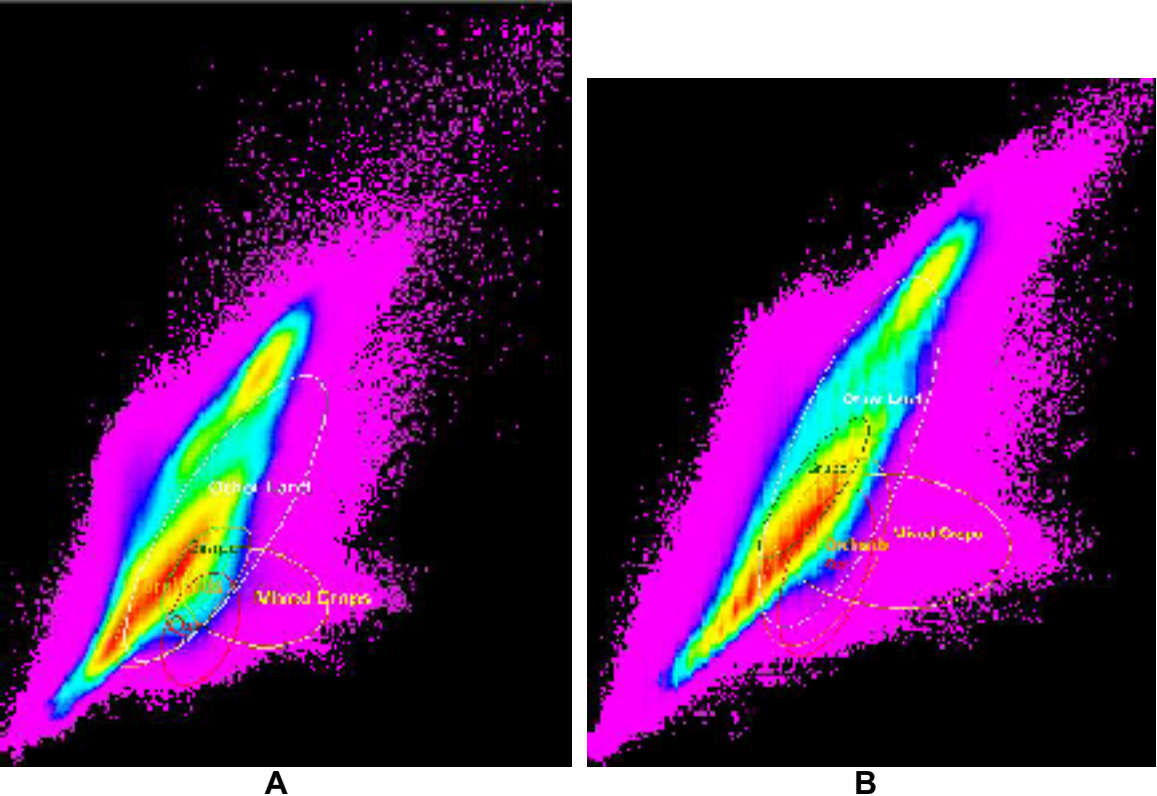


Figure 22: Scattergrams with NIR/SWIR band from Sept. 2004 (A) und Feb. 2005 (B)



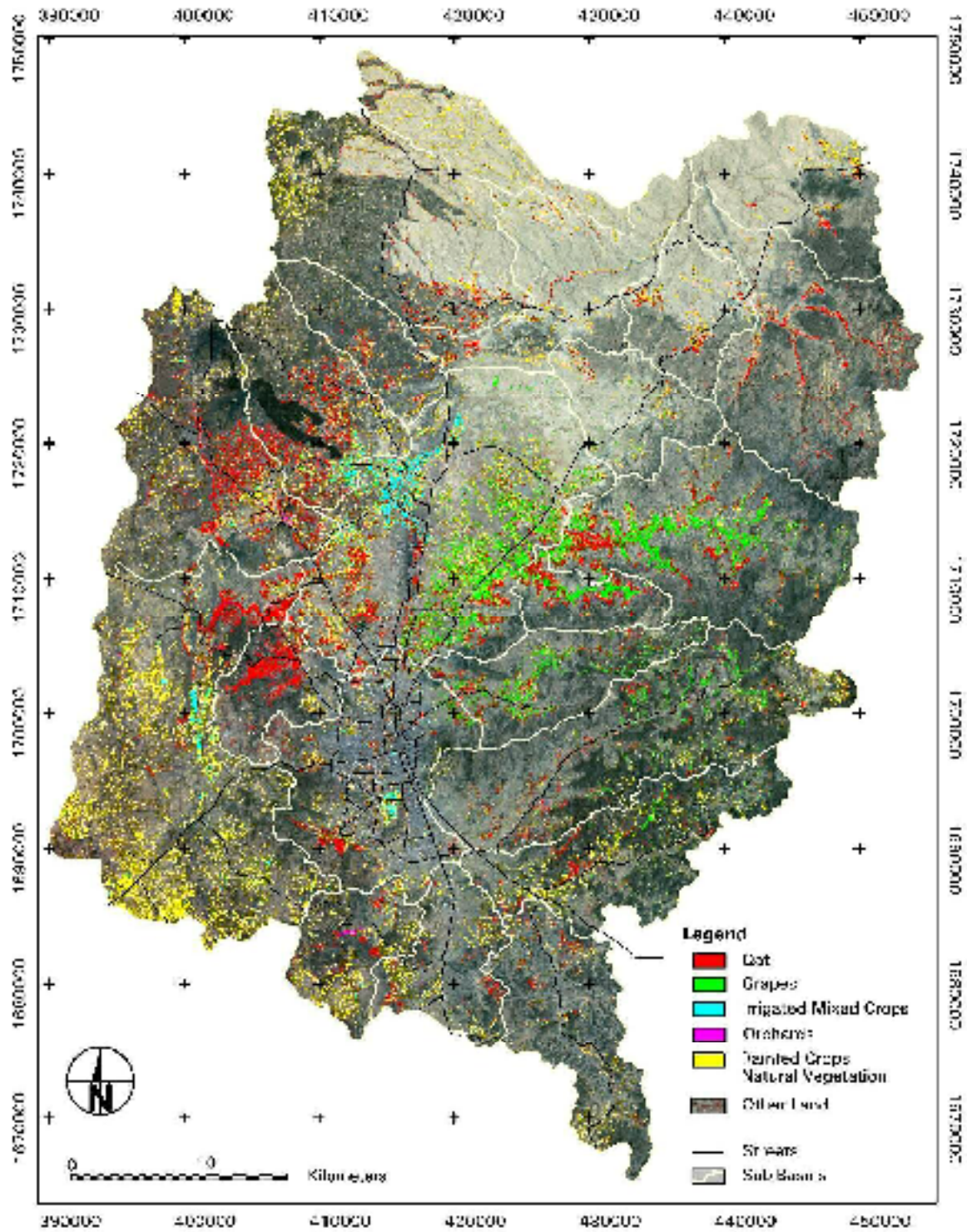


Figure 23: Cropping pattern in the Sana'a Basin (2004/2005)

Table 8: Cropping pattern broken down by sub-catchments

Class	Qat			Grapes		Irrigated Mixed Crops		Rainfed Corps/Nat. Veget		Orchard		Other Land	
	Sub-Catchment	No.	Area (qm)	Area (ha)	Area (%)	(ha)	(%)	(ha)	(%)	(ha)	(%)	(ha)	(%)
Wadi al Mashamini	1	77778536	7777,9	2,4	69,0	0,6		582,2	2,9			7125,9	2,5
Wadi al Madini	2	213300000	21330,0	6,6	350,0	3,1	1,6	1106,0	5,5			19871,8	6,9
Wadi al Ma'adi	4	111330000	11133,0	3,4	100,2	0,9	0,0	211,3	1,1			10820,6	3,8
Wadi al Kharid	3	138210000	13821,0	4,3	228,0	2,0	5,9	449,6	2,3			13133,3	4,6
Wadi A'sir	5	208750000	20875,0	6,4	593,2	5,2		186,3	0,9			20095,2	7,0
Wadi Khulaqah	6	75677104	7567,7	2,3	180,5	1,6		217,7	1,1			7169,5	2,5
Wadi Qasabah	7	64517144	6451,7	2,0	185,4	1,6	0,7	257,0	1,3			6008,6	2,1
Wadi al Huqah	8	120270000	12027,0	3,7	965,0	8,4	126,8	820,5	4,7			10030,1	3,5
Wadi al Iqbal	13	202940000	20294,0	6,3	1384,0	12,1	58,7	1366,6	7,1	62,9	55,6	17389,1	6,1
Wadi Thumah	10	77045984	7704,6	2,4	61,8	0,5		163,2	0,8			7416,0	2,6
Wadi bani Huwat	9	327030000	32703,0	10,1	1753,0	15,3	931,8	2713,6	18,2	9,1	8,1	25163,8	8,8
Wadi as Sirr	11	218550000	21855,0	6,7	1039,1	9,1	5,1	437,0	2,2			18814,2	6,6
Wadi Zahr & al Ghayl	14	360830000	36083,0	11,1	1010,3	8,8	277,5	5412,8	28,4	9,5	8,4	29372,2	10,3
Wadi al Furs	12	45815372	4581,5	1,4	427,1	3,7		66,9	0,3			3658,8	1,3
Wadi Sa'wan	17	95936120	9593,6	3,0	415,1	3,6	0,7	171,7	0,9	8,9	7,9	8367,0	2,9
Wadi Shahik	18	238660000	23866,0	7,4	500,8	4,4		731,0	3,6			22102,7	7,7
Wadi Hamdan	15	63496708	6349,7	2,0	783,4	6,8	5,0	182,7	0,9	0,4	0,3	5378,2	1,9
Wadi al Mawrid	16	179160000	17916,0	5,5	526,5	4,6	106,9	835,1	4,7	0,7	0,6	16341,9	5,7
Wadi Ghayman	19	143340000	14334,0	4,4	288,8	2,5	1,0	846,4	4,2			12954,1	4,5
Wadi Hizyaz	21	81874360	8187,4	2,5	197,0	1,7	7,6	526,5	2,7	1,0	0,9	7454,8	2,6
Wadi al Mulaikhy	20	69657048	6965,7	2,2	227,1	2,0	21,3	730,8	3,8	20,6	18,2	5965,7	2,1
Wadi Akhwar	22	125600000	12560,0	3,9	186,4	1,6	3,7	483,8	2,4			11884,9	4,1
<b>Total</b>	<b>22</b>	<b>3239768376</b>	<b>323976,8</b>	<b>100,0</b>	<b>11471,5</b>	<b>3,5</b>	<b>1554,3</b>	<b>18498,7</b>	<b>5,7</b>	<b>113,1</b>	<b>0,03</b>	<b>286518,2</b>	<b>88,4</b>

Table 9: Irrigation acreage and cropping pattern broken down by sub-catchments

Class	No.	Area (qm)	Area (ha)	Irrigation acreage		qat (%)	grapes (%)	Irrigated mixed crops (%)	Orchards (%)
				Area (%)	(ha)				
Wadi al Mashamini	1	77778536	7777.9	2.4	69.0	100.0	0.0	0.0	0.0
Wadi al Madini	2	213300000	21330.0	6.6	351.6	99.5	0.0	0.5	0.0
Wadi al Ma'adi	4	111330000	11133.0	3.4	100.2	100.0	0.0	0.0	0.0
Wadi al Kharid	3	138210000	13821.0	4.3	237.5	96.0	1.5	2.5	0.0
Wadi A'sir	5	208750000	20875.0	6.4	593.2	100.0	0.0	0.0	0.0
Wadi Khulaqah	6	75677104	7567.7	2.3	180.5	100.0	0.0	0.0	0.0
Wadi Qasabah	7	64517144	6451.7	2.0	186.1	99.6	0.0	0.4	0.0
Wadi al Huqqah	8	120270000	12027.0	3.7	1176.1	82.0	7.2	10.8	0.0
Wadi al Iqbal	13	202940000	20294.0	6.3	1538.1	90.0	2.1	3.8	4.1
Wadi Thumah	10	77045984	7704.6	2.4	125.5	49.3	50.7	0.0	0.0
Wadi bani Huwat	9	327030000	32703.0	10.1	4825.5	36.3	44.2	19.3	0.2
Wadi as S'irr	11	218550000	21855.0	6.7	2603.2	39.9	59.9	0.2	0.0
Wadi Zahr & al Ghayl	14	360830000	36083.0	11.1	1297.2	77.9	0.0	21.4	0.7
Wadi al Furs	12	45815372	4581.5	1.4	85.9	49.9	50.1	0.0	0.0
Wadi Sa'wan	17	95936120	9593.6	3.0	1054.9	39.4	59.7	0.1	0.8
Wadi Sha'lik	18	238660000	23866.0	7.4	1032.4	48.5	51.5	0.0	0.0
Wadi Hamdan	15	63496708	6349.7	2.0	788.8	99.3	0.0	0.6	0.0
Wadi al Mawrid	16	179160000	17916.0	5.5	739.0	71.2	14.2	14.5	0.1
Wadi Ghayman	19	143340000	14334.0	4.4	533.2	54.2	45.7	0.2	0.0
Wadi Hizyaz	21	81874360	8187.4	2.5	205.6	95.8	0.0	3.7	0.5
Wadi al Mulaikhy	20	69657048	6965.7	2.2	269.0	84.4	0.0	7.9	7.7
Wadi Akhwar	22	125600000	12560.0	3.9	190.8	97.7	0.4	1.9	0.0
<b>Total</b>	<b>22</b>	<b>3239768376</b>	<b>323976.8</b>	<b>100.0</b>	<b>18953.2</b>	<b>60.5</b>	<b>30.7</b>	<b>8.2</b>	<b>0.6</b>



Table 10: Confusion matrix of cropping pattern

	Ground Truth Classes				
	Classes	Qat	Grapes	Mixed Crops*	Orchards
The mati c Map Clas ses	Qat	274	8	21	12
	Grapes	13	57	6	1
	Mixed Crops	8	5	134	5
	Orchards	4	0	0	38
	No. Ground Truth Totals	299	70	161	56

\* The class "Mixed Crops" includes the classes "rainfed crops/natural vegetation" and "irrigated mixed crops", because separation of these classes were performed via evapo-transpiration measures

Table 11: Accuracy matrix of cropping pattern

	No. of Ground Truth Samples	Correct Classified Pixel	Accuracy
Qat	299	274	91.64%
Grapes	70	57	81.43%
Mixed Crops*	161	134	82.23%
Orchards	56	38	67.86%
Total	586	503	85.84%

\* The class "Mixed Crops" includes the classes "rainfed crops/natural vegetation" and "irrigated mixed crops", because separation of these classes were performed via evapo-transpiration measures

### 4.1.3 Discussion of Results

#### 4.1.3.1 Irrigation Acreage

Irrigation acreage derived from satellite images records the current status of the vegetation and does not consider that some parcels are only partly cultivated or just harvested. To minimize this problem the extension of the vegetation cover was derived from all three SPOT acquisitions dates and accumulated.

Giving the fact that the class "rain fed crops/natural vegetation" covers in total 5,7% of the Sana'a Basin and all irrigated classes 5,9%, the main issue influencing the results of irrigation acreage is the separation of the class "rain fed crops/natural vegetation". Due to the great extension of the class "rain fed crops/natural vegetation" in the September 2004 and June 2005 imageries and because irrigation per se cannot be classified spectrally, evapo-transpiration measurements were used in addition to outline areas irrigated by groundwater.

The threshold of 240 mm/qm evapo-transpiration for the separation of the class "non irrigated vegetation" (rain fed crops/natural vegetation), corresponding to longtime average rainfall over the last years, was chosen to be on the save side. Therefore, the outlined irrigation acreage is rather underestimated than overestimated because irrigated areas with a very sparse vegetation cover and resulting in a low evapo-transpiration are also excluded using this technique.

A comparison of the final results with the winter irrigation acreage (February, 2005) gives an additional indication on the correctness of this approach because the

February 2005 imagery has with 2,7 % the lowest fraction of the class “rain fed crops/natural vegetation” due to the winter season (Figure 24).

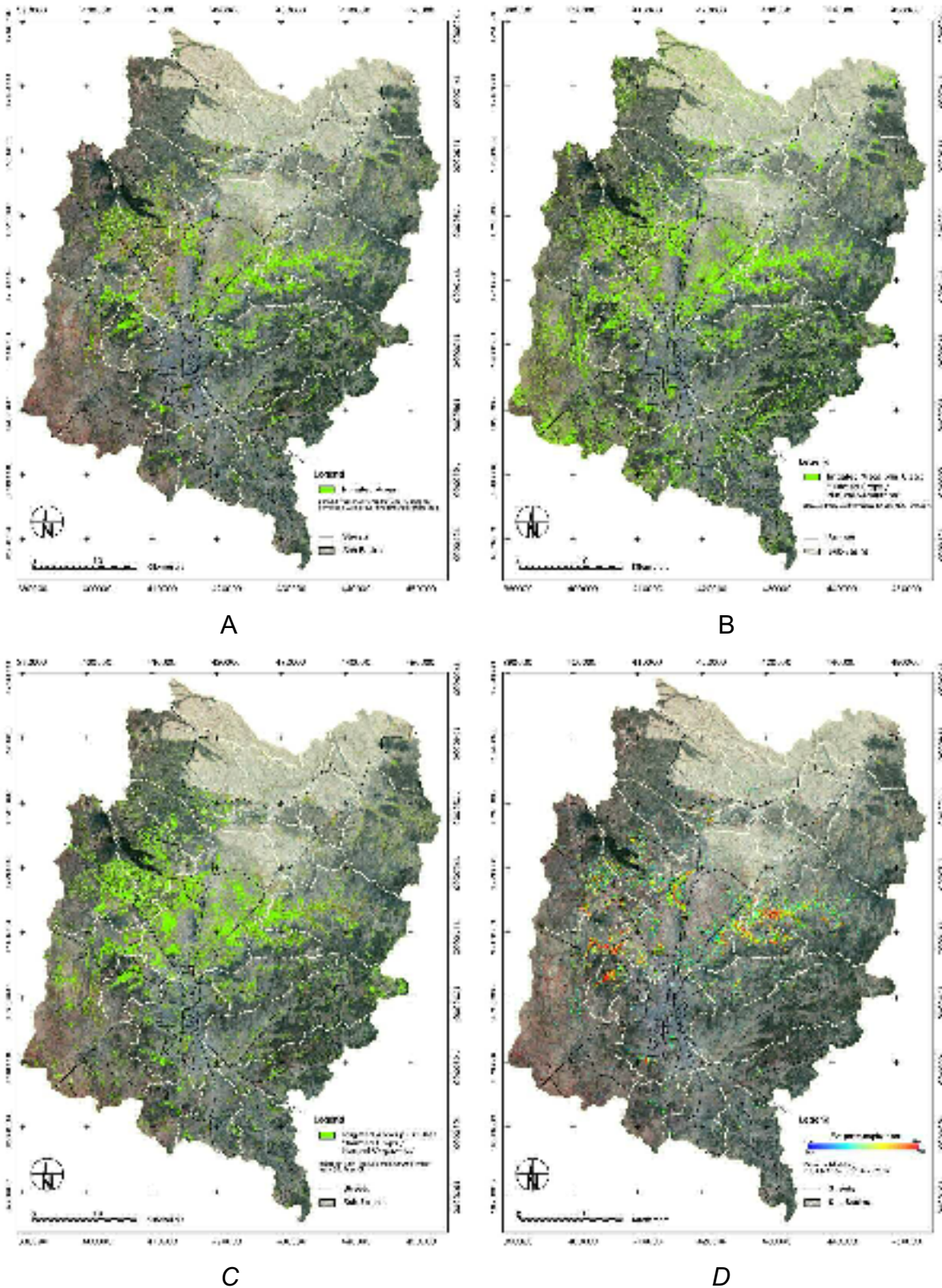


Figure 24: Irrigation acreage (A), irrigation acreage including the class “rain fed crops/natural vegetation” (B), irrigation acreage in Feb. 2005 (C) and evapo-transpiration map (D)

### 4.1.3.2 Cropping Pattern

The results finally demonstrate that sufficient classification accuracy could be achieved on the base of three SPOT 5 data acquisitions despite the following issues which have made the classification difficult.

- Cultivation of very small parcels
- Variable underground / background story
- Intercropping practice
- Partly very sparse vegetation cover / high background signal
- Difference in density/growing stage

The objective of this classification was the derivation of the irrigation “**acreage**” broken down by crop type. Figure 25 shows a comparison between SPOT 5 PAN/MS Merge with 2,5m spatial resolution and SPOT MS with 10m resolution. Despite of the fact that the 2,5m merge gives a much better visual discrimination basis it was decided to perform the automatic classification on the 10m SPOT MS data. The reason for this was that the SPOT 2,5m merge indeed allows visually the identification of single trees or grape rows but the main problem is to outline on this basis the irrigated parcel itself automatically giving at last the irrigation acreage. Figure 27 shows an schematic example of grapes cultivated in rows covered by 1 Landsat TM pixel of 30x30m, by 9 SPOT 5 pixel of 10x10m and by 144 SPOT 5 pixel of 2,5x2,5m spatial resolution. The Landsat TM pixel (30x30m) reflects a mixed information on the grapes and the underground story, problem is that only 3-4 pixels are available for classification per parcel and the mixed pixel problem with adjacent parcels. Also the SPOT 5 MS pixel (10x10m) contains a mixed information on the grapes and the underground story but the great advantage is that much more pixels are being available per parcel for classification and the mixed pixel problem with adjacent parcels is much lower. In contrast to both, the high resolution SPOT 5 PAN/MS Merge Pixel (2,5x2,5m) varies highly in its information content: It covers:

- Pure grapes
- Pure background story
- Mix of both at different portions

These great variations in the information content mainly hamper the automatic classification approach based on the spectral behaviour.

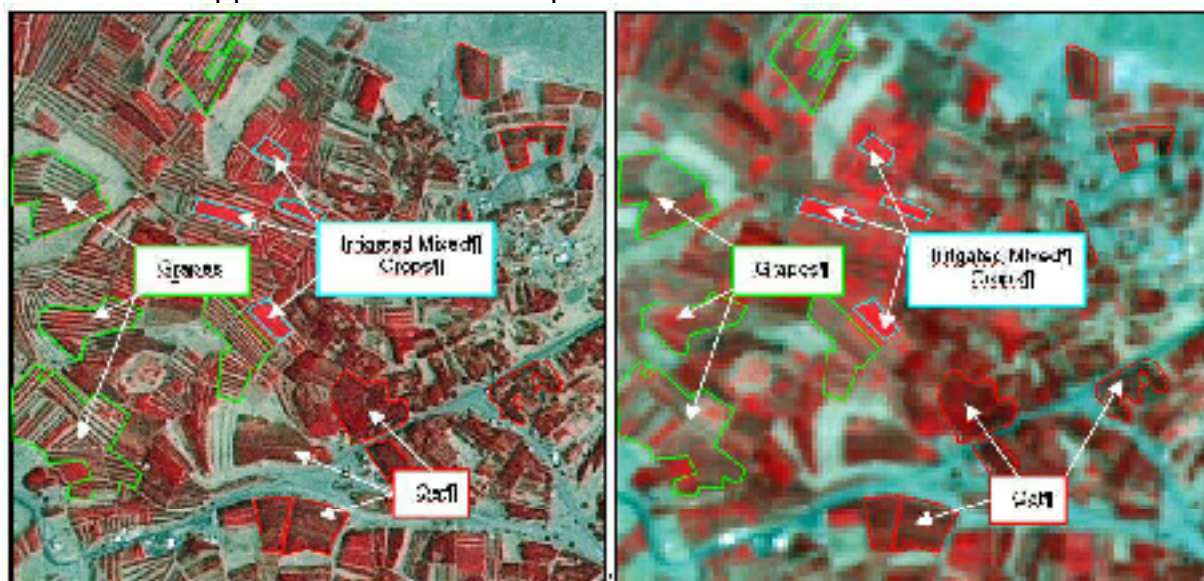


Figure 25: Comparison between SPOT 5 PAN/MS Merge with 2,5m spatial resolution and SPOT MS with 10m resolution



The average parcel size in the Sana'a Basin is about 0,3 ha corresponding to 3000 m<sup>2</sup>. One Landsat TM pixel corresponds to 900 m<sup>2</sup> on the ground and one SPOT 5 MS pixel to 100 m<sup>2</sup>. Accordingly one parcel can be covered with about 3,3 Landsat TM pixels respectively 30 SPOT 5 MS pixels (Fig. 26). Therefore, with SPOT 5 MS data much more pixels are available to classify one parcel and in addition the relative number of mixed pixel is lower in comparison to Landsat TM. Taking all these facts into account the result of this SPOT 5 MS based study gives a more detailed information about the cropping pattern like previous studies based on Landsat TM data.

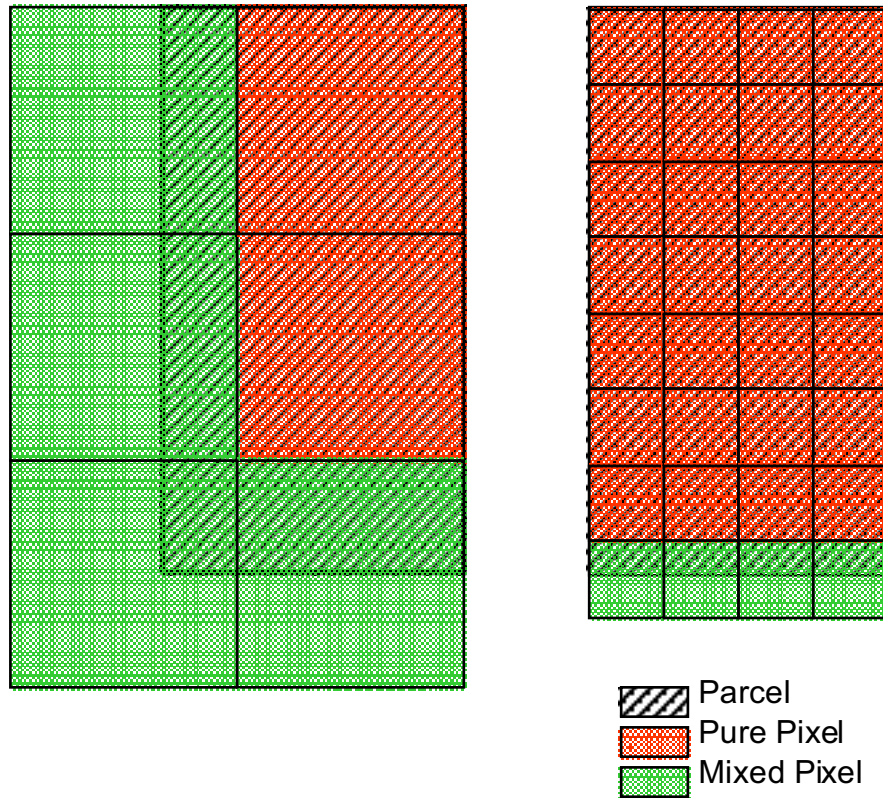


Figure 26: Optimal coverage of a typical parcel (0,3ha; 40x75m) with Landsat TM (30x30m) and SPOT 5 data (10x10m) demonstrating the mixed pixel problem

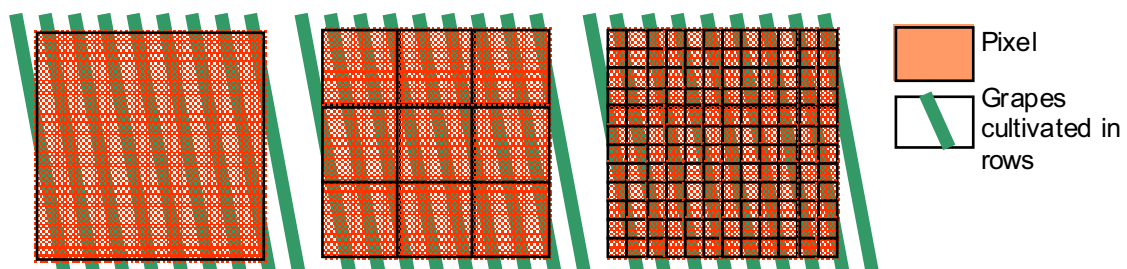


Figure 27: Grapes cultivated in rows covered by 1 Landsat TM pixel of 30x30m (A); by 9 SPOT 5 pixel of 10x10m (B) and by 144 SPOT 5 pixel of 2,5x2,5m (C)

## 4.2 ETa Measurements and ETa Model Results

### 4.2.1 Results from the MBR Station

The station started measurements on Feb 11 2005. Since then it provides meteorological data in mostly good quality. Fig. 28 and 29 illustrate the measured data for February 2004. The plots are created within the COMGRAPH32 software that was delivered together with the hardware of the station. The wet temperature represents the dew point. From the difference between wet and dry temperatures, the humidity can be calculated. The temperature and humidity measurements at the two height levels allow the derivation of the sensible and latent heat fluxes. A special program is included in the software package (EvapoMBR) that enables the direct calculation of the actual evapo-transpiration from the measurements. Training for the maintenance of the station, the use of the software delivered with the station and the data analyses was given to NWRA staff.

Figure 28 and Figure 29 show resulting measurements during February after some data quality check. The upper wet temperature sensor started to produce data errors in the second half of February, which slowly got worse. While in February only single measurements during a day had to be corrected, the data loss summed up to 1 to 3 hours per day in the following months. Therefore it was decided to exchange one sensor. A new sensor was made available in Sana'a in April 2005. The installation was successfully conducted by NWRA staff in May 2005.

Another sensor failure caused by a lack of water occurred at the lower wet sensor. The used psychrometers provide very high accuracy data, but require a good and regular maintenance. Unfortunately this sensor failure happened shortly after the NWRA staff, in charge for the weekly maintenance, went on training to Germany. Therefore this failure could not be corrected immediately. This resulted in a data loss of humidity values of approx. 6 weeks (23. March to 4. Mai 2005).

Another time the farmer happened to cut the power cable of the MBR station during his work in the fields. This problem was immediately transmitted to AQUATECH and the cable fixed already the other day. So no severe data loss occurred.

In general one can conclude that the station worked reliably. Maintenance is the most important and crucial issue in order to obtain high quality meteorological data. NWRA staff proved that they can provide professional maintenance and that they could handle very well all kinds of problems that occurred so far.

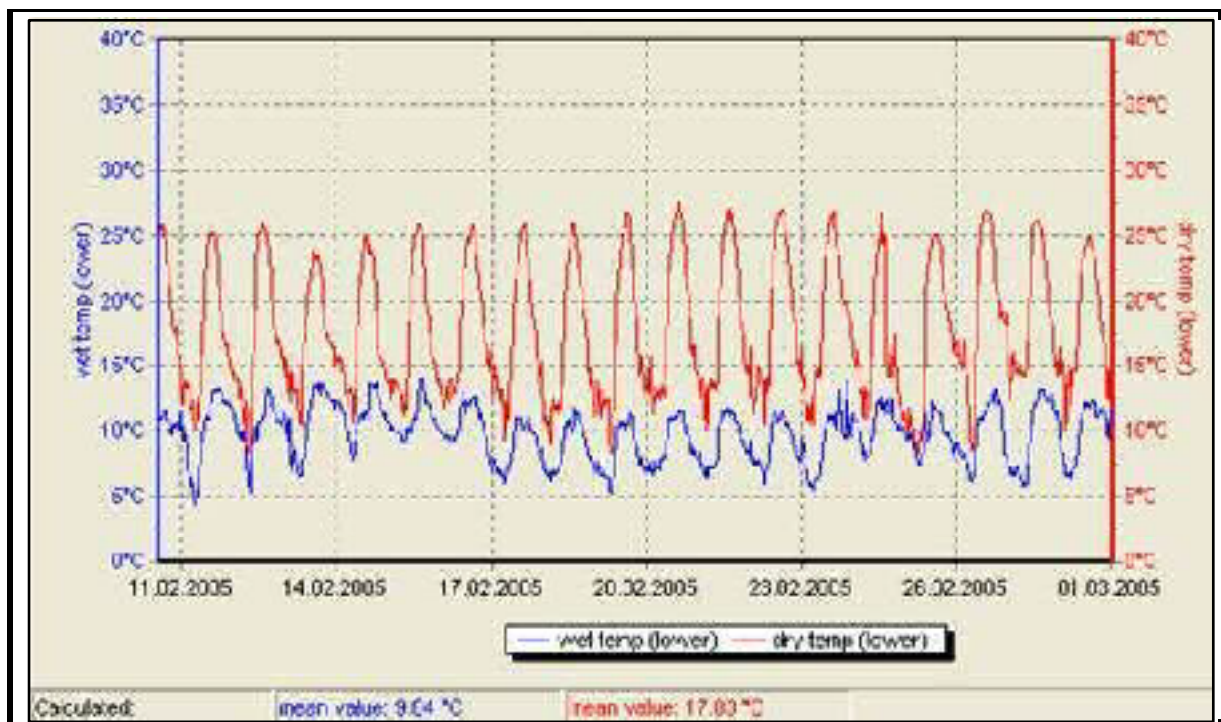
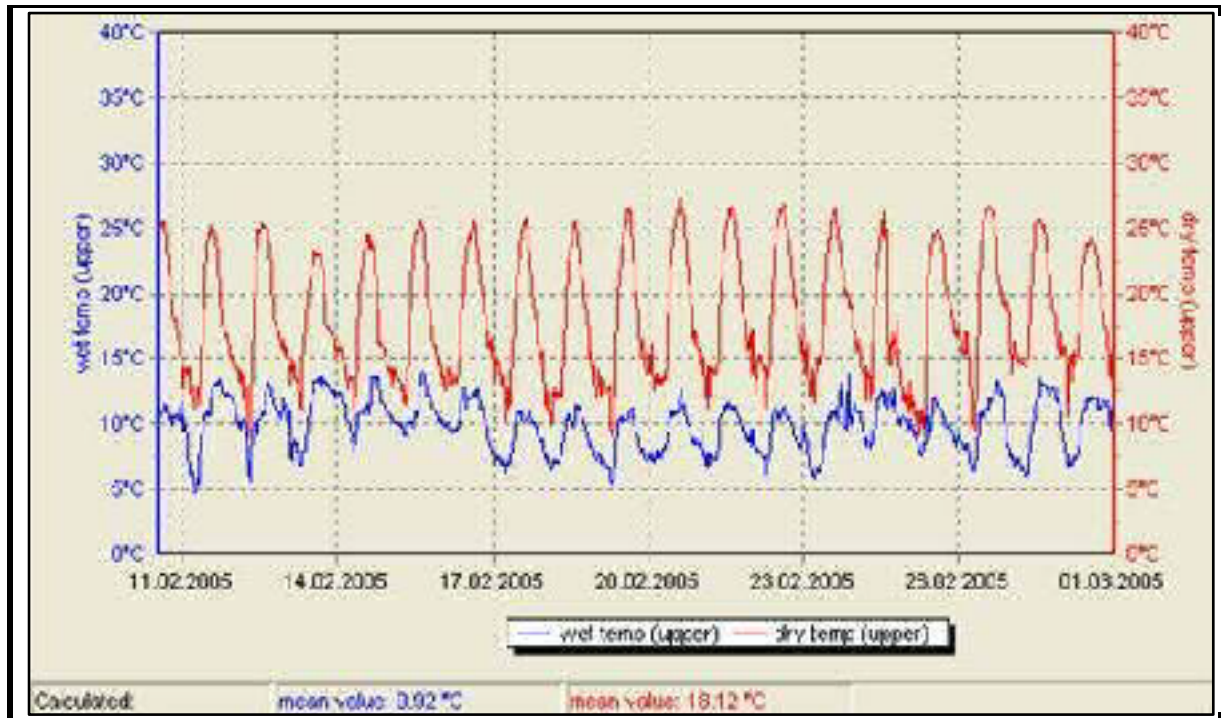


Figure 28: Temperature measurements during February 2005 at the MBR station at Al-Qabil, lower figure: 2m level, upper figure: 5 m level;

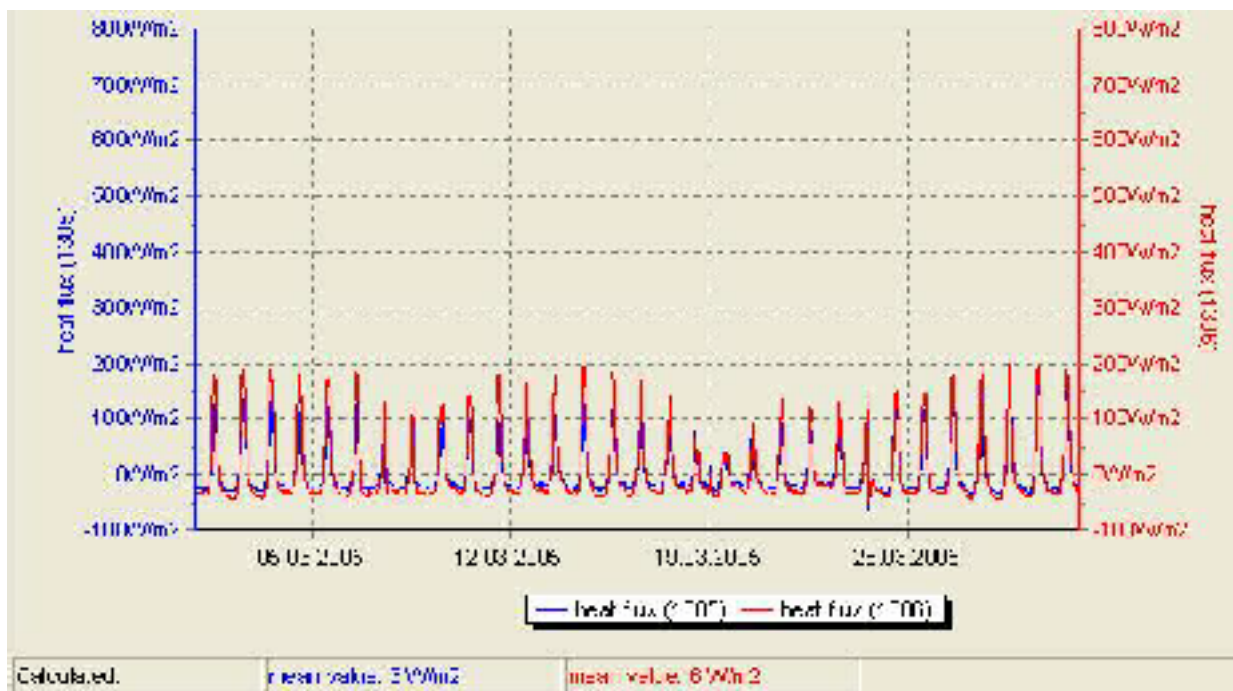
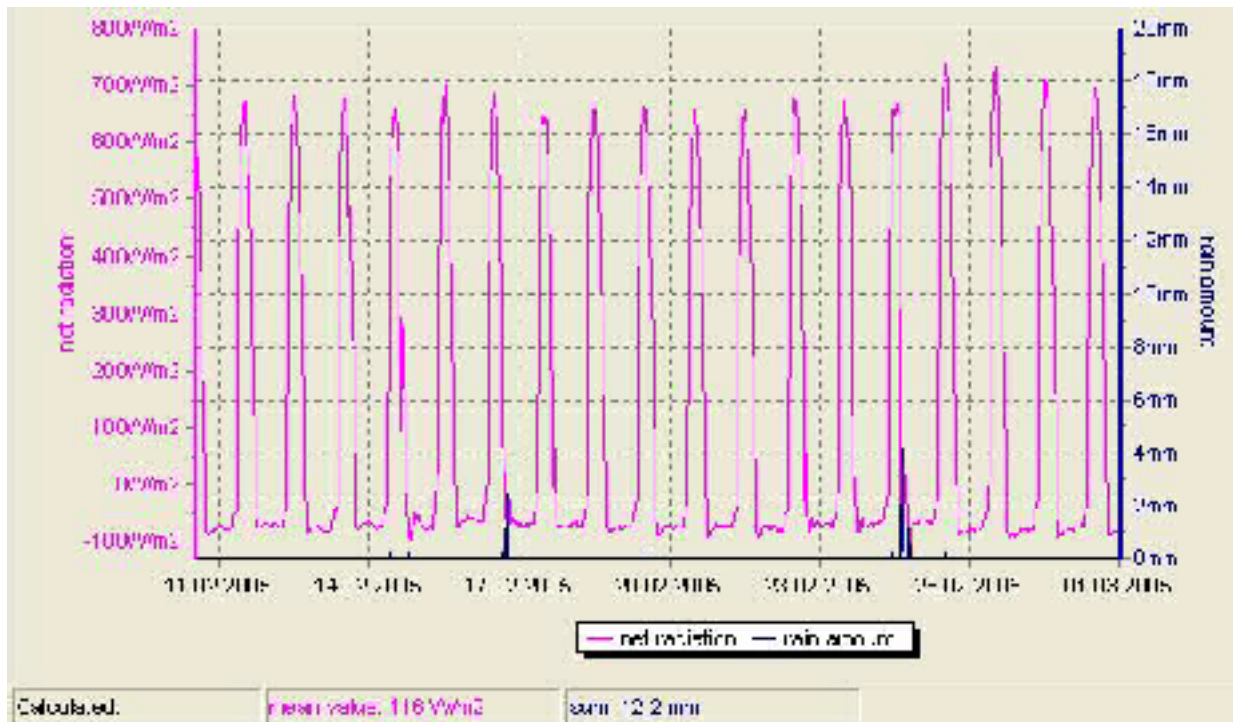


Figure 29: Measurements of energy fluxes and rainfall during February 2005 at the MBR station at Al-Qabil

Figure 30 shows the measured  $ET_a$  values during February 2005. The values are obtained with the software EvapoMBR that is delivered with the meteo-equipment. The graph shows the values for each 20 minute interval. Evapo-transpiration of up to 0.24 mm/20 minutes thus 0.72 mm/hour are measured in February. The effect of rainfall during 25<sup>th</sup> of February can be observed in the  $ET_a$  values with reduced evapo-transpiration during this cloudy day and an increased evapo-transpiration the following days, when enough water was available in the soil. The  $ET_a$  values are only displayed for valid values, which is the case approx. 70% of the time during this



month. A quality parameter is provided within the EvapoMBR software that flags dubious values. These questionable values are not considered further in order to use only valid  $ET_a$  results for further analyses.

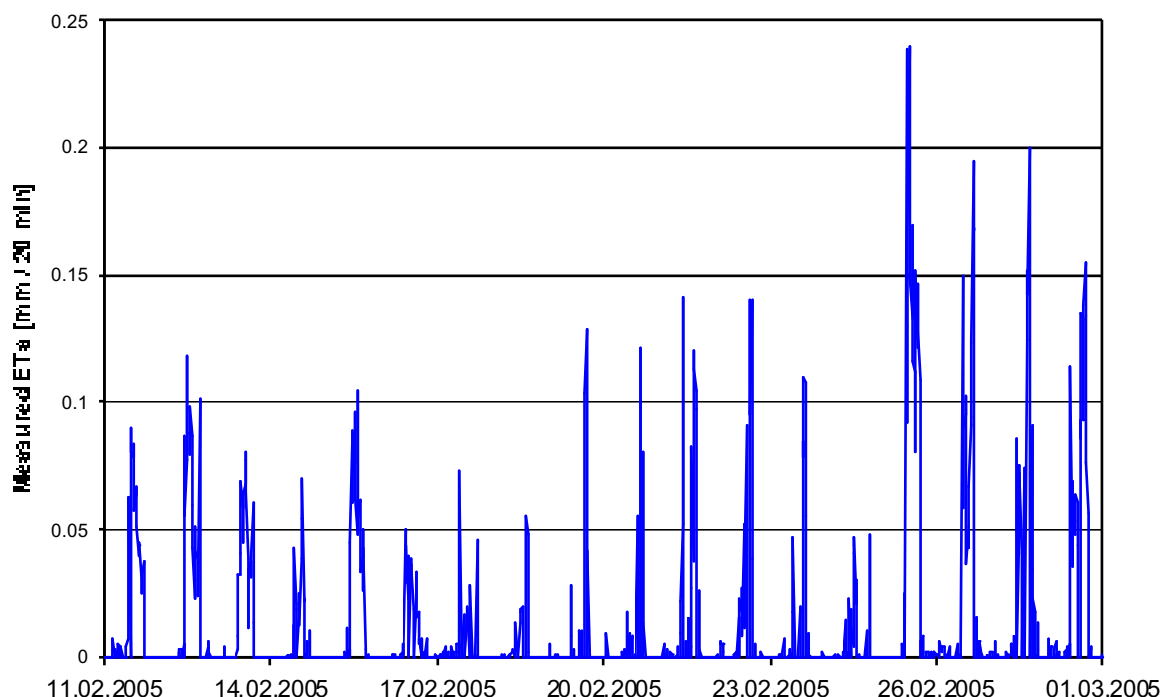


Figure 30:  $ET_a$  measured during February 2005 at the MBR station at Al-Qabil

#### 4.2.2 Spectral Unmixing for Assessing the Fractional Vegetation Cover

Shortage of water and its influence on evapo-transpiration is modelled using information on fractional ground cover from satellite measurements. This reduction factor will be applied to reduce the calculated crop evapo-transpiration to its actual value for each raster cell. Using this approach a map of calculated actual evapo-transpiration was provided on a daily basis.

Spectral mixture analysis can be employed to estimate the fraction of photosynthetic vegetation (PV), non-photosynthetic vegetation (NPV) and bare soil extent from multi-spectral or hyperspectral imagery. The spectral mixing model, which is assumed to be linear, can be written as:

$$M(\lambda) = \sum_{i=1}^n P_i \times R_i(\lambda) \text{ and } \sum_{i=1}^n P_i = 1$$

- with :  $M$  = Reflectance of a pixel at wavelength  $\lambda$
- $P_i$  = Proportion of endmember  $i$  in the pixel
- $R_i(\lambda)$  = Reflectance of endmember  $i$  in the pixel
- $n$  = number of endmembers

The unmixing procedure requires the spectral signatures of the endmembers as input and retrieves the fraction of endmembers in a mixed pixel.

Using this spectral unmixing approach the fractional ground cover was calculated. Endmember spectra for bare soil and for each land use class were selected from the images for this task and linear spectral unmixing was performed. This method provides for each pixel a value for the abundance of the land use class in %, which can be interpreted as fractional ground cover relative to a maximum fractional cover. In terms of the FAO guideline, this analysis retrieves values for  $(f_c/f_{c\_dense})$  for each pixel of the satellite image.

Figure 31 illustrates the endmember spectra that were used. It was differentiated between qat, grapes, orchards and other mixed crops. For each raster cell (pixel) in the SPOT image depending on the classified land use the respective endmember set was applied. The distribution of land use classes used in these preliminary analyses are illustrated in Figure 32. In this illustration also the subareas that were selected for illustration purposes are indicated.

A time series of three satellite images is analysed during the course of the project. This provides information not only of the spatial, but also of the temporal dynamics of the fractional cover of the crops and fields, so that also temporal aspects of  $K_a$  will be observed.

Results for the three satellite acquisitions are illustrated in the Figures 33 to 48 first for each land use class and the subareas and then for the whole Sana'a basin. Statistics of the retrieved results are listed in Tab. 12 and 13.

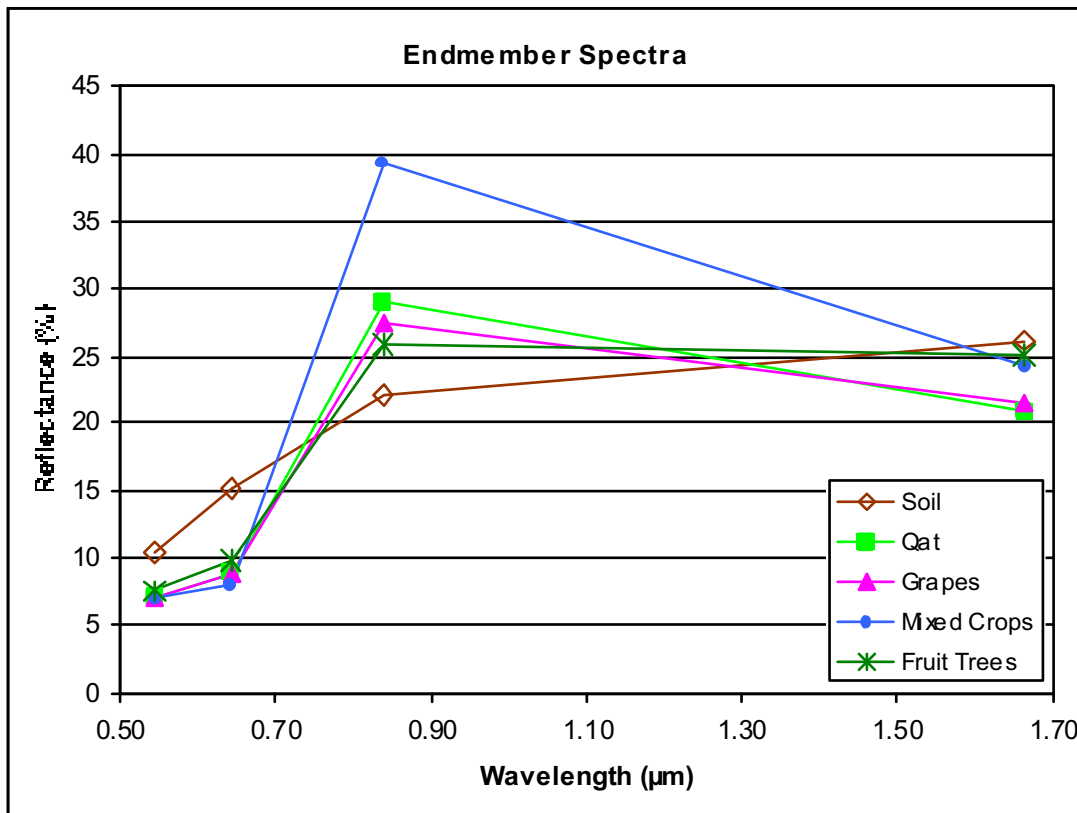


Figure 31: Endmember spectra used for the calculation of the fractional vegetation cover from the SPOT images

The statistics in Tab. 12 reveal that qat was on average more dense (by approx. a factor of 2) in September 2004 than on February 2005. This can be explained by the

harvesting practice. Many farmers harvested qat after Ramadan in October 2004. Also grapes were much denser in June, since in February they had no leaves yet.

*Table 12: Statistics of retrieved fraction cover values for the four land use classes*

Fractional vegetation cover	Mean values	Standard deviation	Maximum
Qat 05.09.2004	29.6 %	23.9 %	100
Qat 24.02.2005	17.6 %	20.1 %	100
Qat 13.06.2005	31.9 %	25.5 %	100
Grapes 05.09.2004	17.9 %	22.5 %	100
Grapes 24.02.2005	0.7 %	3.8 %	100
Grapes 16.06.2005	33.3 %	28.6 %	100
Mixed Crops 05.09.2004	9.4 %	15.2 %	100
Mixed Crops 24.02.2005	2.5 %	9.6 %	100
Mixed Crops 13.06.2005	7.5 %	14.3 %	100
Fruit Orchards 05.09.2004	40.2 %	28.5 %	100
Fruit Orchards 24.02.2005	27.6 %	30.0 %	100
Fruit Orchards 13.06.2005	46.8 %	32.5 %	100

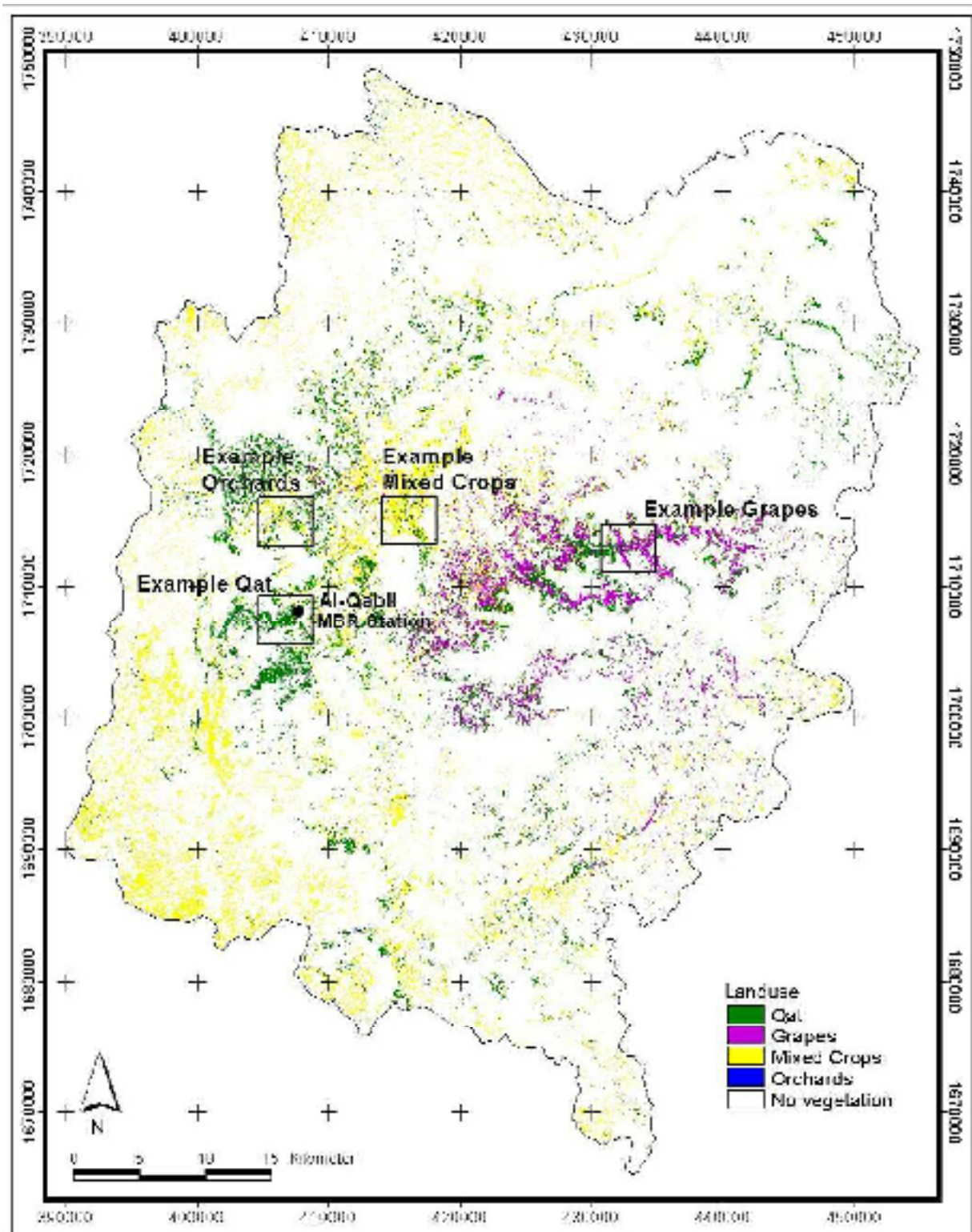


Figure 32: Land use map and illustration of location of example subareas and the installed micro-meteorological station at Al-Qabil



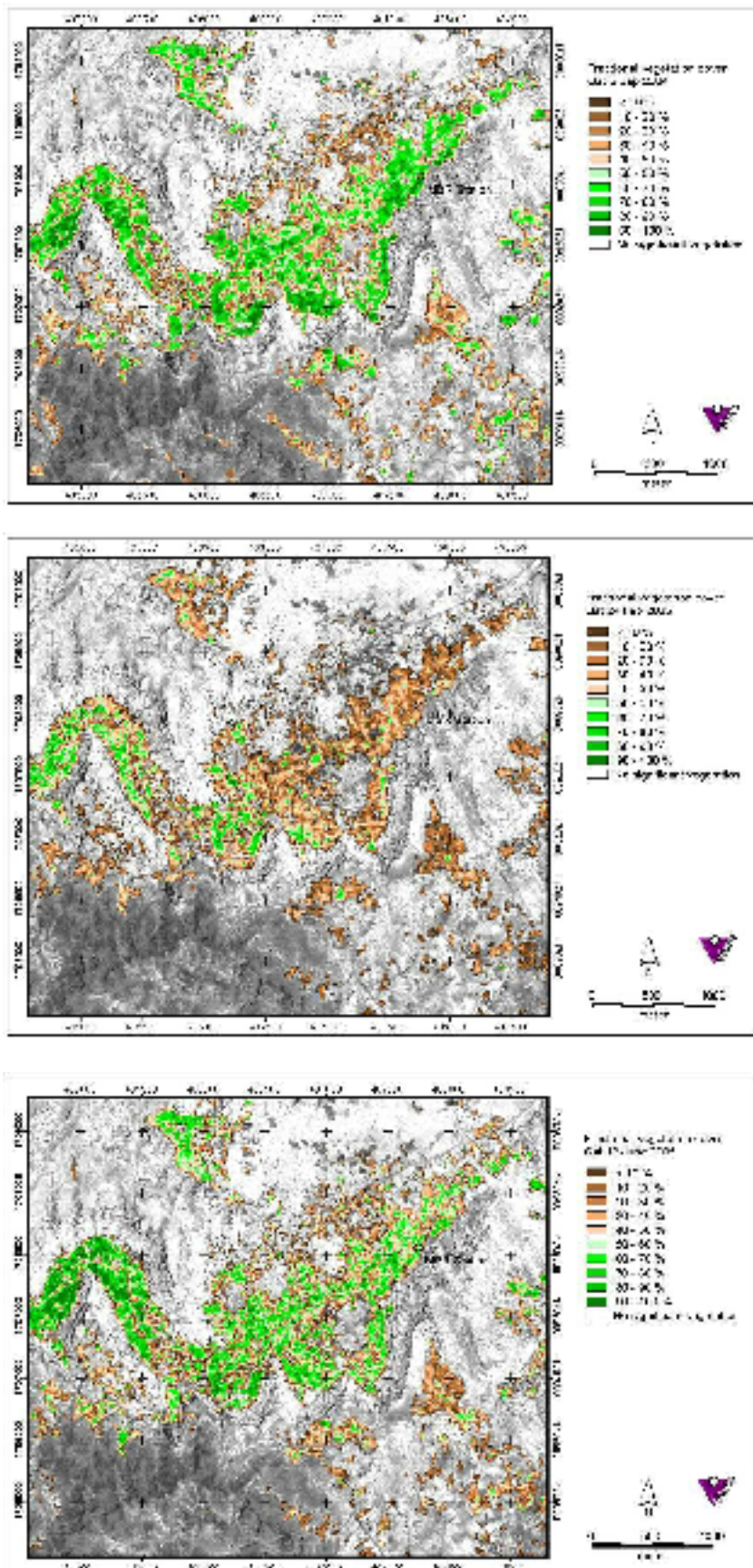


Figure 33: Subarea of calculated fractional vegetation cover of qat on 5th Sep 2004 (top), 24th Feb 2005 (center) and 13th June 2005 (bottom), fc is calculated on 10m pixel

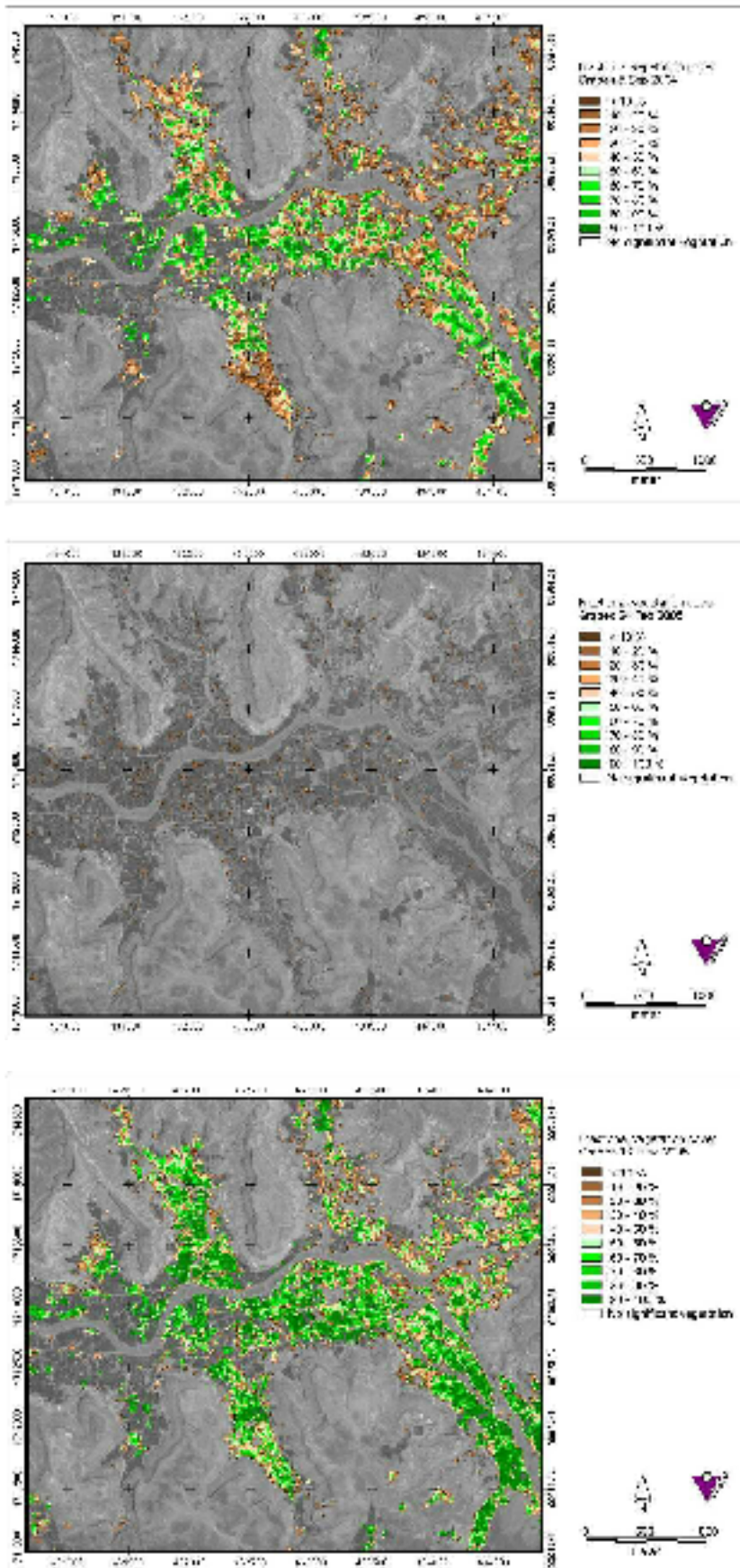


Figure 34: Subarea of calculated fractional vegetation cover of grapes on 5th Sep 2004 (top), 24th Feb 2005 (center) and 13th June 2005 (bottom), fc is calculated on 10m pixel



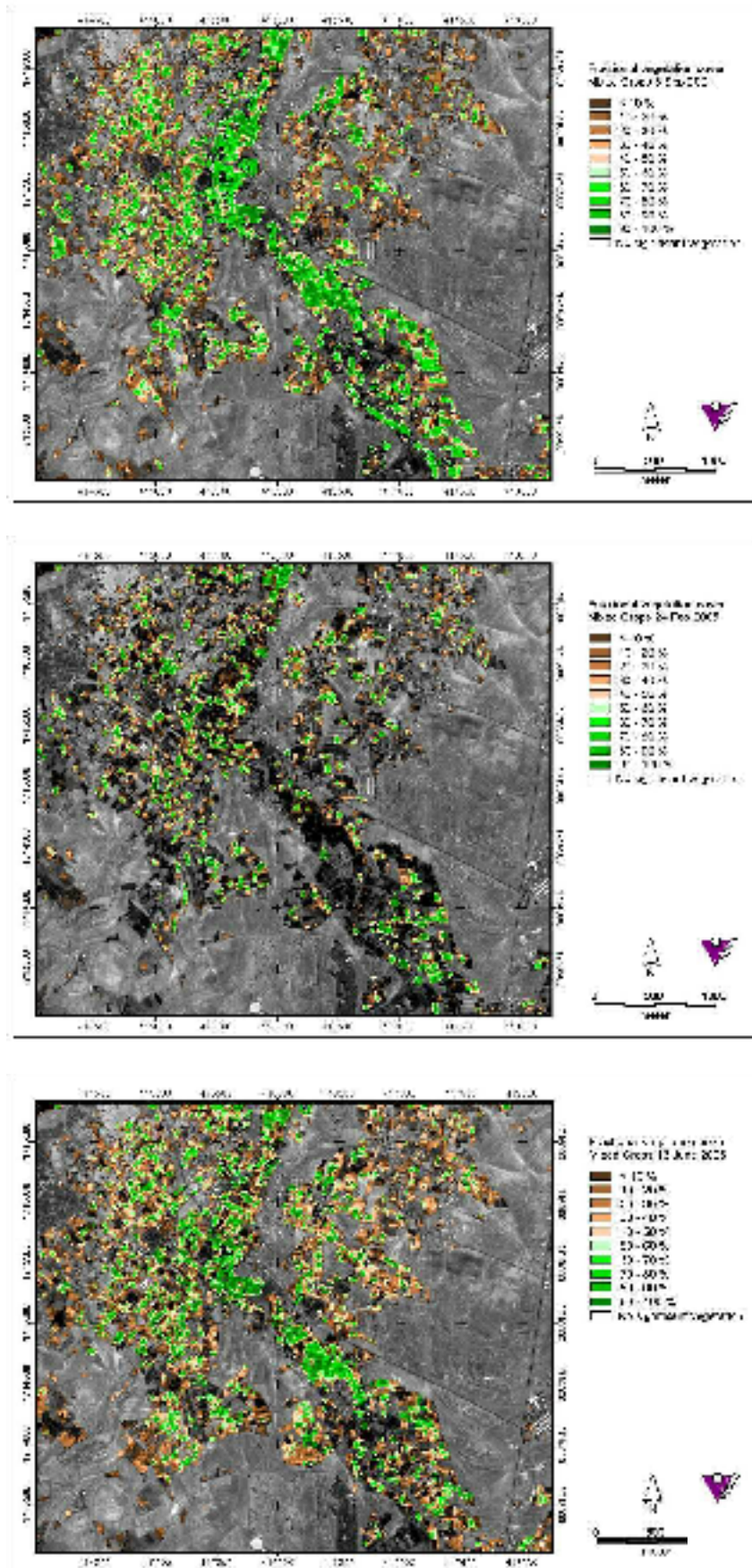


Figure 35: Subarea of calculated fractional vegetation cover of mixed crops on 5th Sep 2004 (top), 24th Feb 2005 (center) and 13th June 2005 (bottom); fc is calculated on 10m pixel



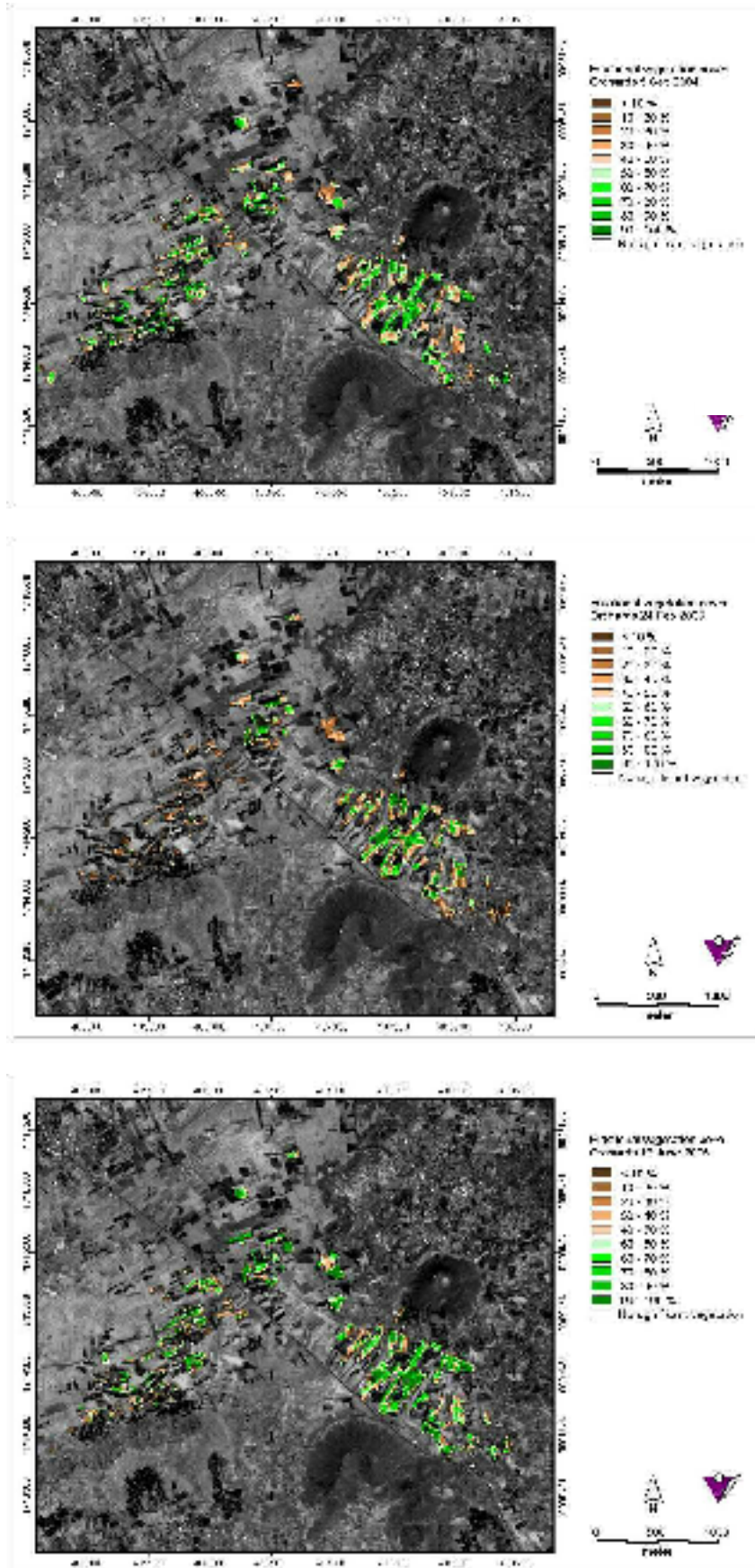


Figure 36: Subarea of calculated fractional vegetation cover of fruit orchards on 5th Sep 2004 (top), 24th Feb 2005 (center) and 13th June 2005 (bottom); fc is calculated on 10m pixel